



UNIVERSITÀ DEGLI  
STUDI DI SALERNO



*Ministero dell'Istruzione,  
dell'Università e della Ricerca*



## **Facoltà di Ingegneria**

Dipartimento di Ingegneria dell'Informazione ed Elettrica e  
Matematica Applicata.

Dottorato di Ricerca in Ingegneria dell'Informazione  
XIV Ciclo - Nuova Serie

TESI DI DOTTORATO

# **Electric Mobility: Smart Transportation in Smart Cities**

CANDIDATO: **GIUSEPPE GRABER**

COORDINATORE: **PROF. MAURIZIO LONGO**

RELATORE: **PROF. VINCENZO GALDI**

CORRELATORE: **DR. PIERLUIGI MANCARELLA**

Anno Accademico 2014 - 2015



*“Our imagination is stretched to the utmost, not, as in fiction, to imagine things which are not really there, but just to comprehend those things which are there”.*

*Richard Feynman,*

*THE CHARACTER OF PHYSICAL LAW*



## Acknowledgements

*I would like to thank and dedicate my dissertation to all those who were close to me during these years. First of all, my family who was always ready to offer me so much support and encouragement.*

*I would like to express my sincere gratitude to prof. V. Galdi for the valuable teachings he has given me during my PhD course, and for the care with which I was constantly followed in every step of my work.*

*I especially thank Dr. P. Mancarella for his willingness to support me in the realization of this PhD dissertation.*

*Finally, warm thanks to my mates in the S.I.S.T.E.M.I. lab. and to the colleagues of the PhD program in Information Engineering with I shared these years, cause they made this period of my life an experience I will never forget and it will be always one of my dearest memories.*

Fisciano, 05/03/2016

*Giuseppe Graber*



# Table of Contents

|   |             |
|---|-------------|
| <b>Acknowledgements</b> .....   | <b>VI</b>   |
| <b>Table of Contents</b> .....  | <b>VIII</b> |
| <b>List of Acronyms</b> .....   | <b>XII</b>  |
| <b>Introduction</b> .....   | <b>2</b>    |
| <b>Chapter 1 - Transport Systems in the Smart Cities of the Future</b> .6 |             |
| 1.1 Energy Demand in Transport Sector .....                               | 7           |
| 1.2 Transport Systems for Sustainable Mobility .....                      | 12          |
| 1.2.1 Electrification of Urban Transport .....                            | 14          |
| 1.3 Tram, Metro and Light Railway Systems.....                            | 16          |
| 1.3.1 Sustainability in Electrified Transport Systems .....               | 19          |
| 1.4 E-Mobility: Electric Vehicles Future Penetration .....                | 21          |
| 1.4.1 Market Growth & CO <sub>2</sub> Reduction .....                     | 22          |
| 1.5 Sustainable Transportation into Modern Power Systems...               | 26          |
| References .....  | 31          |
| <b>Chapter 2 - Smart Grids: Power Systems in Smart Cities</b> .....       | <b>34</b>   |
| 2.1 The Smart Grid Concept.....   | 35          |
| 2.1.1 The Smart Grid Technologies.....                                    | 38          |
| 2.2 Reliability in Smart Grids.....                                       | 40          |
| 2.2.1 Resiliency of Smart Grid Functions .....                            | 42          |
| 2.3 Overloading and Outages: what to do .....                             | 44          |
| 2.3.1 Scheduling of Generators .....                                      | 45          |
| 2.3.2 Load Shedding.....  | 47          |
| 2.4 Uncertainty in Power Systems.....                                     | 49          |
| 2.4.1 Possibility Theory.....   | 49          |
| 2.4.2 Fuzzy Numbers.....  | 51          |
| 2.5 GRLS Problem under Uncertainty Conditions.....                        | 54          |
| 2.5.1 Mathematical Formulation .....                                      | 55          |
| 2.5.1.1 Rescheduling Problem .....  | 56          |
| 2.5.1.2 Load Shedding Problem.....  | 57          |
| 2.5.2 Solution Algorithm.....   | 59          |

Electric Mobility: Smart Transportation in Smart Cities IX

|  |  |            |
|--|--|------------|
| 2.6  | Simulation Framework.....                      | 61         |
| 2.6.1  | Case Study.....                                | 61         |
| 2.6.2  | Numerical Results.....                         | 63         |
|  | References.....                                | 67         |
| <b>Chapter 3 - EVs in Smart Grid: a Smart Charging Solution.....</b> |  | <b>70</b>  |
| 3.1  | Electric Vehicles Technology.....              | 71         |
| 3.2.1  | EVs Charging Options.....                      | 74         |
| 3.2  | Factors Affecting EVs Charging Demand.....     | 78         |
| 3.3  | EVs Charging Profile Prediction.....           | 81         |
| 3.4  | Vehicle Usage Data Analysis.....               | 83         |
| 3.4.1  | Data Acquisition: COSMO Research Project.....  | 84         |
| 3.4.2  | Data Clustering.....                           | 85         |
| 3.5  | EVs Charging Scheduling Algorithm.....         | 86         |
| 3.5.1  | Mathematical Formulation.....                  | 88         |
| 3.5.1.1  | Charging Modes.....                            | 89         |
| 3.5.1.2  | Optimized EVs Scheduling Problem.....          | 90         |
| 3.5.2  | Solution Algorithm.....                        | 91         |
| 3.5.3  | Scheduler Architecture and Protocol.....       | 93         |
| 3.6  | Simulation Framework.....                      | 95         |
| 3.6.1  | Case Study.....                                | 95         |
| 3.6.2  | Numerical Results.....                         | 97         |
| 3.6.2.1  | Data Clustering Results.....                   | 97         |
| 3.6.2.2  | Scheduled EV Charging Results.....             | 101        |
|  | References.....                                | 106        |
| <b>Chapter 4 - Energy Efficiency in Metro Systems.....</b>           |  | <b>110</b> |
| 4.1  | Innovative Solution for Energy Efficiency..... | 111        |
| 4.1.1  | Energy Storage Systems.....                    | 114        |
| 4.1.2  | Eco Drive Speed Profiles.....                  | 117        |
| 4.2  | Models of the Metro Systems.....               | 120        |
| 4.2.1  | Metro Vehicle.....                             | 120        |
| 4.2.2  | Energy Storage System.....                     | 122        |
| 4.2.2.1  | Power Converter Control Algorithm.....         | 123        |
| 4.2.3  | Feeding Network.....                           | 125        |
| 4.3  | ESSs Sizing and Positioning Problem.....       | 127        |
| 4.3.1  | Mathematical Formulation.....                  | 127        |
| 4.3.2  | Solution Algorithm.....                        | 129        |
| 4.4  | Eco-Drive Speed Profiles Problem.....          | 131        |
| 4.4.1  | Mathematical Formulation.....                  | 131        |
| 4.4.2  | Solution Algorithms.....                       | 133        |

---

|         |  |            |
|---------|--|------------|
| 4.5     | Simulation Framework .....               | 136        |
| 4.5.1   | Case Study .....                         | 136        |
| 4.5.2   | Numerical Results .....                  | 137        |
| 4.5.2.1 | SCs Positioning and Sizing Results ..... | 138        |
| 4.5.2.2 | Eco-Drive Speed Profiles Results .....   | 142        |
|         | References .....                         | 147        |
|         | <b>Chapter 5 - Conclusions.....</b>      | <b>150</b> |
| 5.1     | Summary of Dissertation .....            | 150        |
| 5.2     | Future Research Direction.....           | 153        |



## List of Acronyms

|      |   |
|------|---|
| AC   | Alternate Current                                 |
| BEV  | Battery Electric Vehicle                          |
| BP   | British Petroleum                                 |
| CF   | Control Function                                  |
| CHP  | Combined Heat and Power                           |
| CS   | Charging Station                                  |
| DAS  | Driver Advisory System                            |
| DC   | Direct Current                                    |
| DCFC | Direct Current Fast Charge                        |
| DER  | Distributed Energy Resource                       |
| DG   | Distributed Generation                            |
| DSM  | Demand Side Management                            |
| DN   | Distribution Network                              |
| DPO  | Dynamic Programming Optimization                  |
| EIA  | U.S. Energy Information Administration            |
| ESS  | Energy Storage System                             |
| EV   | Electric Vehicle                                  |
| EVSE | Electric Vehicle Supply Equipment                 |
| FCEV | Fuel Cell Electric Vehicle                        |
| FS   | Ferrovie dello Stato Italiane                     |
| GA   | Genetic Algorithm                                 |
| GHG  | GreenHouse Gas emission                           |
| GRLS | Generation Rescheduling and Load Shedding         |
| GTO  | Gate Turn-Off thyristor                           |
| HEV  | Hybrid Electric Vehicle                           |
| HTSC | High Temperature Superconductors                  |
| ICE  | Internal Combustion Engines                       |
| ICT  | Information and Communication Technology          |
| IEA  | International Energy Agency                       |
| IEEE | Institute of Electrical and Electronics Engineers |
| IGBT | Insulated-Gate Bipolar Transistor                 |

---

|            |   |
|------------|---|
| LDV        | Low Duty Vehicle  |
| LV         | Low Voltage   |
| $\mu$ G    | Microgrid   |
| MEMS       | Microgrid Energy Management System                        |
| MILP       | Mixed Integer Linear Programming                          |
| MINLP      | Mixed Integer Non-Linear Programming                      |
| MV         | Medium Voltage  |
| <i>nec</i> | Necessity   |
| OECD       | Organisation for Economic Co-operation and<br>Development |
| PCC        | Point of Common Coupling                                  |
| pdf        | Probability Density Function                              |
| PEV        | Plug-in Electric Vehicle                                  |
| PHEV       | Plug in Hybrid Electric Vehicle                           |
| <i>pos</i> | Possibility   |
| PSO        | Particle Swarm Optimization                               |
| PV         | Photovoltaic  |
| R&D        | Research and Development                                  |
| RES        | Renewable Energy Source                                   |
| RPS        | Railway Power System                                      |
| SoC        | State of Charge   |
| SC         | Supercapacitor  |
| SG         | Smart Grid  |
| T&D        | Transmission & Distribution                               |
| ToU        | Time of Use   |
| UIC        | International Union of Railways                           |
| UniSA      | University of Salerno                                     |
| VOC        | Volatile Organic Compounds                                |
| V2G        | Vehicle-to-Grid   |
| V2I        | Vehicle-to-Infrastructure                                 |
| V2V        | Vehicle-to-Vehicle  |
| WPT        | Wireless Power Transfer                                   |

## Introduction

One of the mega trends over the past century has been humanity's move towards cities. As many as 60% of the world's population will live in cities by the year 2030, according to the World Health Organization, and this rapid urbanization is putting unprecedented pressure on city infrastructures, services and the environment. Public Administration and Municipalities are facing a challenging task, to harmonize a sustainable urban development offering to people in city the best living conditions.

The growing phenomenon of *Smart Cities* has led city managers and planners to look beyond traditional approach in city planning, finding ways to give to the people a place where to live that is environmentally, economically and socially sustainable. Smart city is now considered a winning urban strategy able to increase the quality of life by using technology in urban space, both improving the environmental quality and delivering better services to the citizens.

Mobility is a key element to support this new approach in the growth of the cities. In fact, transport produces several negative impacts and problems for the quality of life in cities, such as, pollution, traffic and congestion, with a negative impact on the quality of life in cities. Therefore, *Sustainable Mobility* is one of the most promising topics in smart city, as it could produce high benefits for the quality of life of almost all the city stakeholders.

Sustainable Mobility is not a unique initiative, but a complex set of projects and actions, different in goals, contents and technology intensity.

The boldest and imminent challenge awaiting mobility in smart cities is the introduction of the electricity as energy vector instead of fossil fuels, concerning both the collective and the private transports.

Public transport is a very important aspect for a sustainable mobility in urban areas, and it considered one of the most relevant approach to encourage low-carbon growth in cities. Electric public

transport include electric city buses, trolleybuses, trams (or light rail), passenger trains and rapid transit (metro/subways/undergrounds, etc.). Even though railway systems are the most energy efficient than other transport modes, the enhancement of energy efficiency is an important issue to reduce their contributions to climate change further as well as to save and enlarge competition advantages involved. One key means for improving energy efficiency is to deploy advanced systems and innovative technologies. Therefore, the International Union of Railways is funding several research projects aimed to evaluate the current railway energy saving methodologies.

Additionally, electrification of the private road transport has emerged as a trend to support energy efficiency and CO<sub>2</sub> emissions reduction targets. According to the International Energy Agency (IEA), in order to limit average global temperature increases to 2°C - the critical threshold that scientists say will prevent dangerous climate change -, by 2050, 21% of carbon reductions must come from the transport sector. To achieve this goal, the agency says, three fourths of all vehicles sold by 2050 need to be electric, including plug-in hybrid and battery electric vehicles (EVs).

In recent years, many EVs were announced and many prototypes presented. Today, there are more than 20 models offered by different brands covering different range of sizes, styles, prices and powertrains to suit the wider range of consumers as possible. Full EVs uses electric motor and battery energy for propulsion, which has higher efficiency and lower operating cost compared to the conventional internal combustion engine vehicle. The continuous development of lithium ion battery and of fast charging technology will be the major facilitators for EVs roll out in the very near future. However, the present EVs industry meets many technical limitations, such as high initial price, long battery recharge time, limited charging facilities and driving range.

Although it is desirable a fast development from the start of electric mobility, its impact on the existing power grid must be assessed beforehand to see if it is necessary prior an adjustment of power infrastructure or/and the introduction of new services in the power grid. In fact, the interconnection of EVs on the power grid for charging their batteries potentially introduces negative impacts on grid operation: uncontrolled charging can significantly increase average load in the existing power systems, with problems in terms of

reliability and overloads. If uncontrolled EV charging is added to the system, this can have effects both at the distribution and at the generation level. In countries with an advanced development of the distribution grid, no significant risks for distribution or transmission grids could be identified even for high shares of electric vehicles, as long as charging uses low power (household) connections. In countries with relatively weak electricity infrastructure, however, even small-scale EV introduction can cause local power-outages if charging is uncontrolled.

Controlled or smart charging will allow a much greater number of cars in the cities, avoiding local overload and allowing a faster EVs penetration without requiring an imminent improvement of the electricity generating and grid capacity. This results in considerable potential benefit for smart charging, possibly through price incentives such as dynamic tariffs, in order to cut off peak demand and smooth electricity demand curves. Smart charging might also allow load balancing both at sub-station and at the grid level, particularly with charging at peak wind supply times. This kind of use of EV battery capacity for storing electric energy may ease the integration of large scale intermittent electricity sources such as renewable energy sources (RESs).

The proposed PhD Dissertation is developed in the context just described, mainly focusing the attention on the impact that electric mobility will have on the power systems and the effectiveness of solutions aimed to increase the reliability and resilience in the smart grid. In particular, it is addressed a scenario analysis regarding the electric vehicles charging management and some innovative solutions to increase energy efficiency in electrified transport systems. The first chapter emphasizes on the key aspects related to the sustainable mobility in the smart cities of the future. It provides a brief overview on the transport sector energy consumption expected in the next years. In particular, the chapter shows the significant contribution that the electrification of urban transport may provide to the sustainable mobility, and the serious concerns related to its impact on existing power systems.

Chapter 2 proposes a solution method for an optimal generation rescheduling and load-shedding (GRLS) problem in microgrids in order to determine a stable equilibrium state following unexpected

outages of generation or sudden increase in demand. The chapter mainly focuses on the mathematical formulation of the GRLS problem and the proposed solution algorithm. Finally, simulations results carried out by using a real case study data are presented and discussed.

In Chapter 3, a simple and effective methodology is proposed to analyze data acquired during the fulfillment of the *COSMO* research project, and to identify typical load pattern for the EVs charging. The chapter also presents a novel scheduling problem formulation, flattening the demand load profile and minimizing the EVs charging costs, according to the electricity prices during the day. Finally, some simulations results are discussed, showing the effectiveness of the proposed methodology. Chapter 4 introduces some innovative solutions for energy efficiency in urban railway systems focusing, in particular, on energy storage systems and eco-drive operations in metro networks. The mathematical formulation of these optimization problems and the proposed solution algorithms are illustrated and discussed. The obtained results are part of the activity carried out in the *SFERE* research project. Finally, Chapter 5 ends the Dissertation with some concluding remarks and further developments of the proposed research activity.

## Chapter 1

# Transport Systems in the Smart Cities of the Future

Urbanization is accelerating at pace, placing new intense pressures on city resources and infrastructure. Urban mobility will be one of the toughest challenges for cities around the globe. In many cities, existing mobility systems are already inadequate and, thus, urbanization and increasing populations will increase demand still further. Cities traditionally searched to solve such challenges by adding new capacity to match demand. However, a capacity-building approach alone is neither efficient nor sustainable.

A smart city is an efficient and livable city, as well as an economically, socially and environmentally sustainable city. This vision can be realized in the next future integrating the different mobility solutions (rail, automotive, bicycle and walking) into one convenient, easily accessible, time-efficient, affordable, safe and green. An integrated systems approach optimizes infrastructure and energy consumption and provides transportation for city residents exactly where and when they need it.

The electrification of road transport establishes a link between the energy and mobility sectors as well as a new domain of services in regards to the management of *electric mobility* as for the first time it brings together utilities and grid operators. The deployment of electric vehicles in the network will require the provision of the supporting infrastructure and systems, and their integration in the full mobility system in a wide scale. The rail public transport, that uses electric energy, provides a sustainable mobility solution as well and will growingly be an alternative to private vehicles in the future. Given the

limitations of the electric vehicle, its intelligent integration into the existing urban transport infrastructure is essential.

This chapter emphasizes on the key aspects and problems related to the electrification of urban transport for sustainable mobility in the smart cities of the future. The purpose of Section 1.1 is to provide a brief overview on the current transportation energy consumption and expected scenarios in the coming years for transport demand. Developing transport systems that are environmentally friendly and characterized by high energy efficiency values is a prerequisite for sustainable mobility and they are illustrated in Section 1.2. However, Section 1.3 shows the significant contribution that the electrified transport systems may provide to the sustainable mobility, whereas Section 1.4 deals with electric vehicles and their growing penetration in the current car market. Finally, Section 1.5 discusses the impact on existing power systems of the urban transport electrification in smart cities.

## 1.1 Energy Demand in Transport Sector

In the New Policies Scenario, in which recent government policy commitments are assumed to be implemented in a cautious manner, demand increases for all energy sources over the 2035 period, but the pace and trend varies, [1].

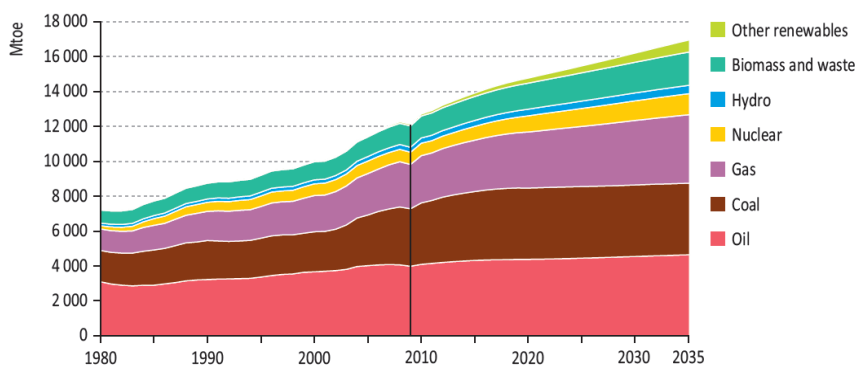
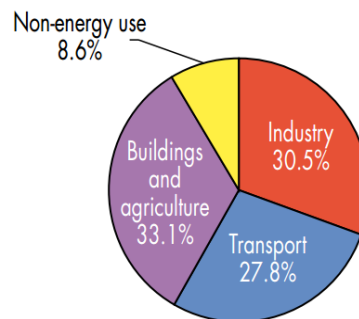


Figure 1 - World primary energy demand by fuel in the New Policies Scenario (source: IEA, WEO-2011).

Around 2000, the transport sector crossed a threshold to account for more than half of total oil demand and it has not looked back. The projected share of the transport sector continues to increase from 55% today to more than 60% in 2040, despite increased fuel efficiency and the growth of alternative fuels. More than three quarters of transport oil demand comes from road transport today, as share which is set to remain broadly unchanged until 2040, [2]. Although aviation is the fastest growing of all transport sectors, road transport is set to account for over two-thirds of oil demand growth for transport. The growth in oil demand for transport occurs almost exclusively in emerging and developing countries, whereas in OECD countries the oil demand of the transport declines across all sub-sectors, except aviation, [3].

In the New Policies Scenario, global demand for oil increases from 84 million barrels per day (mb/d) in 2009 (almost 87 mb/d in 2010) to 99 mb/d in 2035 (Figure 1). All of the net growth in global oil demand in the New Policies Scenario comes from the transport sector in the non-OECD countries, growth being particularly strong in India, China and the Middle East.



**Figure 2 - Total final consumption by sector in the New Policies Scenario, 2040**  
(source: IEA, KWES-2015).

From the energy point of view, the transport sector currently counts for almost 30% of global final energy consumption (Figure 2), including all modes of transportation, from personal vehicles (cars, light trucks) to public transportation (buses, trains) and airplanes, from freight trains to barges, [4].

One might think that airplanes, trains, and buses would consume most of the energy used in this sector but, in fact, their percentages are relatively small-about 9% for aircraft and about 2% for trains and

buses. As reported in Figure 3, personal vehicles, in fact, consume 57% of the energy used for transportation, [5].

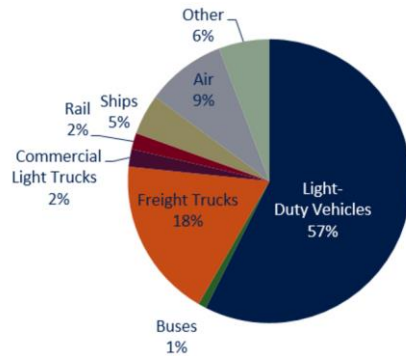
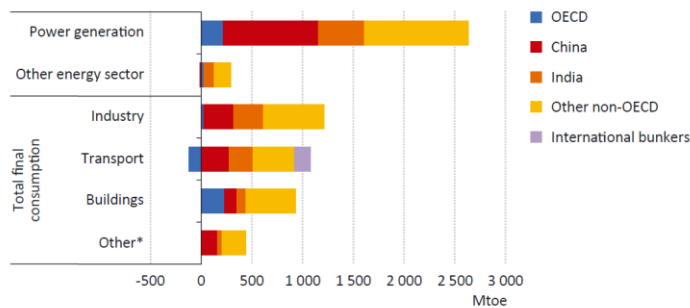


Figure 3 - Transportation energy use by mode (source: U.S. EIA, IEO-2014).

The number of vehicles on the world’s roads doubles between 2012 and 2040, but the increasingly widespread adoption of vehicle fuel-economy standards mitigates the expected impact on transport demand, which rises on average by 1.2% per year - a significantly slower pace than in recent decades, [3].



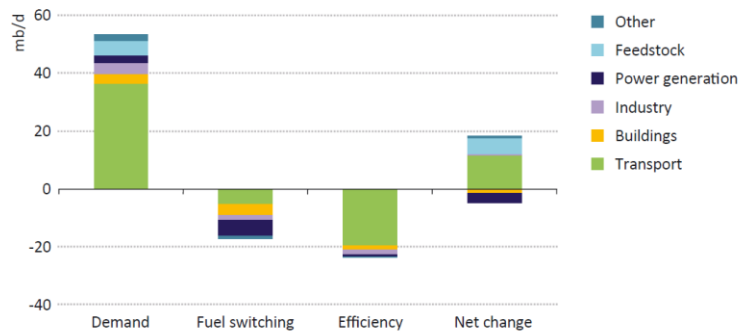
\*Other includes agriculture and non-energy use. Note: Total final consumption includes electricity and heat generated by the power sector.

Figure 4 - Change in energy demand by sector and region in the New Policies Scenario, 2012-2040 (source: IEA, WEO-2014).

All of the growth in transport demand comes from non-OECD countries, notably China; it declines in the OECD, where efficiency gains more than outweigh a modest expansion of the vehicle fleet (Figure 4). Oil-based fuels continue to dominate transport energy demand, although alternative fuels, diesel demand grows strongest and diesel overtakes gasoline as the dominant oil product in the transport

sector by mid-2030s, [3]. While oil still accounts for 85% of total transport demand in 2040, this is a lower share than today's 93%, as alternative fuels, such as natural gas, biofuels and electricity, gain ground. The deployment of alternative fuels is higher in OECD countries, where they account for more than 20% of total transport demand by the end of projection period, [3].

Without the impact of fuel switching and efficiency gains, the increase in oil demand implied by our projections (e.g. from increased vehicle ownership and rising industrial activity) would result in an increase in consumption of 53 mb/d by 2040 (Figure 5). Nevertheless, this - purely theoretical - increase is moderated in practice by the switch to alternative fuels (that determines a reduction of 17 mb/d) and by the adoption of more efficient technologies (that determines a reduction of 23 mb/d). In the New Policies Scenario, energy efficiency has a stronger impact on moderating oil demand growth than fuel switching in transport, while fuel switching plays a more important role in power generation and buildings, [6].



Note: This analysis uses a rolling decomposition technique on a sub-sector level to distinguish three effects: changes in the demand for energy services, such as mobility ("demand"), changes due to the switch from one fuel to another, e.g. from oil to gas in transport ("fuel switching"), and changes related to the use of more efficient equipment ("efficiency").

**Figure 5 - Impact of fuel switching and efficiency on the change in global oil demand by sector in the New Policies Scenario, 2013-2040, (source: IEA, WEO-2014).**

The strong use of fossil fuel results in a very strong impact in terms of greenhouse gas emissions: in the EU-28 in 2011, transport is responsible for around 20% of greenhouse gas (GHG) emissions making it the second largest GHG emitting sector after the energy industry. In addition, despite the fact that emissions from other sectors (energy industry, manufacturing, etc.) present a general decreasing

trend, those from transport have increased by 19% from 1990 to 2011. Emissions from the transport sector showed a continuous growth between 1990 and 2007; followed by a slight dip (-6%) between 2007 and 2011. However, this downward trend is considered to be mainly due to the economic recession.

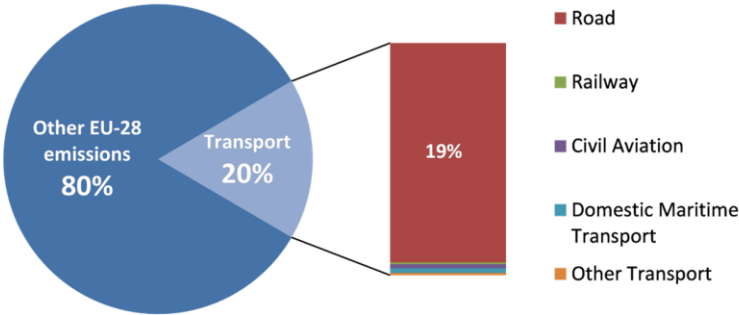


**Figure 6 - EU-28 GHG emissions of the transport sector (source: Eurostat Pocketbook, 2013).**

Over the 1990-2011 period, emissions from road transport and civil aviation grew by 21% and 17% respectively, while emissions from domestic maritime transport presented a 1% growth (Figure 6). In contrast, emissions from railway transportation fell by 46%. A breakdown by sector shows that road transport has dominated emissions from this sector throughout this period (94% in 2011), [7].

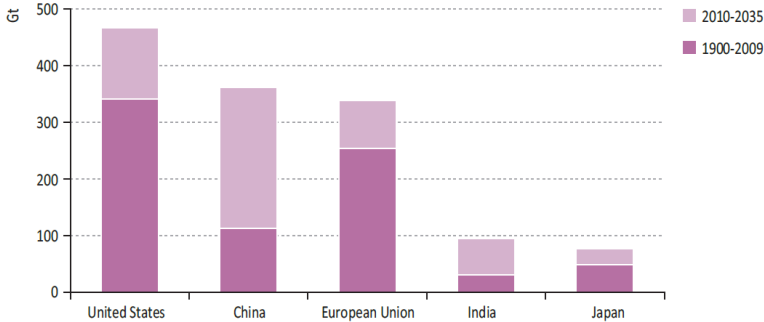


**Figure 7 - Cumulative energy-related CO2 emissions in selected countries and regions, 1900-2035 (source: IEA, WEO-2011).**

As reported in Figure 7, energy-related CO2 emissions are expected to rise in all sectors over the 2035, but the largest increase is expected

in power generation, where emissions increase by 2.3 Gt, and transport, where emissions increase by 2.1 Gt. These two sectors combined account for almost 75% of the increase in energy-related emissions.

## **1.2 Transport Systems for Sustainable Mobility**

People need to move around to secure basic human needs, but mobility is also a luxury, contributing to quality of life by enabling exploration, leisure and recreation. In the city, high quality mobility is a necessity for the success of other urban sectors, the creation of jobs, and plays a key role in cultivating an attractive environment for residents and business. The combined influence of population growth, demographic change and changing urban form leads to increasing demand for travel in city centers, suburbs and between the two. Demand for improved intercity mobility is also growing, to create faster and effective connectivity between settlements. As urban populations increase, existing and emerging cities face the challenge of meeting rising demands for efficient mobility within limited physical infrastructure capacity. As demand rises, so too do concerns about transportation as one of the leading contributors to global greenhouse gas emissions, congestion, noise and poor air quality in cities. Indeed, urban mobility is widely cited as one of the universal challenges faced by cities the world over, [8].

This growing demand converges with an inadequate supply of physical transport capacity in many cities, which can result in crowding, congestion, and an unpleasant experience of the city. In established cities, this problem is attributed to spatial constraints - which inhibit additional growth of transport networks - together with economic limitations on physical infrastructure maintenance and renewal. Meanwhile, in many developing cities the investments in infrastructure constructions are struggling to keep pace with the rapid rate of urban growth, [9].

Sustainable development meets the needs of the present generation without compromising the ability of future generations to meet their own needs. Thus, a sustainable transportation system allows the basic access and development needs of individuals, companies and society

to be met safely and in a consistent way with human and ecosystem health, and promotes equity within and between future generations. It is affordable, operates fairly and efficiently, offers a choice of transport mode, and supports a competitive economy, as well as balanced regional development. Sustainable mobility, also, limits emissions and waste within the planet’s ability to absorb them, uses renewable resources at or below their rates of generation, and uses non-renewable resources at or below the rates of development of renewable substitutes, while minimising the impact of the use of land and the generation of noise.

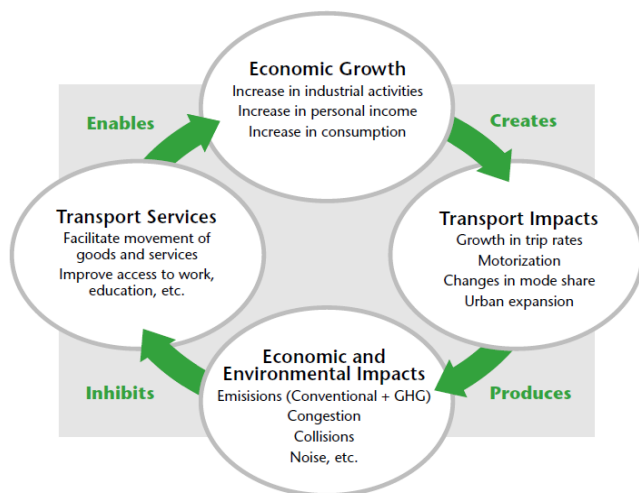


**Figure 8 - The challenges of making mobility sustainable (source: WBCSD - 2004).**

Figure 8 illustrates both the aspects of sustainable mobility - its benefits and its costs - as well as some of the relationships characterizing them - at least until the present. It also reveals points of leverage that, if exploited, can modify some of these relationships in ways that enhance mobility’s benefits and reduce its costs. First, transport services can be made more efficient, increasing the amount of economic growth supported by a given volume of transport services. Second, the level and composition of “induced” mobility demand can be channeled in ways that fulfill growing mobility needs but create fewer transport impacts. Third, the level of adverse economic and environmental impacts associated with any given level

of transport activity can be greatly reduced through significant technology shifts, [8].

### **1.2.1 Electrification of Urban Transport**

In the context of sustainable mobility, transportation electrification is an ideal way to cut down the air pollution while reducing the dependence on fossil fuels. In urban areas in particular, the electric carrier in urban transport can reduce air pollution in the cities, especially when it comes to local pollutants such as particulates, NO<sub>x</sub>, SO<sub>x</sub>, VOCs and ozone. The use of electric buses, trains and light trains can drastically improve the air quality, traffic congestion and noise pollution. Existing electrified transport systems represent an interesting option for governments seeking to increase mobility and choice for commuters. It is an efficient, high-capacity transport mode that can effectively co-exist with other forms of public transport.

Urban public transport systems powered by electricity can trace their origins to 1879 when Berlin launched the world's first electric suburban railway (S-Bahn), followed by electric trams in 1881 and electric trolleybuses a year later. Electric drivetrains are more efficient than the conventional ones due to their high-energy conversion efficiency. They also do not consume energy while at rest or coasting, and some of the energy lost when braking can be captured and used again: in fact, through regenerative braking it is possible capturing as much as one fifth of the energy normally lost during braking, [10].

Electric buses, which require neither great range nor speed and can be partially charged during their journeys as they stop for passengers, are seen as the most promising area for potential growth of green urban public transport. China is the world leader in developing battery electric buses. The southern city of Shenzhen has the world's largest zero-carbon fleet of all-electric buses and taxis, and plans to have 6000 electric buses in service by 2015, [11]. Trolleybuses are electric buses that use spring-loaded trolley poles to draw their electricity from overhead lines, generally suspended from roadside posts, as distinct from other electric buses that rely on batteries. Because they do not require tracks or rails, they are more flexible than trams and drivers can cross the bus lane, making the installation of a trolleybus system much cheaper.

In the 1960s, the tram saw a decline in favour of diesel driven buses, but the backlash in recent years against pollution and dependence on fossil fuels has seen a resurgence of interest in electric trams as another urban transport system that can carry large numbers of passengers efficiently without generating emissions at the point of use. Tram systems do not need vast financing compared with underground systems, which are typically four times more expensive to construct. However, in addition to its relative high cost, compared to that of buses or trolleybuses, the greatest disadvantage of the tram is its confinement to a set route by the wires and tracks it requires. The largest tram networks are in Melbourne, St Petersburg, Vienna, Berlin, Milan, Toronto, Budapest, Bucharest and Prague, while many cities in North America are exploring or planning tram systems, [11].

Market growth is mainly driven by new metro and electric light rail urban transport projects under way on most continents, from major cities in Asia and the Persian Gulf to North and South Africa and North American urban areas. A metro rapid transit system is an electric passenger railway in an urban area with a high capacity and frequency, typically located either in underground tunnels or on elevated rails above street level. It allows higher capacity with less land use, less environmental impact and a lower cost than typical light rail systems. Light rail systems use small electric-powered trains or trams that generally have a lower capacity and lower speed than normal trains to serve large metropolitan areas. They usually operate at ground level, but can include underground or overhead zones, [9].

With transport systems estimated to account for between 20% and 25% of world energy consumption and CO<sub>2</sub> (carbon dioxide) emissions, electric vehicles offer greater efficiency than their conventional counterparts, [3]. Several European countries, as well as the US, Japan, China and others, have recently announced bold plans for the introduction of electric vehicles. These include fiscal incentives, funding research on batteries and electric vehicles and plans for the deployment of a charging infrastructure. Major cities, such as London and Paris, have announced electric car-sharing systems, while public administrations and companies using large captive fleets are purchasing electric vehicles.

During operation, the energy efficiency of electric vehicles is much higher than that of conventional cars and they do not emit any CO<sub>2</sub> or other pollutants while driving. At the local level, improved air quality

and reduced noise are major advantages of electricity as a fuel. In particular, electric vehicle 'tank-to-wheels' efficiency is a factor of about 3 higher than internal combustion engine vehicles.

There are now four types of electric cars: battery electric vehicles (BEV), plug-in hybrid electric vehicles (PHEV), conventional hybrids electric vehicles (HEV) and hydrogen fuel cell powered (FCEV). BEVs runs entirely on a battery and electric drive train, without a conventional internal combustion engine. These vehicles must be plugged into an external source of electricity to charge their batteries. Plug-in hybrid vehicles run mostly on batteries that are charged by plugging into the power grid. They are also equipped with an internal combustion engine that can charge the battery and/or to replace the electric drive train when the battery is low and more power is required. Because PHEVs can be charges on the public network, they are often cheaper to run than tradition hybrids though the amount of savings depend on the distance driven on the electric motor alone, [12]. HEVs on the road today have two complementary drive systems: a gasoline engine and fuel tank and an electric motor, battery and controls. The engine and the motor can simultaneously turn the transmission, which powers the wheels. HEVs cannot be charged from the power grid. Their energy comes entirely from gasoline and regenerative braking. Finally, FCEVs are another type of electric vehicle expected to be widespread on the market in the next few years. Instead of storing and releasing energy like a battery, fuel-cell electric vehicles create electricity from the chemical reaction between hydrogen and oxygen that happen in the FC. Because of these vehicles' efficiency and water-only emissions, some experts consider these cars to be the best electric vehicles, even though they are still in development phases.

### **1.3 Tram, Metro and Light Railway Systems**

Urban congestion has focused attention on the need for improved public transportation. Many cities worldwide are recognizing that trams and light rail systems are effective in transporting large volumes of commuters efficiently and without detriment to the environment. As a result, transport authorities are opting either to restore their

existing light rail infrastructure or to construct complete new systems from scratch. Railway systems offering excellent economics, environmental performance, and punctuality are recognized as a core element of smart city development. Together with the pursuit of efficiency, safety, reliability, and energy savings, the concepts likely to prove key to the future of railways systems include making railways into a more attractive service business, [13]. The adoption of advanced information systems in stations, trains, as well as in the passenger's smartphone and other railway industry applications will help reduce the distance between public transport and private mobility perceived by users, even more encouraging their development in smart cities. At the United Nations Climate Change Summit in 2014, UIC (International Union of Railways) has presented the "Low Carbon Rail Transport Challenge", aimed to promote railway transport as a sustainable alternative to other modes of transportation with higher carbon intensity, such as road or aviation. The three main targets of UIC for world railways are to improve efficiency, to decarbonize power and to achieve a more sustainable balance of transport modes. In order to reach those goals, railways are developing the electrification of the infrastructure, improving load factors, procuring more efficient rolling stock, developing energy and traffic management systems and efficient driving, [13].

The key figures in the 2012 statistics shows the global contribution of rail to energy use and CO<sub>2</sub> emissions: railway systems were responsible for 0.6% of global energy consumption and less than 1% of global CO<sub>2</sub> emissions, while an energy share of 21% and a CO<sub>2</sub> share of 17% can be attributed to road transport, [13]. Even accounting for the much higher share of passengers transported by road versus by rail, the difference between road and rail energy use and emissions is striking. The rail sector's energy intensity has declined globally since 1975, achieving in 2012 about half of its original 1975 level for passenger and freight transport (Figure 9). Not only energy intensity has been improving, but the energy sources used in rail have also become cleaner since 1990, with the progressive phasing out of coal and the growing electrification of the sector, enhanced by the growing share of renewable electricity used in rail. This resulted in a drop in specific CO<sub>2</sub> emissions close to 60% for passenger and 41% for freight rail transport since 1975 (Figure 10).

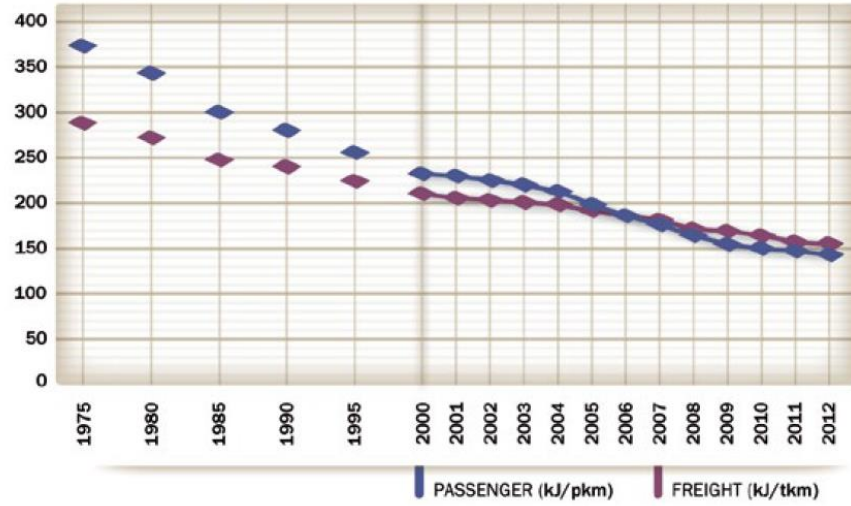


Figure 9 - Railway specific energy consumption, 1975-2012 (source: EIA, RH-2015).

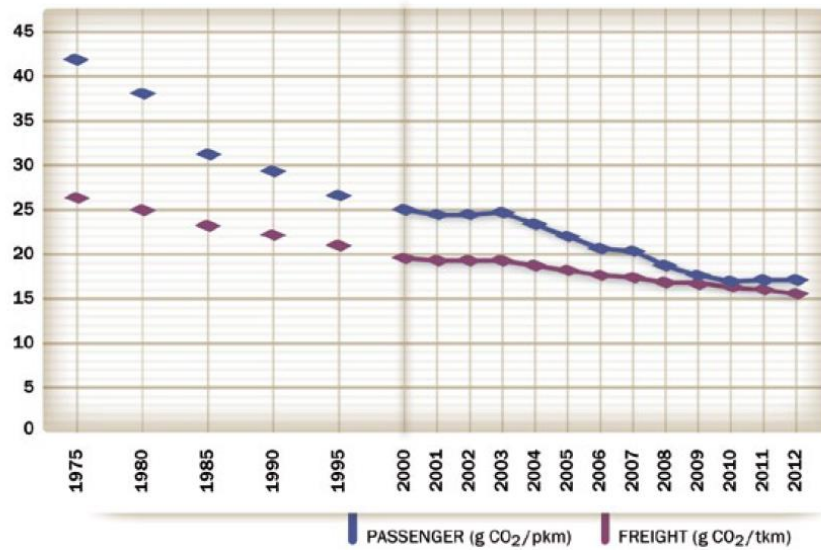


Figure 10 - Railway specific CO<sub>2</sub> emissions, 1975-2012 (source: EIA, RH-2015).

UIC sets internal targets to reduce specific final energy consumption (50% by 2030 and 60% by 2050) and specific average

CO<sub>2</sub> emissions from train operations (50% by 2030 and 75% by 2050), all relative to a 1990 baseline. UIC has also launched a “Modal Shift Challenge”, calling for investments that will increase the modal share of railways at the expense of high carbon transport. The target is increase the rail share of passenger transport up to 50% by 2030 and up to 100% by 2050, relative to a 2010 baseline; and for the rail share of freight land transport to be equal with road by 2030 and 50% greater than road by 2050, [13].

### 1.3.1 Sustainability in Electrified Transport Systems

As part of a wider industry and government agenda for sustainability and energy savings, the way in which the railway industry consumes energy has been researched. Enhancing energy efficiency enables the dual benefits of improving the economics of railway operators and of reducing GHG emissions (Figure 11). However, considering the energy efficiency opportunities available in the existing infrastructure and the upcoming expansion, there is immense scope to learn, adopt and upscale use of innovative energy efficiency technologies, solutions and best practices, [13].

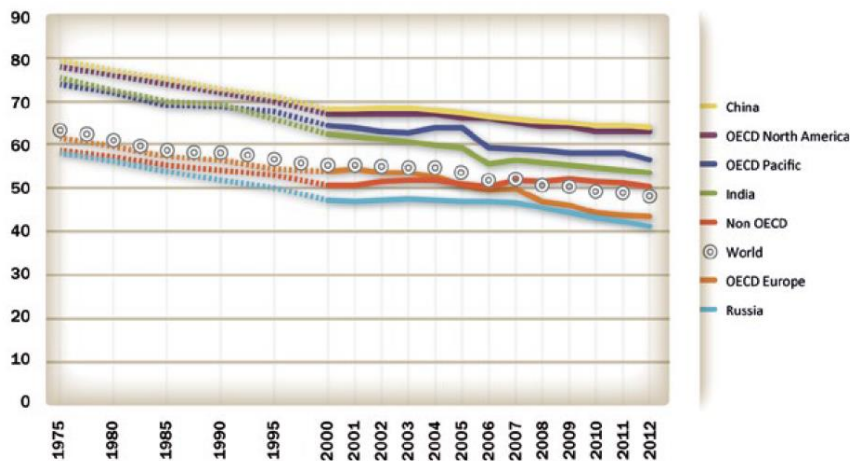


**Figure 11 - Evolution of electric intensity for passenger rail in selected countries and geographic areas, 1975-2012 (MJ/train-km) (source: EIA, RH-2015).**

The railway sector is considering or has already implemented several technological solutions that will facilitate energy efficiency

improvements in the next decades, such as installing energy meters, recovering energy from braking, implementing Driver Advisory Systems (DAS) or leveraging on better infrastructure management. An increasing number of trains are being equipped with technology to recover electric energy from braking, [14].

The energy recovered can be used both internally to the train for the operation of auxiliary systems (e.g. to power lights, air conditioning, door opening and closing, or to charge a battery for later usage when possible) and externally. The recovered electricity can be sent back to the grid and it is used to power other trains in the same section of catenary. In the absence of special equipment, part of the energy recovered is lost by dissipation when the electricity both cannot be stored or used inside the train and when there is no train accelerating in the same section of the grid. In these circumstances, specialized equipment can be used to boost the efficiency of energy recovery from braking: reversible substations, for example, are able to collect the recovered electricity and provide it to the power grid.

On the other hand, railway infrastructure managers play a key role in improving energy efficiency by working closely with railway operators. By allowing trains to ride unhindered and at the most efficient speed, well-managed infrastructure can save a significant amount of energy. Infrastructure managers are adopting advance traffic management systems, which can perform various scheduling and logistic operations and help reduce energy consumption. For example, they can detect and avoid possible conflicts between train journeys, which could cause delays and waste energy due to avoidable braking and stopping of trains; they can assist infrastructure managers in compiling energy-efficient timetables where train trips are optimised, both for passengers (combining the right departure and arrival times) and for freight (to minimise empty trips), [14].

Finally, the human factor has also a significant impact on the energy efficiency of trains. There are a series of operational measures and best practices that can reduce energy consumption, such as turning off the traction power when acceleration is not needed. Training programs for drivers can lead to several percentage points of reduction in energy consumption. The use of additional tools like DAS can further augment the energy performance of the driver. The DAS monitors relevant journey characteristics: upward and downward

slopes, stops and possible leeway in the timetable, and can also interact with a central system that communicates events happening on the road. After analysing these parameters, the system suggests changes in driving behaviour to reduce energy consumption.

## **1.4 E-Mobility: Electric Vehicles Future Penetration**

Electric Mobility is an increasingly popular term used to describe the electrification of transport. More specifically, it describes vehicles that are partly or fully powered by an electric motor. E-mobility, together with alternative fuels such as ethanol and biogas, represents a broad transition toward cleaner transport fleets. The current interest in electric vehicles (EVs) can be attributed to the interaction of a number of favourable environmental, political and technical conditions. Local pollution, global climate change, concern over the supply and security of fossil fuels, rising fuel prices and an automotive industry struggling in the wake of global economic downturn, all combine to create favourable conditions for increased investment in electric mobility. As result of these issues, many countries have introduced legislation and implemented specifically targeted programmes designed to encourage the development and uptake of more efficient, alternative-fuelled vehicles. At the same time, advances in battery technology have enabled EVs to be considered a viable and promising alternative to the internal combustion engine (ICE) vehicle that dominates the passenger vehicle market today, [12].

The world is moving away from a dependence on a single ICE power train model to a portfolio of power trains designed for every possible driving scenario. E-mobility is characterized by a diversification of technological solutions designed to meet individual mobility requirements at a specific place and time: according to vehicle size and travel distance requirements, a number of different drive technology solutions can be applied. No single power train set-up can satisfy all of the different economic, environmental and performance factors at play. Moreover, a number of different technologies will likewise have to undergo a process of evolution until

all vehicles are driven purely by electric means. This means that the conventional ICE still has a bridging role to play - for some time to come - in a number of hybrid EVs scenarios, [15].

In addition to zero tailpipe emissions, electric motors feature a number of other advantages over the internal combustion engine. They contain far less moving parts that contributes to reduced manufacturing costs and lower maintenance requirements. Electric motors are also far more efficient at converting primary energy into vehicular propulsion, with an on-board average efficiency of up to 80% compared to a maximum of 30% for internal combustion engines, where much of the energy is lost in the form of heat. The major disadvantages of EVs - namely high cost and limited range - can be directly attributed to an immature battery market, [12]. Expensive to produce, battery costs are also negatively affected by low manufacturing volumes, and this in turn is reflected in the premium purchase price demanded of EVs. The disadvantages affecting today's EVs are not expected to be an enduring feature of electric mobility, as large amounts of capital is being invested into battery R&D in the hope of a solution. Steady improvements are being achieved in battery storage capacity and the anticipated scaling up of manufacturing volumes will effectively drive prices down.

### **1.4.1 Market Growth & CO<sub>2</sub> Reduction**

The BLUE Map scenario sets an overall target of a 50% reduction in global energy-related CO<sub>2</sub> emissions by 2050 compared to 2005 levels, [15]. Transportation contributes to this overall reduction by cutting CO<sub>2</sub> emissions levels in 2050 to 30% below 2005 levels. This reduction is achieved in part by accomplishing an annual sale of approximately 50 million light-duty EVs and 50 million PHEVs per year by 2050, which is more than half of all LDV sales in that year. Achieving the BLUE Maps requires that EV/PHEV technologies for LDVs evolve rapidly over time, with very aggressive rates of market penetration once deployment begins (Figure 12). By 2030, sales of EVs are projected to reach 9 million and PHEVs are projected to reach almost 25 million. After 2040, sales of PHEVs are expected to begin declining as BEVs achieve even greater levels of market share. The

ultimate target is to achieve 50 million sales of both types of vehicles annually by 2050, [15].

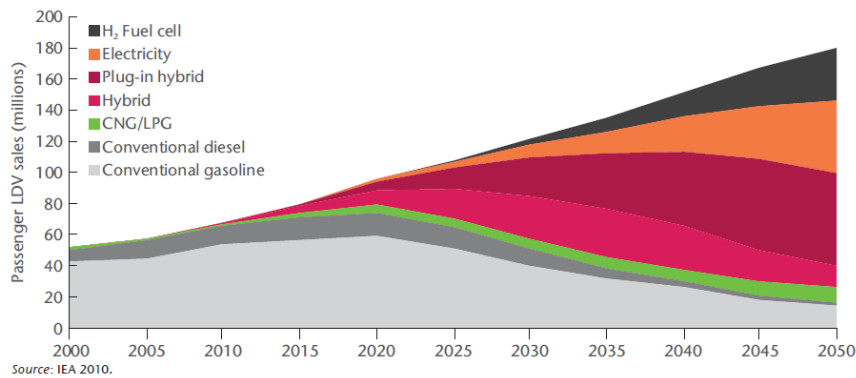


**Figure 12 - Annual light-duty vehicle sales by technology type, BLUE Map scenario (source: IEA, Technology Roadmap-2013).**

**Table 1 - Global EV and PHEV sales in BLUE Map, 2010-2030 (millions per year) - IEA 2010.**

|              | 2010       | 2015       | 2020       | 2025        | 2030        | 2035        | 2040        | 2045        | 2050         |
|--------------|------------|------------|------------|-------------|-------------|-------------|-------------|-------------|--------------|
| <b>PHEV</b>  | 0.0        | 0.7        | 4.9        | 13.1        | 24.6        | 35.6        | 47.7        | 56.3        | 59.7         |
| <b>EV</b>    | 0.0        | 0.3        | 2.0        | 4.5         | 8.7         | 13.9        | 23.2        | 33.9        | 46.6         |
| <b>TOTAL</b> | <b>0.0</b> | <b>1.1</b> | <b>6.9</b> | <b>17.7</b> | <b>33.3</b> | <b>49.5</b> | <b>70.9</b> | <b>90.2</b> | <b>106.4</b> |

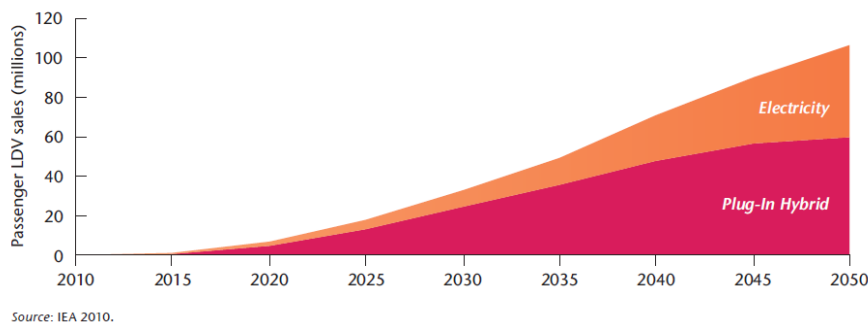


**Figure 13 - Annual global EV and PHEV sales in BLUE Map scenario (source: IEA, Technology Roadmap-2013).**

In order to achieve the deployment targets in Table 1 and Figure 13, a variety of EV and PHEV models with increasing levels of production is needed. Figure 14 demonstrates a possible ramp-up in

both the number of models offered and the annual sales per model. This scenario achieves 100'000 units of production per model for both EVs and PHEVs by 2020, [15]. This rate of increase in production will be extremely challenging over the short time frame considered (about ten years). However, the number of new models for EVs and PHEVs in Figure 14 easily fits within the total number of new or replacement models expected to be offered by manufacturers around the world over this time span (likely to be hundreds of new models worldwide) and typical vehicle production levels per model.

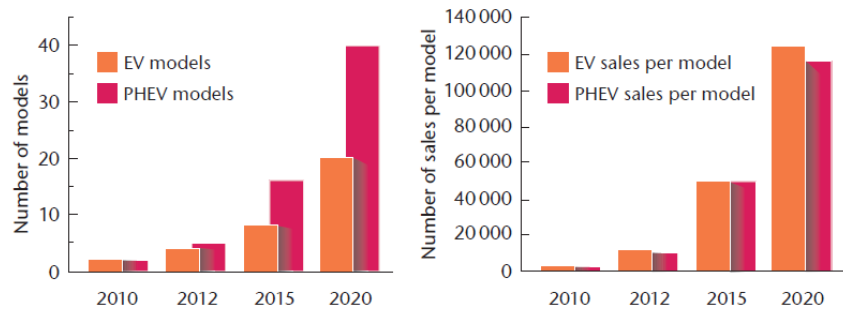


**Figure 14 - EV/PHEV number of models offered and sales per model through 2020 (source: IEA, Technology Roadmap-2013).**

On a regional basis, Figure 15 offers a plausible distribution of EV/PHEV sales by region, consistent with this roadmap's global target of achieving an annual sale of approximately 50 million light duty EVs and PHEVs by 2050. Regional targets reflect the expected availability of early-adopter consumers and the likelihood that governments will aggressively promote EV/PHEV programs.

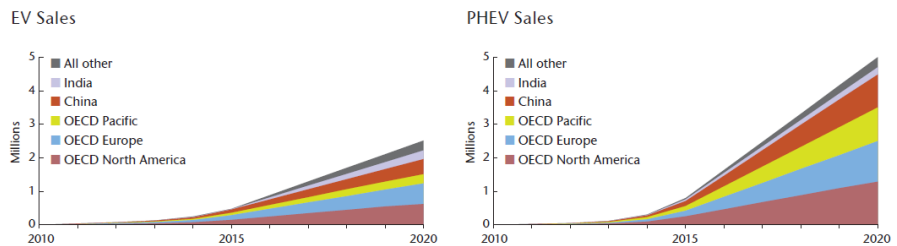


**Figure 15 - EV/PHEV total sales by region through 2020 (source: IEA, Technology Roadmap-2013).**

EV and PHEV sales by region are also based on assumed leadership by OECD countries, with China following a similar aggressive path. Sales in other regions are assumed to follow with a market share lag of five to ten years, [15]. The estimates of EV and PHEV sales and use in this roadmap are based on achieving the BLUE Map scenario's 2050 CO<sub>2</sub> reduction targets, which can only be met with the enactment of aggressive policies. CO<sub>2</sub> reductions also depend heavily on changes in electricity generation; BLUE Map targets require the nearly full decarbonisation of electricity generation around the world by 2050.

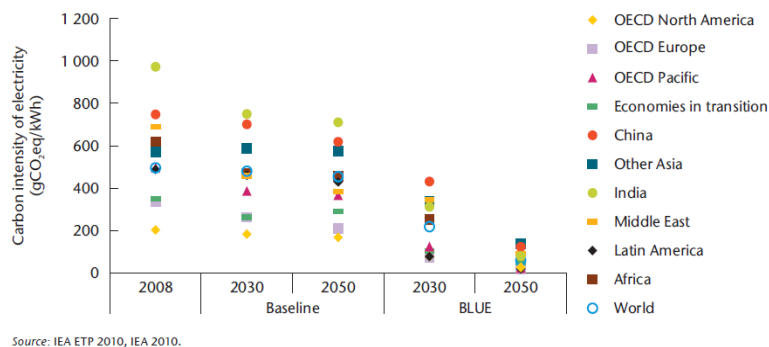


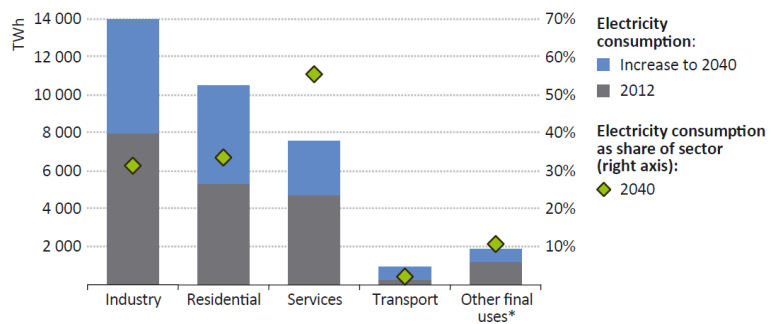
**Figure 16 - CO<sub>2</sub> intensity of electricity generation by region, year and scenario (source: IEA, Technology Roadmap-2013).**

As shown in Figure 16, the CO<sub>2</sub> intensity of electricity generation in the BLUE Map scenario drops steadily over time until, by 2050, all regions have nearly decarbonised their electricity, [15]. This steady decrease is an important assumption; if the achievement of low CO<sub>2</sub> electricity generation around the world does not occur in the 2030 to 2050 timeframe, as shown in Figure 16, the CO<sub>2</sub> benefits of EVs and PHEVs will be much lower.

Overall, given the BLUE Map scenario projections for the numbers of EVs and PHEVs deployed in the locations specified, and assuming that these vehicles replace conventional gasoline vehicles (which themselves improve over time in the baseline), about 0.5 billion tonnes of CO<sub>2</sub> are projected to be saved per year worldwide in 2030, and about 2.5 billion tonnes are projected to be saved worldwide in 2050, [15].

## 1.5 Sustainable Transportation into Modern Power Systems

Electric transport modes such as electric light rail, trolley, electric buses and EV fleets are power demanding transport modes and are likely to add significant pressure on the power system (Figure 17), including the local power utilities, [16].



\* Includes other energy sector and agriculture.

**Figure 17 - World electricity consumption by sector in the New Policies Scenario (source: IEA, WEO-2014).**

Robust networks are vital to delivering electricity reliably to consumers. Reinforcement and expansion of network capacity will be needed in the future to accommodate demand growth, integrate greater renewables-based generation, improve access to electricity in developing countries, facilitate the use of electricity in road transport and increase electricity trade across borders. Indeed, transmission and distribution infrastructure accounts for 42% of all power sector investment over the 2040 period, [3]. At global level, the share of electricity use in each sector increases over the 2040 period. In particular, the fastest rate of expansion in percentage terms is the transport sector, primarily due to the increasing take up of electric vehicles (plug-in hybrid and battery-electric vehicles), but electricity's share of total transport energy demand still reaches only 2.4%, compared with 1% at present, [3].

Electrified urban railways play an important role for public transportation in smart cities; but to serve such a mass public transport system, the reliability of the whole power network is significant for the full performance of the urban railway system. An electrified railway line resembles a typical power distribution system but the major difference is the changes in the positions of the trains called as the frequently moving loads. Power demand varies over a wide range and a load may even become a power source when regenerative braking is allowed. Other factors such as train speed, traffic and service schedule and track layout have also great influence on the power demand of the electrified railway system, [17]. The electrical power system feeding the railway should be able to keep the voltages at the train sets in the admissible range and the conductor currents and transformer powers smaller than their rated values. The overload problems of the railway power system due to the increasing transport demand in the smart cities should be solved through load flow analysis which can lead to highlight any critical issues about the ratings of the transformers and feeder cables and enhancing the operation efficiency of the power system. The current power substations were designed so that sufficient capacity can be provided for the normal operation and the scheme of load transfer can be implemented for the emergency condition when only one outage occurs, [17].

Grid issues have also surfaced as a result of the EVs charging station installations. Due to the lack of a large-scale EV charging infrastructure, many EVs are currently being charged at the EV owners' home, which can draw between 3.3-20 kW from the grid equivalent to adding up to three houses onto the grid, (Figure 18). In many cases, local grids sized for smaller electrical loads would struggle with the rapid addition of such new electric loads. The issue can be accentuated because most EV sales are not evenly distributed across regions but instead occur in clustered markets, which feel the bulk of the impact, [18].

Most of the consumers need their EVs' batteries to be charged as soon as they get home after their working hours. However, if all batteries start charging at the same time, assuming that they are at fully discharged state, the peak demand for the electrical grid will increase, the distribution transformer would be overloaded, the power quality and the reliability of the whole system would be degraded.

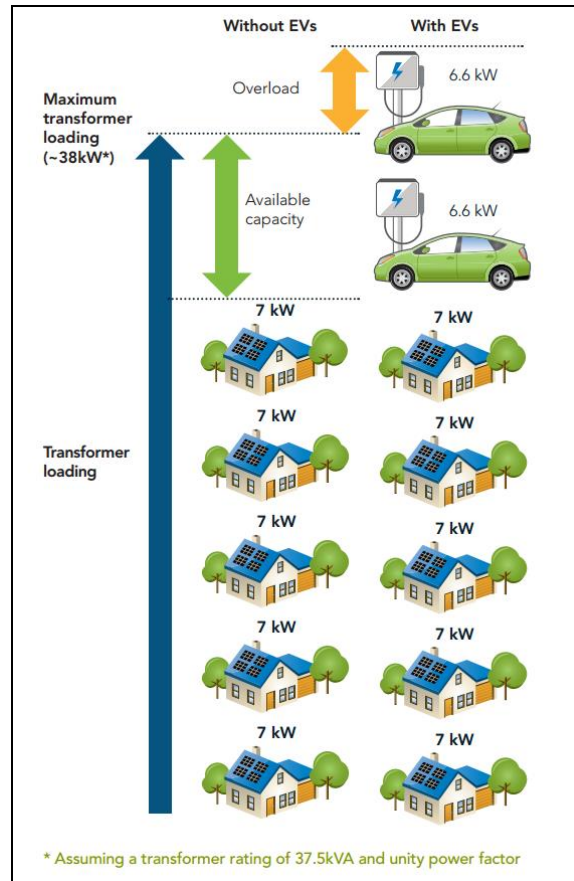


**Figure 18 - Potential Transformer Overloading (source: [20]).**

To overcome these issues, utilities need to reinforce their generation, transmission, and distribution infrastructure. Another recommended solution is that the utilities would either apply financial incentives for off-peak charging or utilize EVs' smart charging that enables communication between utilities and vehicles to control charging pattern, [19].

Smart Grid (SG) technologies offer a potential solution to these problems, and, in so doing, contribute to the establishment of a power system that is more energy efficient, more secure and more sustainable from a growing base of renewable resources. Smart grids allow for better co-ordination of the needs and capabilities of all generators, grid operators, end-users and electricity market

stakeholders in operating all parts of the system as efficiently as possible, minimising costs and environmental impacts while maximising system reliability, resilience and stability, [20]. The process of “smartening” the electricity grid, which has already begun in many regions, involves significant additional upfront investments, though this is expected to reduce the overall costs of electricity supply to end users over the long term. Smart-grid technologies are evolving rapidly and will be deployed at different rates around the world, depending on local commercial attractiveness, compatibility with existing technologies, regulatory developments and investment frameworks.

The most important aspect of the railway SGs is the improvement of controllability that can be achieved, which makes it possible to adapt the operation in real time to the oncoming events originated inside or outside the domain of the railway power system (RPS). Because of their relative size, RPSs have an impact on the T&D grids where are connected, which has to be carefully analyzed to avoid nuisances to other customers. Nevertheless, for the same reason, they can also efficiently help the grid operator performing an appropriate operation, [21]. Here are some examples of the benefits that will be possible with the adoption of SG technologies:

- when an incident occurs in the T&D grid and its capacity has been reduced temporarily, the T&D grid operators can prioritize other customers and ask the railway to reduce its consumption from a specific set of substations: the railway SG allows it;
- in a conventional railway system, the electrical energy generated while train stop is fed immediately into the overhead power lines that has a very limited capacity for absorbing a sudden flood of electrical energy. As a result, the voltage of the third rail rises considerably. By using SG technologies in railway, the power can be efficiently recovered, and is fed back into the regional power grid;
- with SG technologies, in the future, railways could also provide ancillary services (e.g., secondary regulation) to help balance the generation and the demand in an electrical system.

Smart grids will also provide charging facilities for electric vehicles. Home chargers deliver efficient, low power vehicle charging that can refill a battery during the night, reaching full capacity before morning. Charging overnight ensures that the load on the grid is low, and the car is refilled economically using low cost night rate power. Public chargers are semi-fast charging solutions that can charge a battery in a few hours while the driver is at work, or be used to keep the car charged up during everyday activities such as shopping or dining out. Future ultrafast chargers will allow a ‘fuel stop’ equivalent for EVs, charging the car in the shortest possible time. Combined with the latest battery technologies, this could allow a full recharge in less than five minutes. These chargers will be installed in highway rest areas and in convenient city refueling points.

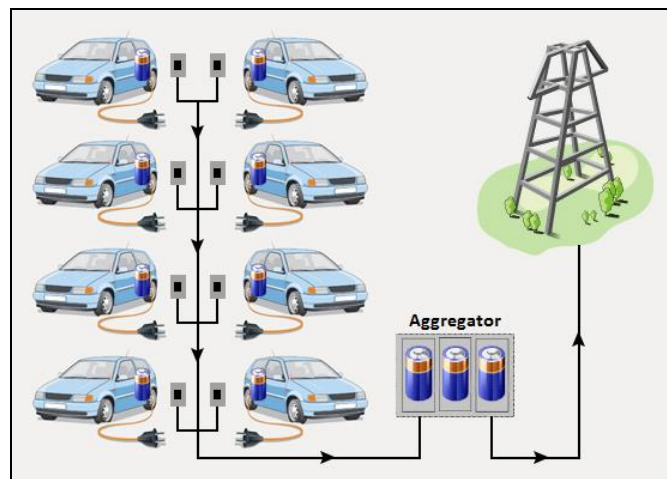


**Figure 19 - Vehicle to Grid Concept**  
(source: <http://www.jarman-international.com/>)

The most conventional charging scheme is to plug in the vehicle and get it charged like any other regular load. This is often referred to as dumb charging. When using dumb charging, obviously no active power charging control is used. Smart charging schemes allow the vehicle to be charged when the grid allows or needs it to. To make this charging scheme possible, there have to be communications between the grid and the vehicle. The smart grid concept with advanced metering infrastructure facilitates this application. Controlled charging architectures allow for time shifting and the reduction of peak power on the grid. In particular, demand side management reducing charging

rate at peak load and rescheduling charging process at appropriate time such as low grid load can be used to solve these issues, [22].

In the longer term, there may be some potential for smart-grid technology to enable EVs to be used as distributed storage devices, either to feed the energy stored in their batteries back into the system when needed (vehicle-to-grid, V2G) or for use within the home or office (vehicle-to-home, or V2H). Vehicles are parked an average of 95% of the time, providing ample opportunity for their batteries to be used for V2G supply. This can help to reduce electricity system costs by providing a cost-effective means of providing regulation services, spinning reserves and peak-shaving capacity. EV batteries may be particularly useful in handling sudden, very brief surges in load, such as during television breaks during or just after major sporting events. When an EV owner has no immediate need to use his vehicle, he may be willing to feed power into the grid if the price obtained for the power is high enough (Figure 19). With V2G, power supply to the grid would need to be metered separately from the power consumption in the home. The total storage capacity potentially available for V2G is a function of the number of EVs and the capacity of the batteries that fuel them; the capacity of BEVs is typically much higher than that of PHEVs, [20].

## References

- [1] International Energy Agency (IEA), “World Energy Outlook 2011”, available on line at url <http://www.worldenergyoutlook.org/weo2011/>
- [2] Oak Ridge National Laboratory, “Transportation Energy Data Book”, Edition 33 Released July 31, 2014, available on line at url [http://cta.ornl.gov/data/tebd33/Edition33\\_Full\\_Doc.pdf](http://cta.ornl.gov/data/tebd33/Edition33_Full_Doc.pdf)
- [3] International Energy Agency (IEA), “World Energy Outlook 2014”, available on line at url <http://www.worldenergyoutlook.org/weo2014/>
- [4] International Energy Agency (IEA), “Key World Energy Statistics”, 2015, available on line at url [https://www.iea.org/publications/freepublications/publication/KeyWorld\\_Statistics\\_2015.pdf](https://www.iea.org/publications/freepublications/publication/KeyWorld_Statistics_2015.pdf)
- [5] U.S. Energy Information Administration (EIA), “International Energy Outlook 2014”, available on line at url [http://www.eia.gov/forecasts/ieo/pdf/0484\(2014\).pdf](http://www.eia.gov/forecasts/ieo/pdf/0484(2014).pdf)
- [6] International Energy Agency (IEA), “Energy Technology Perspective - Scenarios & Strategies to 2050”, 2010, available on line at url <https://www.iea.org/publications/freepublications/publication/etp2010.pdf>

- [7] Eurostat, Energy, transport and environment indicators, Pocketbook ISSN 1725-4566, 2013.
- [8] C. Aoun, “Smart Cities cornerstone series - Urban Mobility in the Smart City Age”, Schneider Electric, 2014.
- [9] The International Council on Clean Transportation (ICCT), “Global Transportation Energy and Climate Roadmap”, Nov. 2012 available on line at url <http://www.theicct.org/sites/default/files/publications/ICCT%20Roadmap%20Energy%20Report.pdf>.
- [10] International Energy Agency (IEA), “EV City Casebook”, 2014, available on line at url [https://www.iea.org/topics/transport/subtopics/electricvehicles/initiative/EVI\\_2014\\_Casebook.pdf](https://www.iea.org/topics/transport/subtopics/electricvehicles/initiative/EVI_2014_Casebook.pdf)
- [11] Federal Ministry for Economic Cooperation and Development (BMZ), “Urban Transport and energy Efficiency”, module 5h, 2012 available on line at url [http://www.sutp.org/files/contents/documents/resources/A\\_Sourcebook/SB5\\_Environment%20and%20Health/GIZ\\_SUTP\\_SB5h\\_Urban-Transport-and-Energy-Efficiency\\_EN.pdf](http://www.sutp.org/files/contents/documents/resources/A_Sourcebook/SB5_Environment%20and%20Health/GIZ_SUTP_SB5h_Urban-Transport-and-Energy-Efficiency_EN.pdf)
- [12] International Energy Agency (IEA), “Global EV Outlook - Understanding the Electric Vehicle Landscape to 2020”, 2013, available on line at url [https://www.iea.org/publications/globalevoutlook\\_2013.pdf](https://www.iea.org/publications/globalevoutlook_2013.pdf)
- [13] International Energy Agency (IEA), “Railway Handbook 2015 - Energy Consumption and CO<sub>2</sub> Emissions”, 2015, available on line at url [http://www.uic.org/IMG/pdf/iea-uic\\_2015-2.pdf](http://www.uic.org/IMG/pdf/iea-uic_2015-2.pdf)
- [14] International Energy Agency (IEA), “Transport, Energy and CO<sub>2</sub>”, 2009, available on line at url <https://www.iea.org/publications/freepublications/publication/transport2009.pdf>
- [15] International Energy Agency (IEA), “Technology Roadmap - Electric and plug-in hybrid electric vehicles”, 2011, available on line at url [https://www.iea.org/publications/freepublications/publication/EV\\_PHEV\\_Roadmap.pdf](https://www.iea.org/publications/freepublications/publication/EV_PHEV_Roadmap.pdf)
- [16] A. Grenier, S. Page, “The impact of electrified transport on local grid infrastructure: A comparison between electric cars and light rail”, in *Elsevier Energy Policy*, Vol. 49, Oct. 2012, pp. 355-364.
- [17] F. Shahnia, S. Tizghadam, S. H. Hosseini, “Power Distribution System Analysis of Urban Electrified Railways”, available on line at url [http://www.emo.org.tr/ekler/16e5cf0acb7e553\\_ek.pdf](http://www.emo.org.tr/ekler/16e5cf0acb7e553_ek.pdf)
- [18] SilverSpring Networks, “How the Smart Grid Enables Utilities to Integrate Electric Vehicles”, whitepaper, 2013, available on line at url <http://www.silverspringnet.com/wp-content/uploads/SilverSpring-Whitepaper-ElectricVehicles.pdf>
- [19] U.S. Department of Energy (DOE) - “Plug-in Electric Vehicle Handbook for Fleet Managers”, April 2012, available on line at url [http://www.afdc.energy.gov/pdfs/pev\\_handbook.pdf](http://www.afdc.energy.gov/pdfs/pev_handbook.pdf)
- [20] T. Morgan, “Smart Grids and Electric Vehicles: Made for Each Other?”, in *OECD - International Transport Forum* - discussion paper, 2012.

- [21] E. Pilo de la Fuente, S. K. Mazumder, I. G. Franco, "Railway Electrical Smart Grids", in *IEEE Electrification Magazine*, September 2014, available at url [http://www.ece.uic.edu/~mazumder/railway\\_electrification\\_magazine.pdf](http://www.ece.uic.edu/~mazumder/railway_electrification_magazine.pdf).
- [22] U.S. Department of Energy (DOE), "Evaluating Electric Vehicle Charging Impacts and Customers Charging Behaviors - Experiences from Six Smart Grid Investment Grant Projects", December 2014, available on line at url <http://energy.gov/sites/prod/files/2014/12/f19/SGIG-EvaluatingEVcharging-Dec2014.pdf>

## Chapter 2

# Smart Grids: Power Systems in Smart Cities

The load increasing, aging infrastructures and equipment, as well the widespread distributed energy generation lead to highly utilized networks during peak load conditions. In addition, to the high power system loading, other technical challenges for ensuring reliable energy supply include the emerging new loads (e.g. from hybrid/electric vehicles, energy storage systems and demand response programs).

Addressing these challenges in traditional power systems by increasing and upgrading network capacity entails costly and time-intensive interventions. However, the *Smart Grid* concept enables new ways of operating power systems, improving reliability, security, and efficiency of the electric grid through a dynamic optimization of grid operations and resources. The Smart Grid enables for adaptation of electricity demand to grid and market conditions, automatic grid reconfiguration to prevent or restore outages, and the safe integration of distributed generators, electric vehicles and large-scale electrified transport systems. In particular, the charging behaviours of various EV users as well distributed generation by renewable energy sources have some uncertainties elements.

In power systems, problems that treat the uncertainty with the classical probabilistic approach can be critical because in many cases, there are not enough data to build reliable probabilistic distributions, and practical applications suffer the lack of information. In fact, often it is necessary to take into account both aleatoric and epistemic effects, so that the uncertainty can be modelled by *possibility distributions*.

This chapter proposes a solution method for an optimal generation rescheduling and load-shedding (GRLS) problem in microgrids in order to determine a stable equilibrium state following overloads or outages. To address this problem taking into account generation and load uncertainty, a new solution methodology based on the use of fuzzy numbers is proposed. The purpose of Section 2.1 is to provide a brief overview of smart grids and its role in the future development of the power systems. Section 2.2 reviews the reliability impact due to unexpected outages of generation or sudden increase in demand, whereas Section 2.3 deals with the main technical solutions to better manage distribution systems in case of congestion or outages in one or more distribution lines. Following, Sections 2.4 briefly presents the possibility theory and fuzzy set theory used to describe the uncertainty in power systems. Mathematical formulation of the GRLS problem and the proposed solution algorithm are illustrated in Section 2.5. Finally, Section 2.6 show and discuss simulations results carried out by using a real case study data.

## 2.1 The Smart Grid Concept

The development of the smart grid concept is an evolutionary process that happens over time, and not in a single step. Often the deployment of smart grid technologies is referred to as *smartening the grid* or *modernizing the electricity system*. From a starting point of an existing grid, or a construction/extension of new networks, the deployment of smart grid technologies is not a goal in itself, but rather an enabler to the provision of secure, reliable, clean, economic electricity required by end-users. Numerous definitions seek to describe smart grids: the International Energy Agency (IEA) offers the following one, [1].

*A smart grid is an electricity network that uses digital and other advanced technologies to monitor and manage the transport of electricity from all generation sources to meet the varying electricity demands of end-users. Smart grids co-ordinate the needs and capabilities of all generators, grid operators, end-users and electricity market stakeholders to operate all parts of the system as efficiently as possible, minimizing costs and environmental impacts while maximizing system reliability, resilience and stability.*

A smart grid is an electricity network that incorporates a suite of information, communication and other advanced technologies to monitor and manage the transport of electricity from all generation sources to meet the varying electricity demands of end-users. Smart grids allow for better co-ordination of the needs and capabilities of all generators, grid operators, end-users and electricity market stakeholders in operating all parts of the system as efficiently as possible, minimizing costs and environmental impacts while maximizing system reliability, resilience, and stability [1]. The process of *smartening* the electricity grid, which has already begun in many regions, involves significant additional upfront investment, though this is expected to reduce the overall cost of electricity supply to end users over the long term. Smart-grid technologies are evolving rapidly and will be deployed at different rates around the world, depending on local commercial attractiveness, compatibility with existing technologies, regulatory developments, and investment frameworks. The evolutionary nature of this process is stylistically illustrated in Figure 20.

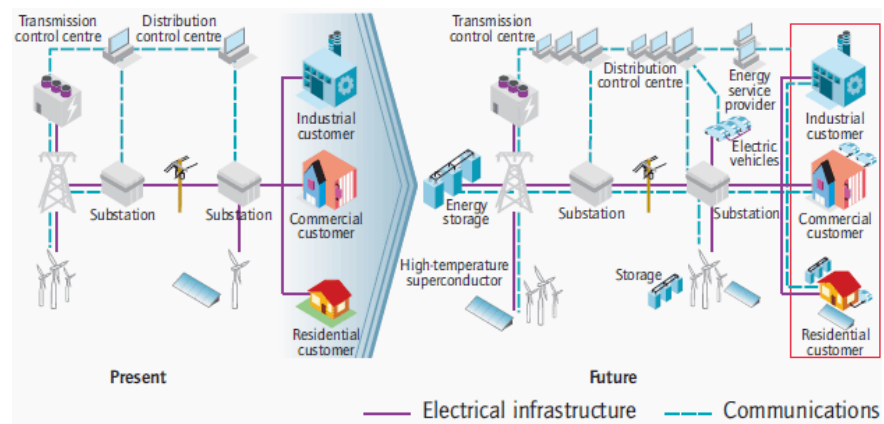


**Figure 20 - Evolutionary character of smart grids (source: IEA-2011).**

Electricity systems worldwide face a number of challenges, including ageing infrastructure, continued growth in demand, shifting load patterns (including changes resulting from the increased use of electric vehicles), the need to integrate new sources of supply and the variability of some sources of renewables-based supply. Smart-grid technologies offer a cost-effective means of helping to meet these challenges and, in so doing, contribute to the establishment of an

energy system that is more energy efficient, secure, and more sustainable. They do this by:

- enabling and incentivizing customers to adjust their demand in real time to changing market and network conditions;
- accommodating all generation sources and storage options;
- tailoring power quality to customer needs;
- optimizing the utilization and operating efficiency of generation, transmission and distribution assets;
- providing resiliency to unplanned supply disruptions and outages;
- accommodating variable generation technologies such as the wind and solar power is a major driver of smart-grid investment;

The importance of such technologies is growing rapidly in many regions in response to the need to reduce greenhouse-gas emissions and reliance on imports of fossil fuels. According to the IEA’s latest World Energy Outlook, they will account for 37% of the net increase in generating capacity worldwide between 2009 and 2035 on planned policies [2].

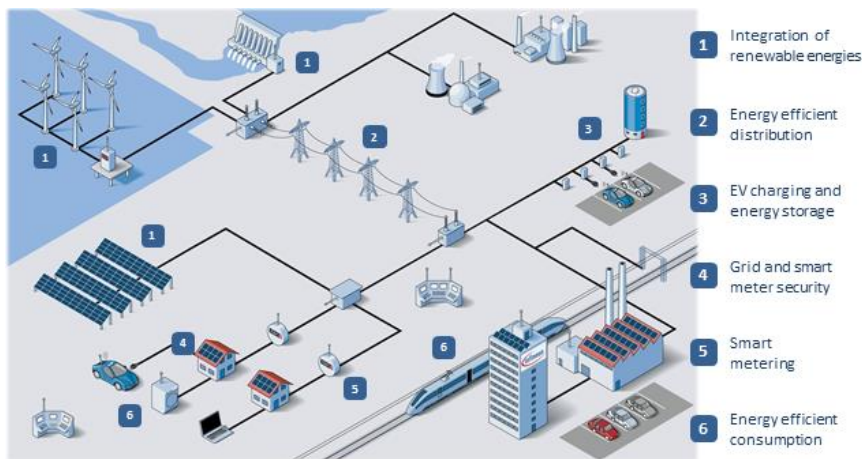


Figure 21 - An interconnected and integrated electricity system of the future (source: Infineon).

As the share of variable generation increases, it becomes increasingly difficult to ensure the reliable and stable management of the electricity system where it relies solely on conventional grid architecture and technology. Smart grids can support greater deployment of variable generation technologies by providing operators with real-time system information that enables them to manage the generation, load and power quality, thus increasing system flexibility and maintaining stability and balance (Figure 21).

### 2.1.1 The Smart Grid Technologies

There are a number of different types of smart-grid technology, all of which make use of information and communication technology (hardware and software) such as internet and radio, cellular and cable networks (Table 2), [3]. Smart grids involve the gathering, by means of sophisticated metering systems, and exchange of large amounts of information in real time at different levels of the supply chain. Sensors can be installed on each device on the network (such as power meters, voltage sensors, and fault detectors) to gather and transmit data while two-way digital communication between the device in the field and the utility's network operations center, which enables the utility to adjust and control each individual device remotely. A key feature of the smart grid is automation technology, which lowers the cost and increases the efficiency of load-management operations (for example, automatic adjustments to the operation of the power system in response to a sudden breakdown of one component). Importantly, information flows between suppliers and end users can also be bi-directional, allowing both parties to adjust their behavior in response to changes in pricing at short notice.

The various smart-grid technology areas - each consisting of sets of individual technologies - span the entire grid, from generation through transmission and distribution to the different categories of the electricity consumer. Not all the different technology areas need to be installed to increase the *smartness* of the grid, which can be accomplished incrementally over time. Companies manufacturing smart-grid equipment or developing software include technology giants, established communication firms and new start-ups.

Electric vehicles charging infrastructure could form an important part of the smart grid of the future. This includes physical charging facilities (connectors and meters), as well as billing, scheduling and other intelligent features for smart charging during off-peak periods. As the share of electric vehicles charging in overall electricity load increases, the grid would need to incorporate other assets in order to enhance the capacity to provide power-system ancillary services (reserve generating capacity and peak-shaving facilities), and, potentially, power discharging hardware and software to enable electric vehicles batteries to be used as storage devices.

**Table 2 - Principal smart grid technologies.**

| <i>Technology area<br/>(level of maturity)</i>                         | <i>Hardware</i>  | <i>System and software</i>  |
|--|--|---|
| Wide-area monitoring and control ( <i>developing</i> )                 | Phasor measurement units (PMU) and other sensor equipment  | Supervisory control and data acquisition (SCADA), wide-area monitoring systems (WAMS), wide area adaptive protection, control and automation (WAAPCA), wide area situational awareness (WASA) |
| Information and communication technology integration ( <i>mature</i> ) | Communication equipment (Power line carrier, WIMAX, LTE, RF mesh network, cellular), routers, relays, switches, gateway, computers (servers)     | Enterprise resource planning software (ERP), customer information system (CIS)  |
| Renewable and distributed generation integration ( <i>developing</i> ) | Power conditioning equipment for bulk power and grid support, communication and control hardware for generation and enabling storage Technology  | Energy management system (EMS), distribution management system (DMS), SCADA, geographic Information system (GIS)  |
| Transmission enhancement ( <i>mature</i> )                             | Superconductors, FACTS, HVDC   | Network stability analysis, automatic recovery systems  |
| Distribution grid management ( <i>developing</i> )                     | Automated re-closers, switches and capacitors, remote controlled distributed generation and storage, transformer sensors, wire and cable sensors | Geographic information system (GIS), distribution management system (DMS), outage management system (OMS), workforce management system (WMS)  |
| Advanced metering infrastructure ( <i>mature</i> )                     | Smart meters, in-home displays, servers, relays  | Meter data management system (MDMS)   |
| EV battery charging infrastructure ( <i>developing</i> )               | Charging equipment (public and private), batteries, inverters  | Energy billing, smart grid-to vehicle charging (G2V) and discharging vehicle-to-grid (V2G) methodologies  |
| Customer-side systems ( <i>developing</i> )                            | Smart appliances, routers, in-home display, building automation systems, thermal accumulators, smart thermostat                                  | Energy dashboards, energy management systems, energy applications for smart phones and tablets  |

## 2.2 Reliability in Smart Grids

Severe power outage events have happened in recent years. These power outages let us realize that the single-contingency criterion (the N-1 principle) that has been used for many years in the power industry may not be sufficient to preserve a reasonable system reliability level. However, it is also commonly recognized that no utility can financially justify the N-2 or N-3 principle in power system planning. Between 1991 and 1995 there were 41 outages that affected more than 50,000 customers, growing steadily to 349 similar outages between 2005 and 2009, as shown in Figure 22, [4].

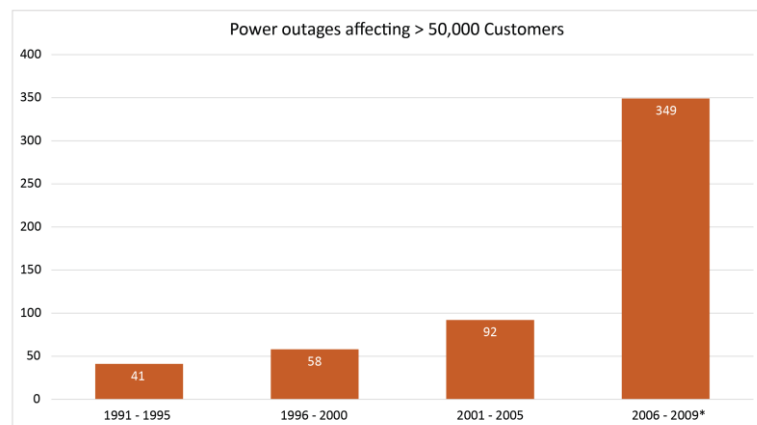


**Figure 22 - US Power Outages 1995 to 2009 (\*EIA data, other data from NERC).**

Reliability of a power system refers to the probability of its satisfactory operation over the long run. It denotes the ability to supply adequate electric service on a nearly continuous basis, with few interruptions over an extended time period. The reliability of electric distribution systems is critically important for both utilities and customers. Electric reliability affects public health and safety, economic growth and development, and societal well-being. Many utilities estimate the value of electric services to consumers to assess the benefits of investments to improve reliability. Power outages in

electric distribution systems are documented and classified by the number of customers affected and by the time interval that power is out. The Institute of Electrical and Electronic Engineers (IEEE) specifies three types of outages:

- *Major Events* are those that exceed the reasonable design and/or operational limits of the electric power system and affect a large percentage of the customers served by the utility.
- *Sustained Interruptions* include outages not classified as momentary events and that last for more than five minutes.
- *Momentary Interruptions* involve the brief loss of power to one or more customers caused by opening and closing of interruption devices.

There are many terms used in reliability discussions, including security, resiliency, risk, robustness, and vulnerability. Reliability is often used to encompass all of these, representing an average or expected level of service provided by the system over a time period (often measured annually).

In power systems, reliability is often measured differently at the distribution (retail service) level and at the bulk transmission/generation (bulk) level. At the distribution level, two of the most common reliability metrics are the System Average Interruption Frequency Index (SAIFI) and the System Average Interruption Duration Index (SAIDI), [5]. SAIFI measures the average frequency of outages per customer and SAIDI measures the average duration of outages, over one year period, per customer (Table 3).

**Table 3 - Reliability indices.**

| <i>Reliability Indices</i> | <b>Description</b>   |
|----------------------------|--|
| <b>SAIFI</b>               | System Average Interruption Frequency Index (outages)          |
| <b>MAIFI</b>               | Momentary Average Interruption Frequency Index (interruptions) |
| <b>SAIDI</b>               | System Average Interruption Duration Index (minutes)           |
| <b>CAIDI</b>               | Customer Average Interruption Duration Index (minutes)         |

Risk, according to New Oxford American Dictionary, is the exposure to the possibility of loss, injury, or other adverse or

unwelcome circumstance; a chance or situation involving such a possibility. In the context of risk analysis, risk is often more formally defined as:

$$\text{Risk} = \text{Exposure} \times \text{Vulnerability} \times \text{Cost}$$

*Exposure* is the extent to which a particular object or system is exposed to potential hazards. When expressed probabilistically, exposure is the probability that a particular object will be contacted by a hazard. *Vulnerability*, in this context, is the probability that an object fails, given that it is contacted by a hazard. Often exposure and vulnerability are combined into an overall probability that a particular component will fail. *Cost* refers to the total system cost that would result from the failure of a particular component. In the case of interconnected infrastructures, this cost needs to account for not only the immediate impact of the component failure (the cost of the transformer, for example), but also the costs incurred from potential cascading failures that might be triggered by a particular outage or set of outages, [6].

It is common in risk analysis to use data on historical outages and simulations to assess the Risk expected value over some range of potential set of failures. This expected value is often reported as a measure of system reliability.

### 2.2.1 Resiliency of Smart Grid Functions

Resilience, on the other hand, refers specifically to the ability of a system to recover from a failure after it has occurred. Resilience is the capability of a system to fulfill its mission in a timely manner, even in the presence of attacks or failures. An operationally resilient system continues delivering essential services even under adverse operating conditions and rapidly recovers its full services when conditions improve. A number of factors such as cyber-attacks, internal system failures, policy changes, configuration changes, or deployment changes can result in adverse conditions and disrupt system operation [7].

In the context of power systems, resilience is closely related to restoration, which is the process of restoring a power grid after a blackout. One of the principal near-term benefits of the smart grid is

the ability to optimize the restoration process. For example, smart meters provide utilities with precise data regarding which locations do not have power, allowing them to more efficiently dispatch restoration crews. In addition, meters with remote disconnect switches should eventually enable utilities to switch off non-critical loads after a major outage, and use distributed generation (which may not be sufficient to supply the entire load) to quickly restore power to more critical ones.

In the following, four main high-level smart grid functions are discussed focusing on the minimum conditions necessary for the functions to be resilient: remote metering, demand response, outage management and cyber security, [7].

**Remote Metering** Automated remote metering requires meters to send meter reads to the utility at a configurable frequency. This function depends on reliable and timely delivery of meter data to the utility by the communication infrastructure. Long-term disruption of the metering function affects the operational resiliency of the smart grid by interfering with revenue. *Remote metering is resilient if data from some percentage of the meters is always delivered to the utility and within a bounded time, where the percentage and time are dependent on utility-specific requirements.*

**Demand Side Management (DSM)** DSM is a set of services based on an automated load management and relies on the ability of the communication infrastructure to reliably send load curtailment requests to end devices for dynamically managing the overall system load. Unlike metering, disruption of DSM operations can have near-term effects on the operational resiliency of the smart grid by destabilizing the power grid. *Demand side management is resilient if required kWh of load is always curtailed within a bounded time, where the required load and time are dependent on utility-specific requirements.*

**Outage Management (OM)** Automated outage management requires smart meters to send outage information in a last gasp message on detection of an outage by the meter. The utility uses the information such as time and location of the outage from the message to re-store power in a timely manner. A disruption of this function directly affects the operational resiliency of the grid by delaying the recovery and restoration of power to end customers. *Outage management is*

*resilient if the utility can always identify and recover from outages within a bounded time, where the time is dependent on utility specific requirements.*

**Cyber Security (CS)** The cyber security are the set of devices and procedure able to protect the smart grid system against attacks and failures and provides integrity, availability and confidentiality services for the smart grid. CS functions such detection, diagnosis and response depend on the underlying communication infrastructure for tasks such as transporting monitored data from different critical points in the system, exchanging detection and diagnosis messages across its components and communicating response actions for responding promptly to adverse situations. Disruption of these functions has direct consequences to the security of the smart grid and affects its overall resiliency. *Cyber security component is resilient if it always detects and responds to security threats before performance and security requirements of other functions are violated.*

### 2.3 Overloading and Outages: what to do

A power system continually experiences changes in its operating state. Usually, as a consequence of the growth in power demand and the requirements of higher power quality levels, power systems are operated in more and more stressful conditions. In the case of congestion or overloads in one or more distribution lines, due to unexpected outages of generation, sudden increase in demand, tripping of lines, or failures of other equipment, the resulting power imbalance could lead to instability and security analysis and contingency plans must be made at regular intervals [8]. Nevertheless, load shedding, demand side management (DMS) and distributed generation control can be an opportunity to better manage distribution systems. In fact, nowadays some distributed energy resource (DER) units can be programmable (dispatchable) in contrast to units intuitively not programmable, (such as wind, solar etc.) and information and communication technology (ICT) tools allow implementing smart strategies to manage the power demand, [9].

In order to take advantage of the new technology opportunities, the distribution network requires advanced management policies as those based on the concept of the microgrid. In fact, in the case of faults, sudden dramatic load changes, and an insufficient generation that can create power mismatch between generation and power demand, it is possible to define operative microgrid strategies based on an optimal use of available dispatchable DERs. These strategies ensure a rapid and effective service recovery incrementing the power system reliability: the microgrid can isolate itself via a utility branch circuit and coordinate generators and load by implementing different controls as below, [10].

- Real power generation scheduling
- Phase shifting transformers
- Flow control through high-voltage DC link
- Line switching
- Load shedding

In the following, the attention is mainly focused on generators rescheduling and load shedding procedures.

### **2.3.1 Scheduling of Generators**

The operation of a microgrid with more than two DG units, especially in an autonomous mode, requires a centralized control system called microgrid energy management system (MEMS) [10]. As shown in Figure 23, MEMS is responsible for the optimization of the microgrid operation, providing power set points, start-up and shutdown decisions for each unit and load control signals for demand side.

The optimal generation scheduling is one of the important functions of the MEMS. Depending on the features of DG sources, load characteristics, and power quality constraints, the required operational strategies of a microgrid can be significantly different from those of the conventional power system. If the load condition exceeds the maximum loading, congestion cannot be relieved by

generation rescheduling. The next possible option is to shut down the load appropriately.

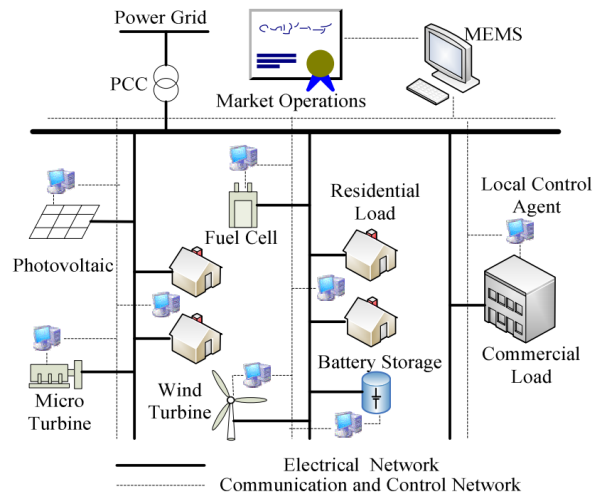


**Figure 23 - The basic architecture of a microgrid (source: [10]).**

The generation rescheduling is carried out when the congestion occurs in a specific transmission line. The change in the generation will reduce the congestion. If the congestion still prevails after the generation rescheduling, the load shedding will be carried out to reduce the congestion. The loads that are connected to the congested line will be removed one by one until the congestion reduces to a satisfied level.

#### State of art

In the literature, a variety of methods for preventive generation rescheduling has been studied. In particular, the steady-state analysis is dealt with [11], where a Particle Swarm Optimization (PSO) algorithm is used to minimize the deviations of rescheduled values of generator power outputs from scheduled levels, and with [12], where a zone-based congestion management approach has been proposed. Transient analysis is considered in [13], in which a sensitivity-based rescheduling method to dispatch the generation and to maximize the power transfer subject to the small-signal stability constraint is proposed, and in [14], where the sensitivity approaches is based on transient energy function methods. Refs. [15]-[17] present other rescheduling strategies based on heuristic stability performance index

[15], coherency identification, extended equal area criterion, trajectory simulation [16], (n-1) steady-state and dynamic security, artificial neural network techniques, and real-time approach [17]. Although many approaches found in the literature face the rescheduling problem in transmission networks, there is an absence of methodologies performing the same problem at distribution system level, neglecting the increasing penetration of DERs in distribution systems and the possibility to exploit the microgrid concept to solve congestion problems [18]. Additionally, the potential advantage of adopting an uncertainty-based approach has been handled only recently and in few research papers [19].

### 2.3.2 Load Shedding

The load shedding or disconnection of non-essential loads is a vital strategy to avoid a major electric power system breakdown during a disturbance, such as with the tripping of a generator during which case the load demand becomes greater than the generation could supply.

Loads that can be shed include non-essential machines, cooling and air conditioning units, motors, furnaces, compressors, pumps, and lighting systems. The main idea is to balance out supply shortages with demand reductions, [20]. To this end, a facility will draw up a priority list that defines which equipment and machines will be shutdown at which times under a given set of circumstances. In the ideal case, an outage should immediately be followed by a power-feed cutoff in fractions of a second, thus minimizing the chance that instabilities might lead to a total collapse of a grid. In the past, control center technicians decided which loads to drop if a generator failed. However, this required too much time to prevent disaster. Later, simple automatic load shedding systems were developed that could shut down specific areas of energy demand in line with previously calculated scenarios.

Scheduled load shedding is controlled by way of sharing the available electricity among all its customers. By switching off parts of the network in a planned and controlled manner, the system remains stable throughout the day, and the impact is spread over a wider base of customers. Load shedding schedules are drawn up in advance to describe the plan for switching off parts of the network in sequence

during the days that load shedding is necessary. On days when load shedding is required, the networks are switched off according to the predetermined plan, to ensure that, as far as possible, customers experience load shedding in accordance with the published load shedding schedules.

In exceptional circumstances, if scheduled load shedding is not achieving the required load reduction and/or unexpected emergencies or failures occur, then it is necessary to shed load outside the published schedules by using emergency switching in order to protect the network. Such events are rare, but if a state of emergency load shedding is declared, then all customers can expect to be affected at any time, and the planned schedules may not necessarily apply.

#### State of art

In the literature, few studies deal simultaneously with generation rescheduling and load shedding (GRLS) problems. In [21], sensitivity-based optimum generation rescheduling and/or load shedding schemes to alleviate overloading of transmission lines are reported. Optimization techniques are used for GRLS in the reliability evaluation of conventional power systems, [22]. More recent works are in [23]-[25]: a particle swarm optimization method is used to solve a GRLS multi objective problem in order to alleviate overload and minimize the operation cost [23], whereas a decision tree-based preventive and corrective method such as GRLS schemes to enhance the security of power system is proposed in [24]. *Wang et al.* propose a risk-based method for coordinating GRLS to enhance overall transient stability of power systems [25]. Other papers deal with congestion management by focusing on load shedding scheme separately, [8]. Many of these algorithms utilize the rate of change of frequency ( $df/dt$ ) to recognize the required speed and amount of load shedding [26]. In [27] for large disturbances that result in a high rate of frequency decline, the amount of load shedding is increased. The methods proposed in [28] use centralized load shedding algorithms and need fast communication of the measured parameters of power system, e.g., the frequency and rate of frequency change of all system generators.

## 2.4 Uncertainty in Power Systems

In power systems, problems that treat the uncertainty with the classical probabilistic approach can be critical because, in many cases, there are not enough data to build reliable probabilistic distributions, and practical applications suffer the lack of information. These considerations led to formulate a theory of possibility based on a fuzzy set approach [29]. In fact, often it is necessary to take into account both aleatoric and epistemic effects so that the uncertainty can be accounted by the model by possibility distributions. Possibility measures are particularly well suited to integrate the judgment of experts regarding the uncertainty or likelihood. For example, an expert may describe a load saying that it could be between 80 and 100 MVA, 90 MVA being the most 'possible' value. He might estimate the power factor between 0.87 and 0.9. In addition, he could guess that between 70 and 80% of the total load is linear and of this percentage, about 30-40% may be because of the induction motors and soon. In general, such information is incomplete, imprecise, even contradictory or deficient in some other way, [30], [31]. Fuzzy numbers allow to modeling in an easy way these non-probabilistic uncertainties. This justifies the increasing interest in theoretical and practical aspects of fuzzy arithmetic in the last years, especially directed to: operations over fuzzy numbers and properties, ranking of fuzzy numbers and canonical representation of fuzzy number. Here, the fundamental concepts of the possibility theory and fuzzy sets are recalled.

### 2.4.1 Possibility Theory

The importance of the theory of possibility stems from the fact that - contrary to what has become a widely accepted assumption - much of the information on which human decisions are based is possibilistic rather than probabilistic in nature. In particular, the intrinsic fuzziness of natural languages - which is a logical consequence of the necessity to express information in a summarized form - is, in the main, possibilistic in origin. Based on this premise, it is possible to construct

a universal language in which the translation of a proposition expressed in a natural language takes the form of a procedure for computing the possibility distribution of a set of fuzzy relations in a database. This procedure, then, may be interpreted as the meaning of the proposition in question, with the computed possibility distribution playing the role of the information, which is conveyed by the proposition [32].

Since Zadeh introduced the concept of possibility, the fuzziness has been handled by possibility distributions, and a fuzzy variable with its membership function is related to a possibility distribution in the same manner as the corresponding probability distribution of the random variable [32]. Let  $A$  a fuzzy set, a subset of a universal set  $U$ , represented by an ordered pair composed of a generic element and its membership value:

$$A = \{(x, \pi_A(x) \mid x \in U)\} \quad (1)$$

A possibility distribution  $\pi_A$  on  $U$  is a mapping from  $U$  to the unit interval  $[0,1]$  attached to the single-valued variable  $A$ . The function  $\pi_A$  represents a flexible restriction, which constrains the possible values of  $A$  according to the available information. The following conventions are adopted:  $\pi_A(x)=0$  means that  $A=x$  is definitely impossible;  $\pi_A(x)=1$  means that absolutely nothing prevents that  $A=x$ . Intermediary levels of plausibility about the possible values of  $A$  are modeled by letting  $\pi_A(x)$  between 0 and 1 for some values  $x$ . The quantity  $\pi_A(x)$  thus represents the degree of possibility of the assignment  $A=x$ . Then one can acknowledge the fact that some values of  $x$  are more possible than others, according to available information.

In order to deep the concept of the possibility distribution, the  $\alpha$ -cut of a fuzzy set  $A$  is introduced: a classical set  $A_\alpha$  containing all the elements in  $U$  with a membership value in  $A$  greater or equal than  $\alpha$ , is:

$$A_\alpha = \{(x \in U \mid \pi_A(x) \geq \alpha \quad \alpha \in [0,1]\} \quad (2)$$

A possibility distribution can be seen as a sequence of nested confidence intervals, coincident with the  $\alpha$ -cuts of a fuzzy set  $A$ . The confidence level regarding the truth of a sentence, like "the value of the uncertain measurement belongs to an interval  $A$ ", represents the necessity (*nec*), which is maximum for  $\alpha=0$  and it decreases as

increases:  $nec_\alpha(A_\alpha)=1-\alpha$ . The possibility ( $pos$ ) is related to necessity through the following:

$$pos(S) = 1 - nec(S^c) \tag{3}$$

where  $S$  is a subset of  $A$ , and  $S^c$  is the complementary subset.

For each possible event  $A=x$  its possibility  $\pi_A(x)$  is the greatest possible probability of the event [33]. The necessity, instead, is the minimal but certain probability value of the event occurrence. If the possibility value  $\pi_A(x)$  and the necessity  $\eta_A(x)$  value are known, then the event  $A=x$  occurs with probability at least equal to the necessity but not exceeding the possibility. The possibility and necessity measures of an event occurrence in the solution of real problems correspond, respectively, to the extremely optimistic and to extremely pessimistic approach to the problem.

### 2.4.2 Fuzzy Numbers

A fuzzy number is a generalization of a regular, real number in the sense that it does not refer to one single value but rather to a connected set of possible values, where each possible value has its own weight between 0 and 1. This weight is called the membership function. A fuzzy number is thus a special case of a convex, a normalized fuzzy set of the real line, [34]. Just like fuzzy logic is an extension of Boolean logic (which uses absolute truth and falsehood only, and nothing in between), fuzzy numbers are an extension of real numbers.

A fuzzy number  $\tilde{a}$  is a fuzzy subset in  $U$  that fulfills the following conditions:

- $\tilde{a}$  is normal
- $\tilde{a}$  is convex
- $\tilde{a}$  has a bounded support
- every  $\alpha$ -cut of  $\tilde{a}$  is a closed interval in  $U$ .

Here, fuzzy numbers with triangular shape are used. The membership function is defined as

$$\begin{aligned} \pi_a(x) &= \pi_a(x, a_1, a_2, a_3) = \\ &= \begin{cases} \frac{(x - a_1)}{(a_2 - a_1)} & \text{if } a_1 \leq x \leq a_2 \\ \frac{(a_3 - x)}{(a_3 - a_2)} & \text{if } a_2 \leq x \leq a_3 \\ 0 & \text{if } x > a_3 \vee x < a_1 \end{cases} \end{aligned} \quad (4)$$

The  $\alpha$ -cut representation is achieved building  $\alpha$  dependent function for left and right edges of  $\pi_A$ . Thus, for the fuzzy number  $\tilde{a}$  is defined:

$$a_\alpha = [a_\alpha^-, a_\alpha^+] \quad (5)$$

where

$$\begin{aligned} a_\alpha^- &= (a_2 - a_1)\alpha + a_1 \\ a_\alpha^+ &= (a_2 - a_3)\alpha + a_3 \end{aligned} \quad (6)$$

In the literature, various operations are defined on Fuzzy numbers. The usual arithmetic operation on real numbers can be extended to the ones defined on fuzzy numbers by means of Zadeh's extension Principle [32]. Following the main operations on fuzzy numbers used for our purposes are recalled. Let  $\tilde{a}$  and  $\tilde{b}$  be two fuzzy numbers and  $a_\alpha = [a_\alpha^-, a_\alpha^+]$  and  $b_\alpha = [b_\alpha^-, b_\alpha^+]$  their  $\alpha$ -cuts, respectively. The sum of  $\tilde{a}$  with  $\tilde{b}$  is a fuzzy number  $\tilde{c}$  with the following  $\alpha$ -cut:

$$c_\alpha = (a + b)_\alpha = [a_\alpha^- + b_\alpha^-, a_\alpha^+ + b_\alpha^+] = [c_\alpha^-, c_\alpha^+] \quad (7)$$

Thus, the fuzzy number is well defined and considering the related membership function, it is possible to obtain the following:

$$\pi_{a+b}(x) = \pi_{a+b}(x, a_1 + b_1, a_2 + b_2, a_3 + b_3) \quad (8)$$

For the absolute value the membership function is:

$$\pi_{|a|}(x) = \pi_{|a|}(x, |a_1|, |a_2|, |a_3|) \quad (9)$$

Here, only the scalar multiplication between a fuzzy number  $\tilde{a}$  with a scalar  $k$  is defined. In particular, the product is a fuzzy number with the following membership function:

$$\pi_{ka}(x) = \pi_{ka}(x, ka_1, ka_2, ka_3) \quad (10)$$

In the literature, quite a few fuzzy ranking methods for comparing fuzzy numbers are present, but they are able to guarantee the comparison only in particular conditions, [33]. Since the method used here is closely related to the addressed problem, in this work is used the ranking method for comparing fuzzy numbers introduced in [34]. For our purpose, three cases are considered: inequality between a fuzzy number and a real number; equality between two fuzzy numbers and inequality between two fuzzy numbers.

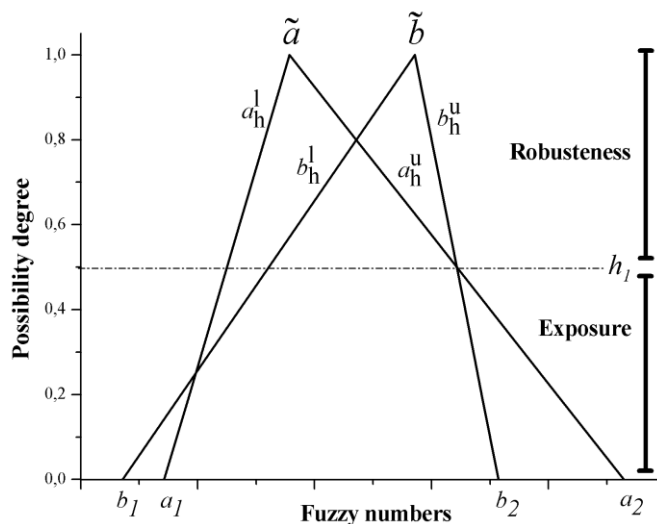


Figure 24 - Comparison between fuzzy numbers.

In particular,

- a fuzzy number is less than a real number if each element of the set of the associate membership function is less than the real number;
- two fuzzy numbers are equals if the correspondent elements of their set are equal to each other;

- a fuzzy number is greater than of a fuzzy number if each element of the first set is greater than of each element of the second set.

The fuzzy constraints can be satisfied in different ways. In this work the Soyster's criterion is considered, [35]. Let consider two fuzzy numbers  $\tilde{a}$  and  $\tilde{b}$  with triangular shapes as in Figure 24, the inequality  $\tilde{a} \lesssim \tilde{b}$  is satisfied up to the level  $h_1$  if  $\tilde{a} \lesssim_{h_1} \tilde{b}$ , that is the left-hand side satisfies  $a'_h \lesssim b'_h$  and the right-hand side satisfied for any  $\alpha$ -cut  $h \in [h_1, 1]$ . The level  $h_1$  ( $\beta$ -level) is a measurement of the corresponding risk accepted by the planner and is called *exposure*. Instead, the value  $1-\beta$  is a measurement of *robustness* of the planning solution.

## 2.5 GRLS Problem under Uncertainty Conditions

Uncertainty in planning studies stems from several sources both internal and external to the distribution power system. The most relevant uncertainty sources are:

- the price of electricity based on competing for energy sources;
- lower and upper limits of power production of some of the dominant constraints, which are not sharp but rather soft;
- weather conditions;
- improvements on the energy end use;
- New loads such as an electric vehicle.

Here, a planning study based on the solution of a GRLS problem is faced. It is modeled by using fuzzy variables that represent the possibility distributions of the demand values and power production in the presence of distributed generation units with aleatory sources. Forecasting these variations involves uncertainty, which could be significant especially in the medium and long term. In the following,

triangular fuzzy numbers will model the uncertainty associated with power demand and power production.

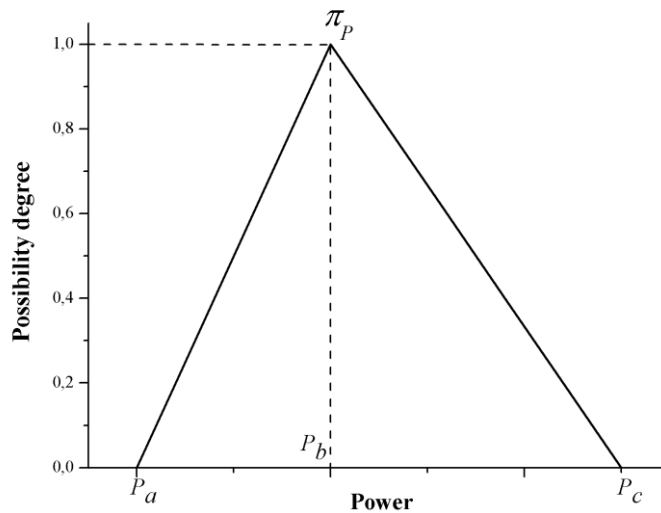


Figure 25 - Example of triangular fuzzy number.

In particular, a linguistic declaration about the absorption of power as "power load may occur between  $P_a$  and  $P_c$  MW but it is likely  $P_b$ " is modeled by the fuzzy number  $\pi_P(x, P_a, P_b, P_c)$  sketched as in Figure 25; then it is possible to distinguish between programmable and not-programmable DERs. In particular, not-programmable DER are assumed connected at the same bus of programmable DER, so that the produced power is affected by an uncertainty degree.

### 2.5.1 Mathematical Formulation

GRLS problem deals with the determination of a new stable equilibrium state (steady state analysis) following an outage in a distribution network hosting DERs. The objective of the problem is to reschedule power generation as close as possible to the power generated in order to minimize production costs and, if necessary, to reduce the load, classified with different priorities, in order to guarantee the maximum continuity of service. The problem formulation is divided into two parts: the first one describes the rescheduling problem; the second one formalizes the load-shedding problem.

### 2.5.1.1 Rescheduling Problem

Rescheduling problem is formulated as an optimization fuzzy problem based on an AC power flow, subject to operating constraints. The mathematical model can be expressed as

$$\begin{aligned} \min_{\tilde{P}_G \in F^{N_g}} \quad & \tilde{F}_1(\tilde{P}_G) \quad \forall \alpha \in [0,1] \\ \text{s.t.} \quad & \tilde{x}(\tilde{P}_G) \in X \end{aligned} \quad (11)$$

where  $F^{N_g}$  is the subset of fuzzy variables,  $\tilde{P}_g$  is the set of the fuzzy active power variables produced by the DER units,  $N_g$  is the number of the programmable DERs, and  $\tilde{F}_1$  is:

$$\tilde{F}_1 = \sum_{i=1}^{N_g} \tilde{P}_{Gi} - \tilde{P}_{TOT}^L \quad (12)$$

In (12)  $\tilde{P}_{Gi}$  represents the active power of the DER at the bus  $i$ ;  $\tilde{P}_{TOT}^L$  represents the overall load active power. The uncertainty on produced active power is due to the presence of not-programmable DERs connected to the same bus of the programmable DERs. The electrical and operational constraints are summarized by

$$X = \left\{ \tilde{r}(\tilde{P}_G) \mid \tilde{r}(\tilde{P}_G) \leq 0 \right\} \quad (13)$$

where the vector function  $\tilde{r}(\tilde{P}_G)$  describes both the equality constraints (i.e. load flow equations) and the constraints for a correct system operation as

$$\left\{ \begin{aligned} \tilde{P}_i^{SP} &= \tilde{V}_i \sum_{j=1}^{N_b} \tilde{V}_j Y_{ij} \sin(\tilde{\delta}_i - \tilde{\delta}_j - \vartheta_{ij}) \quad i \in nP \\ \tilde{Q}_i^{SP} &= \tilde{V}_i \sum_{k=1}^{N_b} \tilde{V}_k Y_{ik} \sin(\tilde{\delta}_i - \tilde{\delta}_k - \vartheta_{ik}) \quad j \in nQ \\ |\tilde{I}_h| &\leq I_h^{\max} \quad h = 1 \dots N_l \\ P_{Gi}^{\min} &\leq \tilde{P}_{Gi} \leq P_{Gi}^{\max} \quad i = 1 \dots N_g \\ Q_{Gi}^{\min} &\leq \tilde{Q}_{Gi} \leq Q_{Gi}^{\max} \quad i = 1 \dots N_g \\ V_{Gi}^{\min} &\leq \tilde{V}_{Gi} \leq V_{Gi}^{\max} \quad i = 1 \dots N_g \end{aligned} \right. \quad (14)$$

where  $N_b$  is the number of load buses,  $nP$  and  $nQ$  are the list of the buses in which the active and reactive power are specified, respectively.  $\tilde{P}_i^{SP}$  and  $\tilde{Q}_i^{SP}$  are the real and reactive specified power at  $i$ -th and  $j$ -th bus (load and generation);  $\tilde{V}_i$  and  $\tilde{\delta}_i$  are the  $i$ -th bus voltage (magnitude and angle) and  $Y_{ij}$  and  $\vartheta_{ij}$  are the  $ij$ -th element of the bus admittance matrix (magnitude and angle).  $\tilde{I}_h$  is the current on the line  $h$ . The terms with *max* and *min* indicate the limits of the corresponding electrical quantities:  $V_{Gi}$  and  $Q_{Gi}$  describe the voltage and the reactive power at the generation  $i$  bus. The terms with the symbol  $\sim$  are fuzzy numbers.

### 2.5.1.2 Load Shedding Problem

In the load-shedding problem, each bus is associated with an aggregate load with a priority degree, so that all buses can be clustered in priority classes. This assumption introduces a constraint in the order of the load reduction. For this reason, a multilevel optimization problem is formulated. Multilevel optimization recognizes that there is a hierarchy of decision makers with the decision made at different levels of the hierarchy [36]. Von Stackelberg introduced the multilevel optimization in 1952: he proposed a two level strategy for systems where policy makers at the top level influence the decision of private individuals and companies. According to this strategy, the problem of load shedding must take into account the load shedding solutions obtained at lower levels to guarantee the correct order of load reduction based on the priority of the loads. Analytically, the optimization problem is formulated as

$$\begin{aligned} \min_{\tilde{P}_L^L \in \mathbb{F}^{N_b}} \quad & \tilde{F}_1(\tilde{P}_L^H, \tilde{P}_L^M, \tilde{P}_L^L) \quad \forall \alpha \in [0,1] \\ \text{s.t.} \quad & \tilde{x}(\tilde{P}_L^H, \tilde{P}_L^M, \tilde{P}_L^L) \in X \end{aligned} \quad (15)$$

where  $\tilde{P}_L^M$  solves

$$\begin{aligned} \min_{\tilde{P}_L^M \in \mathbb{F}^{N_b}} \quad & \tilde{F}_2(\tilde{P}_L^H, \tilde{P}_L^M) \quad \forall \alpha \in [0,1] \\ \text{s.t.} \quad & \tilde{x}(\tilde{P}_L^H, \tilde{P}_L^M) \in X \end{aligned} \quad (16)$$

where  $\tilde{P}_L^H$  solves

$$\begin{aligned} \min_{\tilde{P}_L^H \in \mathbb{F}^{N_b}} \quad & \tilde{F}_3(\tilde{P}_L^H) \quad \forall \alpha \in [0,1] \\ \text{s.t.} \quad & \tilde{x}(\tilde{P}_L^H) \in X \end{aligned} \quad (17)$$

in (15)-(18)  $\tilde{P}_L^H$ ,  $\tilde{P}_L^M$ ,  $\tilde{P}_L^L$  are the sets of the high, medium and low priority load, respectively. Furthermore,

$$\begin{cases} \tilde{F}_1 = \sum_{i=1}^{N_g} \tilde{P}_{Gi} - \sum_{j=1}^{N_b} (\tilde{P}_{Lj}^H + \tilde{P}_{Lj}^M + \tilde{P}_{Lj}^L) \\ \tilde{F}_2 = \sum_{i=1}^{N_g} \tilde{P}_{Gi} - \sum_{j=1}^{N_b} (\tilde{P}_{Lj}^H + \tilde{P}_{Lj}^M) \\ \tilde{F}_3 = \sum_{i=1}^{N_g} \tilde{P}_{Gi} - \sum_{j=1}^{N_b} (\tilde{P}_{Lj}^H) \end{cases} \quad (18)$$

Obviously, in (18), we sum only the demand powers with a priority  $p$ , even though the sum is extended to all buses; demand power at the bus associated with a load with a priority different from  $p$  is considered null. The electrical and operational constraints in (15)-(18) are summarized by

$$X = \{ \tilde{r}(\tilde{P}_L) \mid \tilde{r}(\tilde{P}_L) \leq 0 \} \quad (19)$$

where  $\tilde{P}_L = \{ \tilde{P}_L^H, \tilde{P}_L^M, \tilde{P}_L^L \}$  and the vector  $\tilde{r}(\tilde{P}_L)$  describe both the equality constraints (i.e. load flow equations) and the inequality constraints for a correct system operation as

$$\begin{cases} \tilde{P}_i^{SP} = \tilde{V}_i \sum_{j=1}^{N_b} \tilde{V}_j Y_{ij} \sin(\tilde{\delta}_i - \tilde{\delta}_j - \vartheta_{ij}) \quad i \in nP \\ \tilde{Q}_i^{SP} = \tilde{V}_j \sum_{k=1}^{N_b} \tilde{V}_k Y_{jk} \sin(\tilde{\delta}_j - \tilde{\delta}_k - \vartheta_{jk}) \quad j \in nQ \\ V_i^{\min} \leq \tilde{V}_i \leq V_i^{\max}; \quad |\tilde{I}_h| \leq I_h^{\max} \quad i, h = 1 \dots N_l \\ \tilde{P}_L^{sh} + (\Delta f_{\min})D \leq \Delta \tilde{P}_L \leq \tilde{P}_L^{sh} + (\Delta f_{\min})D \end{cases} \quad (20)$$

where  $D$  is the damping load constant,  $\Delta \tilde{P}_L$  is the active load power to disconnect for the load-shedding.  $\tilde{P}_L^{sh}$  is the active power lost after the outage and  $\Delta f_{\min(\max)}$  is the frequency deviation between the rated value and the minimum (maximum) standard limit, [18]. The last inequality allows steady state frequency to maintain within a

permissible range in steady state analysis. It is obtained ignoring generator droops, [27].

### 2.5.2 Solution Algorithm

The solution method is based on the algorithm whose block diagram is shown in Figure 26. When an outage occurs, and some microgrid are formed, first, the algorithm tries to perform a rescheduling of the dispatchable generators: this operation can lead to an optimal rescheduling valid for each  $\alpha$  value or a feasible rescheduling solution valid only for particular values of  $\alpha$ .

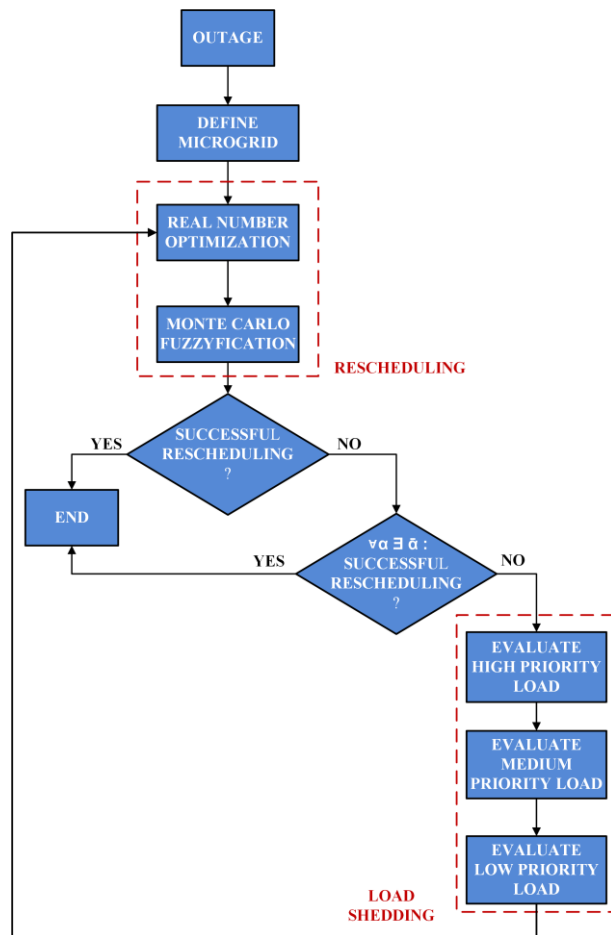


Figure 26 - Block diagram of GRLS problem solution algorithm.

If the total generated power is less than the power absorbed by loads, it will be impossible to perform the rescheduling procedure, thus, a load shedding routine starts, followed by a power rescheduling in order to find an optimal generators operating point. In details, the solution of the rescheduling optimization problem is obtained in two steps: in the first one, the fuzzy optimization problem (10) is translated to a real number based minimization problem by applying  $\alpha$ -cuts ( $\alpha=1$ ), which corresponds to a deterministic classical problem for rated values. It is a constrained non-linear optimization problem that can be solved by using a Hessian, computed by a quasi-Newton approximation. In particular, the power flow is solved assuming that one of the microgrid generators takes the slack node role and limiting its active and reactive power according to power limits. In the second step the rescheduling algorithm allows obtaining the solution in terms of fuzzy numbers in order to verify the possibility degree. The procedure is based on the following sub-steps:

- translate the deterministic solution to a fuzzy number solution by applying the same maximum uncertainty width interval ( $\alpha=0$ ), as defined before the rescheduling to DER buses (PV buses) and load buses (PQ buses). In fact, the imprecise information depends on the not-programmable sources and it is independent of the obtained solution;
- define an interval for all load flow input variables by setting a value of  $\alpha$ ;
- carry out Monte Carlo simulations by using, for all power flow input variables, values selected in the interval;
- check that the power flow solutions are feasible according to technical constraints;
- repeat the last two steps in order to obtain a fuzzy number solution for each  $\alpha$ -cut included in  $A=[0,0.2,0.4,0.6,0.8,1]$  (*Monte Carlo fuzzyfication* block).

The load shedding problem, instead, is traced back to a knapsack problem: given a backpack that can withstand a certain weight and  $N$  objects with their own weight, the problem aims to choose the higher number of these items to put in the backpack without exceeding the sustainable weight of the backpack itself. The problem of load shedding is well described by the knapsack problem because the

backpack weight represents the maximum power that could be supplied by generators and the  $N$  objects are the loads that remain connected to the grid. Each load has a priority value: high, medium, or low. Firstly, the algorithm minimizes high priority loads to disconnect from the microgrid according to the generators maximum power (17), then it repeats the same procedure for the lower priority loads (16)-(15). If two or more loads have the same priority, loads with higher demand power are disconnected from the grid to ensure greater continuity of service to as many as possible connected loads. In order to properly set the slack node, we check the possibility of selecting another bus as slack. So, the procedure is repeated for each slack node candidate.

## 2.6 Simulation Framework

In order to show the effectiveness of the proposed methodology, a real study is presented in which only one outage occur in the network, [30], [37]. Indeed, if one or more outages occurs, the proposed methodology is still applicable because more parts of the network are isolated and more microgrid are formed. Several simultaneous outages increase only the computational time but not the effectiveness of the proposed methodology. To better compare the results obtained by applying the two methods, we suppose the fuzzy membership function and the pdf similar in shape (symmetrical triangular). The solution algorithms are coded in Matlab<sup>TM</sup> R2014b and are run on a workstation with an Intel Core i7 (3.20 GHz, 64 bit) processor, 16 GB of RAM.

### 2.6.1 Case Study

The tests are performed on a 69 branch, 9 lateral test grid derived from a portion of the *PG&E* distribution network (Figure 27) [38]. A comparison is performed between the proposed fuzzy method and an approach well known in the literature, as the stochastic optimization. Total distribution network load is 3802.19 kW for  $\alpha=1$  in the fuzzy approach and corresponds to the maximum value of the probability

density function (pdf) for the stochastic optimization. They are assumed 9 buses with not-programmable and programmable DER units, in correspondence of the buses 4, 14, 35, 38, 46, 47, 52, 58 and 65, able to guarantee the total active power generation equal to 3950 kW, which is the maximum value of the possibility function ( $\alpha=1$ ) and the maximum value of the pdf.

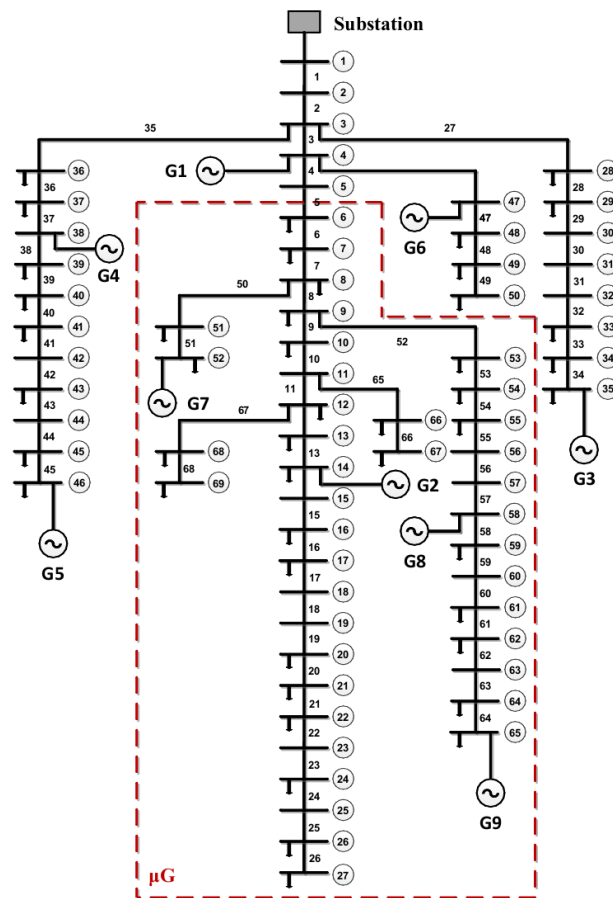


Figure 27 - C69-bus test network.

For each DER unit, we assume an uncertainty of  $\pm 5\%$  described by using fuzzy numbers in the proposed approach, and by a probability density function in the stochastic approach. To better compare the results obtained by applying the two methods, we suppose the fuzzy membership function and the pdf similar in shape (symmetrical

triangular). In order to implement the two methods, Monte Carlo simulations are carried out on 10'000 different values where input variables, in the assumed input bounds, are randomly selected.

## 2.6.2 Numerical Results

In the case study, following to the outage of line 5, the main part of the network is isolated, so the big microgrid ( $\mu G$ ) is formed and joined results of rescheduling and load shedding are discussed. The total rated generation power and the total load are equal to 2.232 MW and 2.676 MW, respectively.

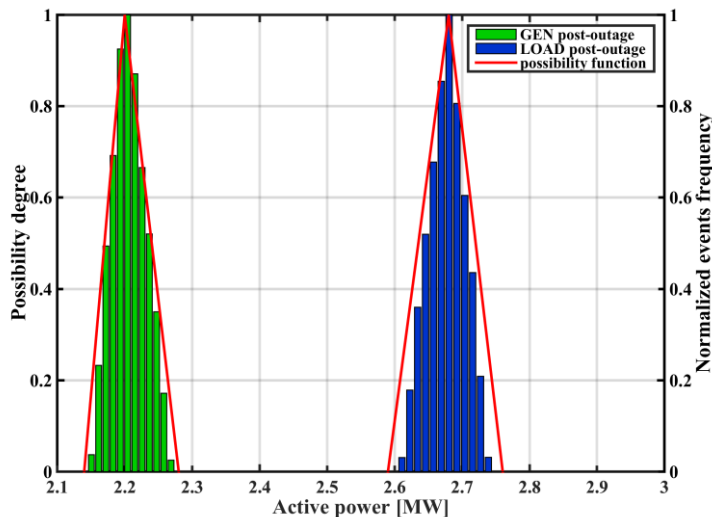
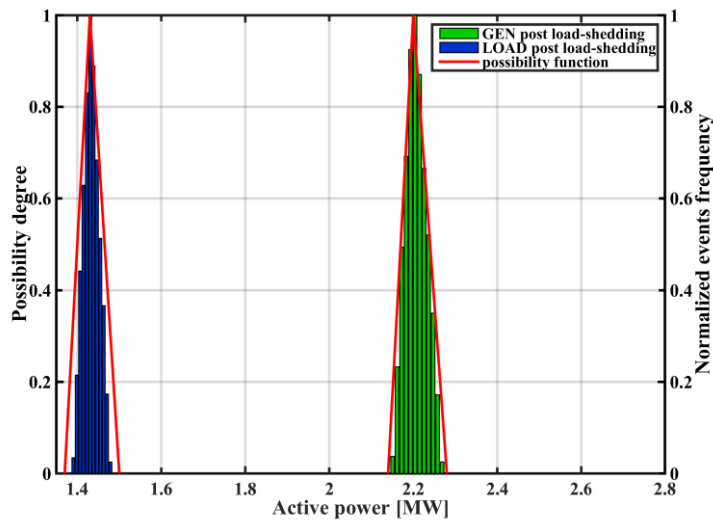


Figure 28 - Total generators and loads active power post outage.

One of the following priority value characterizes the load buses connected to the  $\mu G$ : LOW, MEDIUM or HIGH. Figure 28 shows the fuzzy membership functions (fuzzy approach) and the normalized histograms (stochastic approach) after the outage of the total generation active power and total demand. It is not possible to obtain a feasible solution, applying the rescheduling routines, because the maximum total generation power is lower than the total demand so that the load shedding procedure is run. Figure 29 shows the results obtained by load shedding routines: the algorithm in order to maximize the supplied total load in the  $\mu G$  disconnects only one big load (1.244 MW - bus 61) with LOW priority value. The two

approach allow obtaining similar results. In particular, the fuzzy arithmetic lead to a more conservative solution since the membership functions, for  $\alpha=0$ , are slightly larger than the normalized histograms amplitude. It is worth noting that the fuzzy load shedding procedure implements only arithmetic fuzzy operations without Monte Carlo simulations so that it is possible having a feasible solution with a low computational time-consuming but an increasing amplitude of the solution interval.



**Figure 29 - Total generators and loads active power post load shedding.**

The total generators active power, after the performed load shedding routine, is much greater (2.232 MW) than total load active power (1.433 MW), as shown in Figure 29, thus by applying the rescheduling algorithm, the new total generation active power matches the total power demand, according to the values shown in Figure 30.

**Table 4 - Rescheduling results.**

| <i>Gen number</i> | <i>P<sub>inf</sub></i><br>[MW] | <i>P</i><br>[MW] | <i>P<sub>sup</sub></i><br>[MW] | $\Delta P$<br>[MW] |
|-------------------|--------------------------------|------------------|--------------------------------|--------------------|
| 14                | 0.118                          | 0.122            | 0.126                          | +0.024             |
| 52                | 0.476                          | 0.493            | 0.508                          | -0.309             |
| 58                | 0.337                          | 0.344            | 0.351                          | -0.156             |
| 65                | 0.492                          | 0.525            | 0.550                          | -0.275             |
| <b>Tot</b>        | <b>1.423</b>                   | <b>1.484</b>     | <b>1.535</b>                   | <b>-</b>           |

Table 4 lists the variation of the power generation after the rescheduling; in particular, the second and the fourth columns show the minimum and maximum value for  $\alpha=0$ , the third column the more possible value for  $\alpha=1$ , whereas the fifth column shows the active power variation regarding the rated power pre-outage for  $\alpha=1$ .

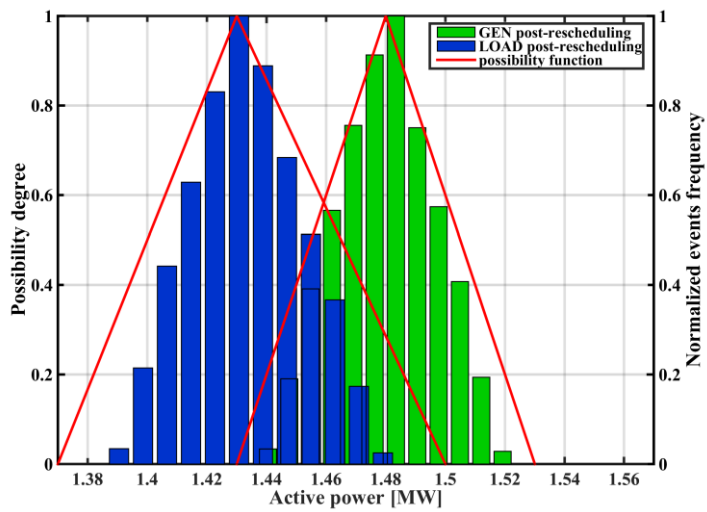


Figure 30 - Total generators and loads active power post rescheduling.

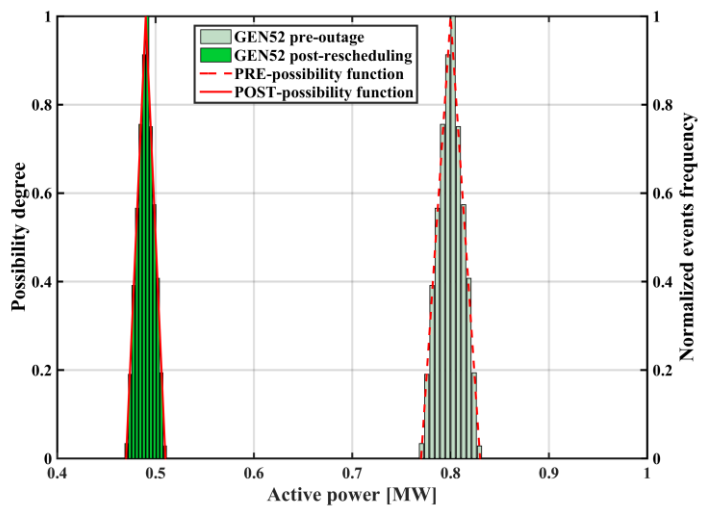


Figure 31 - Active power production of the generator G7.

The rescheduling results in terms of generators active power at the buses 52, and 58 are shown in Figure 31 and Figure 32: the membership function are plotted in stretched red line after the rescheduling procedure and in dotted red line the pre-outage ones. The solution shows a decrease of the active power of both generators in order to match the total load. The results obtained by using the stochastic optimization method are similar in comparison with those achieved by the proposed fuzzy approach.

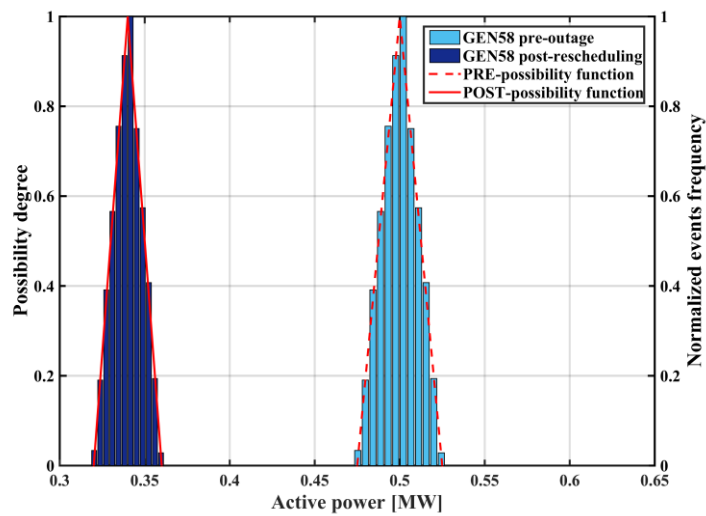


Figure 32 - Active power production of the generator G8.

Table 5 - Slack node impact on rescheduling procedure.

| <i>Gen number</i> | $\Delta P_{14}$<br>[MW] | $\Delta P_{52}$<br>[MW] | $\Delta P_{58}$<br>[MW] | $\Delta P_{65}$<br>[MW] | <i>Loss</i><br>[%] |
|-------------------|-------------------------|-------------------------|-------------------------|-------------------------|--------------------|
| 14                | +0.024                  | -0.309                  | -0.156                  | -0.275                  | 3.4                |
| 52                | -0.003                  | -0.463                  | +0.072                  | -0.185                  | 11.6               |
| 58                | +0.031                  | -0.168                  | -0.288                  | -0.221                  | 7.0                |
| 65                | +0.005                  | -0.082                  | -0.004                  | -0.613                  | 4.9                |

The losses of the system are illustrated in Table 5 by varying the position of the slack bus. In particular, in order to implement the rescheduling algorithm, four rescheduling solutions changing the slack bus are obtained. The best rescheduling solution in terms of losses (3.4%) is achieved assuming the generator 14 as the slack bus.

Keeping in mind that the proposed methodology is addressed in the context of planning studies, the average computational times obtained are about 12 min. and 18 min. by using fuzzy method and stochastic optimization, respectively.

## References

- [1] International Energy Agency (IEA), “Technology Roadmap - Smart Grids”, available on line at url [https://www.iea.org/publications/freepublications/publication/smartgrids\\_roadmap.pdf](https://www.iea.org/publications/freepublications/publication/smartgrids_roadmap.pdf)
- [2] International Energy Agency (IEA), “World Energy Outlook 2015”, available on line at url <http://www.worldenergyoutlook.org/weo2015/>
- [3] T. Morgan, “Smart Grids and Electric Vehicles: Made for Each Other?”, in *International Transport Forum*, 2012.
- [4] S. Massoud Amin, “U.S. Electrical Grid gets less Reliable”, in *IEEE Spectrum*, Jan. 2011.
- [5] P1366/d8, mar 2012, “IEEE draft guide for electric power distribution reliability indices”, available on line at url <http://ieeexplore.ieee.org/servlet/opac?punumber=6194243>, March 2012.
- [6] R. Billington, R.N. Allan, “Reliability Evaluation of Power Systems”, *Plenum Press - New York and London*, 2<sup>nd</sup> edition, 1984.
- [7] A. Aimajali, A.Viswanathan, C. Neuman, “Analyzing resiliency of the smart grid communication architectures under cyber-attack”, in *Proc. of 5th Workshop on Cyber Security Experimentation and Test*, 2012.
- [8] J. Tang, J. Liu, F. Ponci, and A. Monti, “Adaptive load shedding based on combined frequency and voltage stability assessment using synchrophasor measurements”, *IEEE Transactions on Power Systems*, vol.28, no.2, pp. 2035-2047, 2013.
- [9] V. A. Evangelopoulos, P.S. Georgilakis, “Optimal distributed generation placement under uncertainties based on point estimate method embedded genetic algorithm”, in *IET Generation, Transmission, and Distribution*, Vol. 8, No. 3, pp. 389-400, March 2014.
- [10] F. Katiraei, R. Iravani, N. Hatziargyriou, and A. Dimeas, “Microgrids management”, *IEEE Power and Energy Magazine*, vol. 6, pp. 54-65, 2008.
- [11] S. Dutta, S.P. Singh, “Optimal Rescheduling of Generators for Congestion Management Based on Particle Swarm Optimization”, *IEEE Trans. on Power Systems*, vol. 23 n. 4, 2008, pp. 1560-1569.
- [12] A. Kumar, S.C. Srivastava, S.N. Singh, “A zonal congestion management approach using real and reactive power rescheduling”, *IEEE Trans. on Power Systems*, vol. 19 n.1, Feb. 2004, pp. 554-562.

- [13] C.Y. Chung, Lei Wang, F. Howell, P. Kundur, "Generation rescheduling methods to improve power transfer capability constrained by small-signal stability", *IEEE Trans. on Power Systems*, vol. 19 n.1, Feb. 2004, pp. 524-530.
- [14] K.N. Shubhanga, A.M. Kulkarni, "Stability-constrained generation rescheduling using energy margin sensitivities", *IEEE Trans. on Power Systems*, vol. 19 n. 3, Aug. 2004, pp.1402-1413.
- [15] D.Z. Fang, Yang Xiaodong, Sun Jingqiang, Yuan Shiqiang, Zhang Yao, "An Optimal Generation Rescheduling Approach for Transient Stability Enhancement", *IEEE Trans. on Power Systems*, vol. 22 n. 1, Feb. 2007, pp. 386-394.
- [16] T.B. Nguyen, M.A. Pai, "Dynamic security-constrained rescheduling of power systems using trajectory sensitivities", *IEEE Trans. on Power Systems*, vol. 18 n. 2, May 2003, pp.848-854.
- [17] A. Hoballah, I. Erlich, "Online market-based rescheduling strategy to enhance power system stability", *Generation, Transmission & Distribution, IET*, vol. 6 n. 1, January 2012, pp. 30-38.
- [18] Xiong Wu, Xiuli Wang, Zhaohong Bie, "Optimal generation scheduling of a microgrid", in *Proc. of Innovative Smart Grid Technologies (ISGT Europe), IEEE PES International Conference, 2012*, pp. 1-7.
- [19] R. Noroozian, A. Jalilvand, M. Kazemi, H. Vahedi, "Reliability and Availability Modelling of Uninterruptible Power Supply Systems Using Monte-Carlo Simulation", *International Review of Electrical Engineering (IREE)*, vol. 6 n. 5, October 2011, pp. 2401-2410.
- [20] A. Saffarian, M. Sanaye-Pasand, "Enhancement of Power System Stability Using Adaptive Combinational Load Shedding Methods", *Power Systems, IEEE Transactions on*, vol. 26, no. 3, pp. 1010-1020, 2011.
- [21] T.K.P. Medicherla, R. Billinton, and M.S. Sachdev, "Generation rescheduling and load shedding to alleviate line overload Analysis", *IEEE Trans. Power App. Syst.*, vol. PAS-98, no. 6, pp. 1876-1884, 1979.
- [22] C. Dornellas, M. Schilling, A. Melo, J.C.S. Souza, and M.B. Do Coutto Filho, "Combining local and optimized power flow remedial measures in bulk reliability assessment", *IEE Proc. Gener. Transm. Distrib.*, vol. 150, no. 5, pp. 629-634, 2003.
- [23] J. Hazra, and A.K. Sinha, "Congestion Management Using Multiobjective Particle Swarm Optimization", *IEEE Transactions on Power Systems*, vol. 22, no. 4, pp. 1726-1734, 2007.
- [24] I. Genc, R. Diao, V. Vittal, S. Kolluri, and S. Mandal, "Decision Tree-Based Preventive and Corrective Control Applications for Dynamic Security Enhancement in Power Systems", *IEEE Transactions on Power Systems*, vol. 25, no. 3, pp. 1611-1619, 2010.
- [25] Z. Wang, X. Song, H. Xin, D. Gan, and K.P. Wong, "Risk-Based Coordination of Generation Rescheduling and Load Shedding for Transient Stability

- Enhancement”, *IEEE Transactions on Power Systems*, vol. 28, no. 4, pp. 4674-4682, 2013.
- [26] B. Delfino, S. Massucco, A. Morini, P. Scalera, and F. Silvestro, “Implementation and comparison of different underfrequency load shedding schemes”, in *Proc. 2001 IEEE Power Eng. Soc. Summer Meeting, Vancouver, BC, Canada*, Jul. 2001, vol. 1, pp. 307-312.
- [27] P. Kundur, “Power System Stability and Control”, *New York: McGraw- Hill*, 1994.
- [28] V. Calderaro, V. Galdi, V. Lattarulo, and P. Siano, “A new algorithm for steady state load-shedding strategy”, in *Proc. IEEE OPTIM Int. Conf.*, 2010, pp. 48-53.
- [29] D. Dubois, H. Prade, “Possibility Theory. An Approach to Computerized Processing of Uncertainty”, *Plenum Press*, New York and London, 1988.
- [30] V. Calderaro, V. Galdi, G. Graber, A. Piccolo, “Optimal Generation Rescheduling in Microgrids under Uncertainty”, in *International Review of Electrical Engineering* - Num. 5 (October 2013), vol. 8.
- [31] A. Piegat, “On practical problems with the explanation of the difference between possibility and probability”, *Control and Cybernetics*, vol. 34, no. 2, pp. 505-524, 2005.
- [32] L.A. Zadeh, “Fuzzy sets as a basis for a theory of possibility”, *Fuzzy Sets and Systems I*, vol. 100, pp. 9-34, 1999.
- [33] M. Cortes, R. Palma, and G. Jimenez, “Fuzzy load flow based on  $\alpha$ -Cuts arithmetics”, in *Proc. 39th North American Power Symposium*, Las Cruces, NM, Oct. 2007, pp. 683-691.
- [34] M. Cortes-Carmona, R. Palma-Behnke, G. Jimenez-Estevez, “Fuzzy Arithmetic for the DC Load Flow”, *IEEE Transactions on Power Systems*, vol.25, no.1, pp. 206-214, Feb. 2010.
- [35] A.A. Romero, H.C. Zini, G. Rattá, R. Dib, “Harmonic load-flow approach based on the possibility theory”, *Generation, Transmission & Distribution, IET*, vol. 5, no. 4, pp. 393-404.
- [36] A. Migdalas, P.M. Pardalos, and P. Varbrand, ”Multilevel optimization: algorithms and applications”, Dordrecht, *The Netherlands: Kluwer Academic Publisher*, 1998.
- [37] V. Calderaro, V. Galdi, G. Graber, A. Piccolo, “Generation Rescheduling and Load Shedding in Distribution Systems under Imprecise Information”, in *IEEE Systems Journal*, vol. PP, no. 99, pp.1-9, Feb. 2016.
- [38] M.E. Baran, and F.F. Wu, “Optimal capacitor placement on radial distribution systems”, *IEEE Transaction on Power Delivery*, vol. 4, n. 1, pp. 725-734, 1989.

## **Chapter 3**

# **EVs in Smart Grid: a Smart Charging Solution**

Plug-in electric vehicles (PEVs) are becoming a very interesting option to reduce both fuel consumption and greenhouse gas (GHG) emissions in smart cities for the next future. Due to these features, PEV penetration is supposed to reach an amount between 10% and 25% of the overall circulating vehicles in the 2010-2030 horizon. However, this new type of electric load will need careful management. Although electricity needs for EVs are likely to remain small relative to overall load in most countries for many years to come, they could have a much bigger impact on peak load as EV users seek to charge their batteries. The expected impact on distribution networks (DNs) due to the PEVs charging is significant: usually a car requires from 3 kW to 50 kW and more to charge about 15-25 kWh of energy, increasing up to 18% the average load in the existing DN, with problems in terms of reliability and overloads. Several studies show that effective EV charging management strategies are able to support a deeper penetration of electric vehicles within DNs. Thus, optimal scheduling algorithms capable to allow PEVs charging, avoiding negative drawbacks on distribution networks are needed.

This chapter shows a simple and effective methodology to analyze measured data identifying typical load pattern for the PEVs charging. It also proposes a novel scheduling problem formulation, flattening the demand load profile and minimizing the PEVs charging costs, according to the electricity prices during the day. In Section 3.1, the main characteristics of the battery electric vehicles (BEVs) are introduced, focusing on critical issues related to the EVs charging and

most promising solutions for the charging stations. Following, Section 3.2 deals with the key factors affecting the EV charging load, whereas Section 3.3 reviews main methodology to face of the EV charging load prediction. Sections 3.4 describes the data acquisition and clustering methods employed in the proposed vehicle data analysis. Mathematical formulation of the EV scheduling problem and the proposed solution algorithm are illustrated and discussed in Section 3.5. Finally, Section 3.6 show simulations results carried out by using a real case study data. The obtained results are based on the data acquired during the fulfillment of the research project: “*COSMO - Cooperative Systems for Sustainable Mobility and Energy Efficiency*”, co-founded by the European Commission under the Competitiveness & Innovation Program - ICT Policy Support Program.

### **3.1 Electric Vehicles Technology**

PEVs or battery electric vehicles (BEVs) are powered by electric energy stored in large batteries within the vehicles. These batteries are used to power an electric motor, which drives the vehicle. BEVs are equipped with electric motors mechanically very simple and they are often able to achieve 90% energy conversion efficiency over the full range of speeds and power output. BEVs also use regenerative braking, which allows the electric motor to act as a generator in order to save the energy that would be normally lost through heat dissipation and frictional losses. This can be used to reduce the wear on brake systems (and consequent brake pad dust) and reduce the total energy requirement of a trip. Regenerative braking is especially effective for start-and-stop city use, [1].

PEVs benefit from the high levels of torque supplied by electrical motors as well as smooth gearless acceleration and deceleration, and thus they do not need multiple gears to match power curves. This removes the need for gearboxes and torque converters. BEVs provide quiet and smooth operation and consequently have less noise and vibration than internal combustion engines (ICE). They are therefore well suited to urban areas where vehicle emissions represent a large proportion of urban air pollutants. Although BEVs produce zero

emissions at point of use, the electricity source must be taken into account when considering the wider scale environmental benefits; if renewable energy is used then EVs can offer a much-reduced environmental impact over other vehicle technologies. In particular, electricity generated from fossil fuels such as coal will lead to higher carbon dioxide and air quality emissions compared to electricity sourced from renewable sources such as the wind or hydroelectric power, which will have virtually zero emissions during vehicle operation. All of these factors make them ideal for inner city and urban usage.

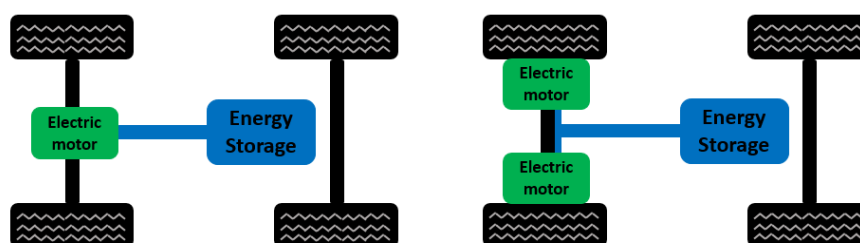


Figure 33 - BEV's powertrain architectures.

BEVs are powered by either a large electric motor connected to a transmission, or smaller electric motors housed within the wheel hubs. The two types of BEV's powertrain architecture are illustrated in Figure 33. The key difference is the positioning and the size of electric motors. The central motor type is currently more common as it works on tried and tested principles of car design. It is also more suited to larger vehicles in which the motor must be quite powerful. However, the requirement to transfer power from the motor to the wheels does involve some losses in efficiency through friction. The hub motor type, however, can avoid many of the transmission losses experienced in the central motor type but, at the current time, is more suited to smaller vehicles due to the power requirements of larger vehicles and as such is a less regularly used technology, [1].

There are a number of rechargeable battery technologies that are used or are likely to be used in the future for hybrid and electric vehicles. EVs batteries are characterized by their relatively high power-to-weight ratio, energy to weight ratio and energy density;

smaller and lighter batteries reduce the weight of the vehicle and improve its performance.

**Table 6 - Battery technologies.**

| <i>Battery type</i>                        | <i>Description</i>   |
|--|--|
| <i>Lead acid<br/>(Pb-acid)</i>             | Lead-acid batteries are the oldest type of rechargeable battery and have a very low energy-to-weight and energy-to-volume ratio. These factors mean that lead acid batteries take up significant amounts of space within vehicles and add significant amounts of weight. However, they can maintain a relatively large power-to-weight ratio and are low cost making them ideal for use in small road vehicles.  |
| <i>Nickel-Metal-Hydride<br/>(NiMH)</i>     | The Nickel Metal Hydride battery technology is similar to a NiCd battery in design, except cadmium is replaced making it less detrimental to the environment. NiMH batteries can also have 2-3 times the capacity of an equivalent size NiCd, with much less significant memory effect. Compared to lithium-ion batteries, energy capacity is lower and self-discharge is higher. Applications include hybrid vehicles such as the Toyota Prius, the Toyota RAV4-EV all-electric plug-in electric car, and consumer.   |
| <i>Lithium-ion<br/>(Li-ion)</i>            | The relatively modern lithium-ion battery technology has a very high specific energy. Current limitations include volatility, the potential for overheating, high cost, and limited shelf and cycle life. The technology has widespread use in consumer electronics (e.g. mobile phones) but has only recently begun to be used in transport applications (e.g. the Tesla Roadster electric car and in Prius conversions to a plug-in hybrid). General Motors and Toyota are now also moving towards using more Lithium-ion batteries.   |
| <i>Li-ion polymer</i>                      | This is a similar technology to Li-ion, but typically has slightly lower charge density, greater life cycle degradation rate and an ultra-slim design (as little as 1 mm thick). Disadvantages include the high instability of overcharged batteries and if the battery discharges below a certain voltage it may never be able to hold a charge again.  |
| <i>Sodium Nickel Chloride<br/>(NaNiCl)</i> | Sodium Nickel Chloride, also known as the Zebra battery, belongs to the class of molten salt batteries. These use molten salts as an electrolyte, offering both a higher energy density, as well as a higher power density making rechargeable molten salt batteries a promising technology for powering electric vehicles. However, the normal operating temperature range is 270-350°C, which places more stringent requirements on the rest of the battery components and can bring problems of thermal management and safety. Furthermore, there are also significant thermal losses when the battery is not in use. |

Compared to liquid fuels, most current battery technologies have much lower specific energy; and this often influences the maximum all-electric range of the vehicles. Rechargeable batteries used in electric vehicles include lead-acid, nickel metal hydride, lithium ion,

Li-ion polymer, and, less commonly, zinc-air and molten salt batteries. The principal technology types are briefly described in Table 6, whereas Figure 34 provides a summary of their performance characteristics, [2].

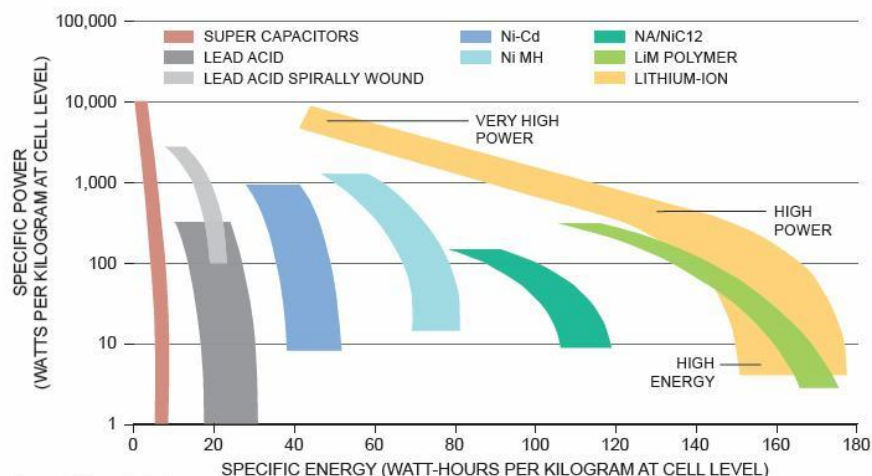


Figure 34 - Batteries specific energy vs specific power (source: Johnson Controls).

### 3.2.1 EVs Charging Options

The rise of BEVs will entail the development of a vast amount of charging infrastructure, also known as EVSE (electric vehicle supply equipment). Actually, particular attention is focused on the development of the PEV charging infrastructure for the urban and multifamily environments. Important choices have to be made on a city, regional, and country level about the required number, location (home parking vs. public), and type of charging infrastructure. PEVs can be charged in three different methods reported in the following, [1], [3].

1. *Conductive coupling* - is a method for connecting the electric power supply network to the EVs for charging the battery by using a physical support to transfer energy.
2. *Inductive coupling* - allows transmitting electrical energy via an alternating magnetic field generated between two coils, without charging cables.

3. *Battery Swap* - consists in exchanging drained or nearly drained batteries (or range extender battery modules) with fully charged batteries, in particular exchange stations.

EV charging stations (CSs) are normally classified as Level 1, Level 2 or DC Fast Charge (DCFC). In general, CS classification pertains to the power level that the equipment provides to charge a PEV's batteries, [3].

#### AC Level 1 (120 V/15 A)

Level 1 charging refers to charging through a standard home or business outlet through a 120 Volt AC plug.

- No installation of other EVSE is necessary for Level 1 charging mode.
- The charging cord has a standard three-pole household plug on one end and a connector on the other end to plug into the vehicle.
- This charging level is ideal for easy charging at home or the office and usually does not require you to make changes to your electric panel or wiring.
- Depending on the vehicle and size of the battery, Level 1 charging can take eight to 20 hours to fully charge a depleted battery.

#### AC Level 2 (230 V/30-10 A)

Level 2 charging refers to charging through 208/240 Volt AC charging equipment.

- This charging level can require the installation of charging equipment or modification of your existing electrical system.
- This charging level can recharge an EV in four to five hours - significantly faster than AC Level 1 charging.
- Charging an EV using 240 Volt is similar to adding a large appliance, such as clothes dryer, which results in a greater electrical draw and might require upgrading electrical service.

DC Fast Charging

DC Fast Charging or Level 3 Charging refers to charging at 480 Volt AC.

- It delivers the fastest charging rate and can recharge a battery EV in less than 30 minutes.
- It requires the installation of charging equipment.
- In the case of DC Fast Charging, the AC/DC conversion occurs in the charging equipment rather than in the vehicle's AC/DC converter so that the power entering the vehicle is already in DC form.
- DC Fast Charging can enable rapid charging between work shifts and during breaks.
- These chargers are also well suited for public areas and highway rest areas.

Main characteristics and average charging times related to Level 1, Level 2 and DC Fast Charging EVSE are summarized in Figure 35.

| Charging Option  | Primary Use | Current Supplied to Vehicle | Charging Current (Amps) | Charger Input (Volts) | Power (kW) | Hrs. to Recharge* |
|------------------|-------------|-----------------------------|-------------------------|-----------------------|------------|-------------------|
| Level 1          | Residential | AC                          | ≤15                     | 120                   | ≤1.8       | 6–20              |
| Level 2          | Residential | AC                          | ≤30                     | 240                   | ≤7.2       | 3–8               |
|                  | Public      | AC                          | 80                      | 240                   | ≤19.2      | 3–8               |
| Level 3          | Public      | AC                          | To be determined        |                       |            | ≤0.5              |
| DC Fast Charging | Public      | DC                          | 200                     | 480                   | 50–150     | ≤0.5              |

\*Varies, depending of battery state of charge; Source: DOE Energy Efficiency and Renewable Energy Vehicle Technologies Program

**Figure 35 - EV Charging Equipment Options (source: DOE).**

Today's EVSE and PEVs have standard connectors and receptacles based on the J1772 standard developed by SAE International. Vehicles with this receptacle can use any Level 1 or Level 2 EVSE. Major vehicle and charging system manufacturers in the United States support this standard, which should eliminate concerns about vehicles' compatibility with charging infrastructure. Most currently available PEVs that are equipped to accept DC fast charging are using the CHAdeMO connector. SAE International recently developed a "hybrid connector" standard for fast charging that adds high-voltage

DC power contact pins to the J1772 connector, enabling the use of the same receptacle for all levels of charging, [3].

Inductive charging, also known as Wireless Power Transfer (WPT), is an emerging technology that allows charging PEVs without the use of a cabled connection. The most common application uses a charging pad installed on or in the pavement and a receiving pad installed underneath the PEV. The pavement pad creates an inductive electrical field that is captured by the PEV's receiving pad to charge the vehicle's batteries as shown in Figure 36. WPT chargers typically use an induction coil to create an alternating electromagnetic field within a charging base station, and a second induction coil in the portable device (i.e., PEV) that takes power from the electromagnetic field and converts it back into electrical current to charge the battery. The two induction coils in proximity combine their self to form an electrical transformer. With a charging rate of 3.6 kW and an efficiency factor of over 80 percent, this method enables the high-voltage batteries in vehicles to be charged efficiently, conveniently and safely [4].

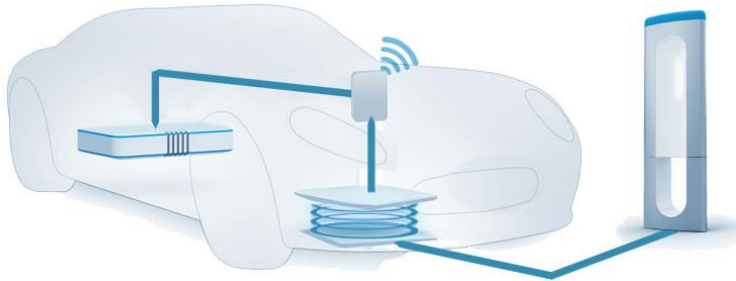


**Figure 36 - Inductive charging solution for electric vehicles**  
(source: [www.fastincharge.eu](http://www.fastincharge.eu)).

A battery swapping (or switching) station is a place at which a vehicle's discharged battery or battery pack can be immediately swapped for a fully charged one, eliminating the delay involved in waiting for the vehicle's battery to charge, [5]. In recent years, Better Place, Tesla Motors, and Mitsubishi Heavy Industries have been involved with integrating battery switch technology with their electric vehicles to extend driving range (Figure 37). The following benefits are claimed for battery swapping:

- Fast battery swapping under five minutes.

- Unlimited driving range where there are battery switch stations available.
- The driver does not have to get out of the car while the battery is swapped.
- The driver does not own the battery in the car, transferring costs over the battery, battery life, maintenance, capital cost, quality, technology, and warranty to the battery switch station company.
- Contract with a battery switch company could finance the electric vehicle at a price lower than equivalent ICE cars.
- The spare batteries at swap stations could participate in vehicle to grid storage.

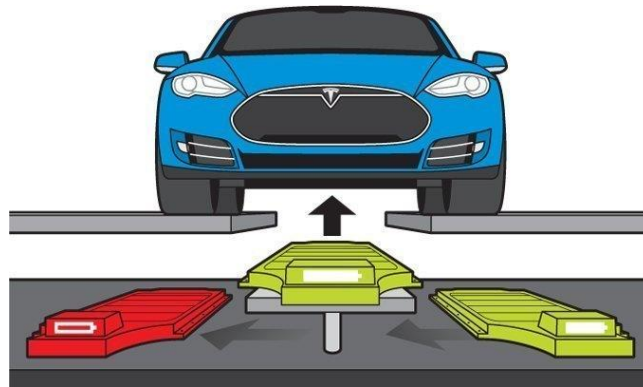


Figure 37 - Tesla's battery swap station (source: Tesla).

### 3.2 Factors Affecting EVs Charging Demand

With such a great number of EVs to be connected into power systems for charging their batteries, the charging demand can potentially increase the peak demand on the utility distribution system significantly. Although it is desired that EV battery charging load can be contained during system off-peak hours without affecting the peak demand, the charging behaviours of various EV users have some elements of randomness, [6-7]. Several factors influence the overall EVs charging demand and their combination determines the amount

of time required to fully charge the PEV's batteries and the additional electric load. In the following, the key factors affecting the EVs charging demand are briefly described focusing attention on power and energy stochastic absorptions.

### Charging location

The charging location represents the site where PEVs are connected for charging. It can be a specific residential, industrial, urban or rural area with some charging EVs, or it can be any site defined to have charging opportunities, [8]. Charging locations at home or in a residential area, can offer available EV Charging outlets and the possibility of starting at any moment the charging session. An EV owner plugs in when he or she returns home, and the vehicle charges overnight by using Level 1 mode.

CSs can also be located in public places such as where there are on-street parking areas, at taxi stands, as well as in parking lots (at places of employment, hotels, airports, shopping centres, convenience shops, fast food restaurants, coffeehouses etc.). Existing filling stations may also incorporate charging stations. Many charging stations are on-street facilities provided by electric utility companies or located at retail shopping centres and operated by many private companies. In general, public charging will use AC Level 2 or DC fast charging, [9].

Fast charging at public charging stations deliver over 100 km of range in 10-30 minutes. These chargers may be at rest stops to allow for longer distance trips. They may also be used regularly by commuters in metropolitan areas, and for charging while parked for shorter or longer periods.

### Charging Level

The charging level is a measure of the power that is supplied to a battery during the charging session. The most common measurement is maximum current. Level 1 charging provides up to 15 A of AC current, Level 2 charging provides up to 40 A of alternating current and DC Fast Charge will provide up to 125 A of DC current. PEVs are equipped with on-board chargers that regulate the amount of power used during battery charging at Levels 1 and 2. Standard equipment chargers are typically rated at 3.3 kW; faster 6.6 kW chargers are usually available from the PEV manufacturer, primarily as part of a

package of optional equipment. Currently, not all vehicles accept DC fast charging equipment (up to 22 kW).

While all of these factors influence how long it will take to charge the PEVs batteries, the driving habits of the PEV owner usually determine how frequently and for how long batteries need to be charged, [10].

#### PEV Battery Size & SoC

PEV battery size requirements increase as the physical size and weight of the PEV increases or if the desired range of travel increases (Table 7). Larger batteries take longer charging times, a fact that can be compensated by using faster charge rates supplied by Level 2 and DC Fast Charge. The battery's ability to hold charge depends also on several factors varying with time - the age of the battery, its temperature, and the rate at which the battery was charged, [11].

**Table 7 - Comparison between commercial EVs battery pack.**

| <i>EV model</i>      | <i>Battery Size<br/>[kWh]</i> | <i>Range<br/>[km]</i> |
|----------------------|-------------------------------|-----------------------|
| Nissan Leaf          | 24                            | 199                   |
| BMW i3               | 19                            | 160                   |
| Mitsubishi i-MiEV    | 16                            | 150                   |
| Smart Electric       | 17                            | 145                   |
| Tesla S 70D          | 70                            | 390                   |
| Tesla S 85/85D/ P85D | 85                            | 426/430/407           |

Battery's SoC refers to the battery charge level at the beginning of the charging cycle. The lower the SoC, the longer it will take to charge the battery, regardless of what level of charging is applied. A battery 50% charged at the beginning of the charging cycle will take longer to charge at Level 1 than a similar battery charging from a 75% SoC using the same charger. In both instances, the time required to charge both batteries can be significantly reduced by applying a Level 2 charge, but again the battery with a beginning charge level of 50% will still take more time than the battery at 75% SoC. The battery size influences charging behavior in that a larger battery requires longer charging time and more energy to charge. However, a larger battery also requires a lower charging frequency, depending on the mobility intensity of the EV.

### Charging start-time

The charging start-time concerns at what time in the day the charging session takes place. Most of the EV drivers starting to charge their vehicles in the evening. They enable EVs to charge when they are parked at home from 09:00 p.m. until 07:00 a.m. over a longer period during the night in which electricity cost is generally is low. On the other hand, the average EV commuter is parked at work from 09:00 a.m. until around 3:00 p.m. For employees, charging at work can be a convenient way to recharge an EV whilst parked during the day, especially if the distance between the home and the workplace is quite long, [12].

The frequency of EV charging session concerns how often an EV is charged. The charging frequency, however, can vary tremendously between a minimum of once a week and a maximum of more than once in a day. The charging frequency of drivers is strongly related to the mobility intensity of the EV. From a sustainability perspective, a high charging frequency is preferred as this would require smaller batteries. This would however require high charging point density, well balanced and well-planned mobility behavior.

The charging time concerns the amount of time a charging session takes. It dependent on the vehicle battery and the charging point type. Longer periods in which the EV is connected to the charging point enable the flexibility and the potential for smart-charging technology: the electricity producer may choose to delay the transaction until the electricity demand has dropped. However, for availability problems of charging points shorter charging session are best, as this brings more potential for the charging points to be used efficiently, [13].

## **3.3 EVs Charging Profile Prediction**

Plug-in electric vehicles are gaining much popularity due to the global call for clean energy. However, there are some concerns about the possible negative impacts of EVs on the distribution networks (DNs) [14]. Indeed, significant EVs charging activities will mostly take place in users' car garages, public or corporate car parks and dedicated charging stations. Thus, EVs integration into DNs has to be

deeply investigated in order to identify the bottlenecks and benefits of their future integration scenarios [15], [16]. Large-scale development of electric vehicles will be a greater impact on the distribution grid (Figure 38). To carry out electric vehicle charging load characteristics is a prerequisite to ensure the safe operation of the grid. Usually, the aggregated power demanded by EVs in a specific area at any given time is referred to the EV charging profile [8]. Thus, the prediction of EVs charging demand is fundamental to evaluate the power system impacts of a deep EVs penetration in terms of overloading, voltage profile changes, power losses, electricity markets and power system reliability [17].

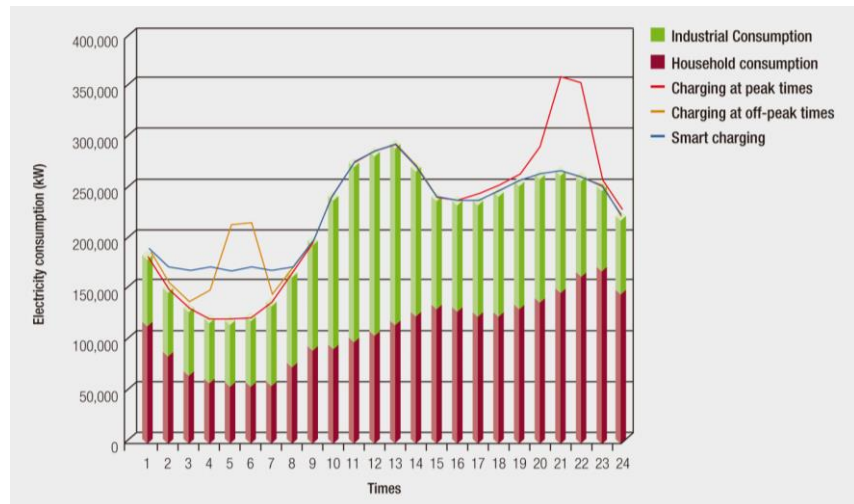


**Figure 38 - Impact of the EVs on electricity distribution grids**  
(source: Lychnos No. 6).

### State of art

Within the literature, it is possible to find many works that use a statistical approach to predict the power consumption due to EVs' charging patterns and the effects of these patterns on distribution and transmission networks [18]. In [17], different charging scenarios are examined by using a Monte Carlo-based model for PEV energy consumption, in order to evaluate the effects of such a scenario on DN transformers insulation life. In [7], results obtained from a deterministic method based on vehicle usage data are compared to the ones of a proposed stochastic approach in order to validate it. A

stochastic methodology to estimate the daily impact of aggregated vehicles charging profiles on DNs is presented in [6] while a stochastic analysis of single phase EV charging strategies impact on a residential grid is analyzed in [11]. In [19], instead, a mixed approach, combining deterministic and probabilistic methods, is discussed. In [16] and [20], the time of occupancy analysis (e.g. time period during which the feeding line provides energy to the EV battery) is performed using Markov-chains based models.

Currently, some PEVs impact studies in the literature assume PEV charging profiles dictated by utilities [14]. Those studies commonly use an arbitrary ideal charging profile optimized from the utilities' perspective. Moreover, any controlled PEV charging profile requires first knowing the uncontrolled charging profiles. Recent PEV studies try to address this issue by using travel survey data [6], [21]. This study demonstrates that accurate prediction of PEV charging profiles requires more sophisticated stochastic modeling than available literature models. Lack of proper stochastic modeling can hinder optimized integration of PEVs into electrical grid and lead to excess infrastructure, [16].

### 3.4 Vehicle Usage Data Analysis

The impact of EVs demand on DNs in terms of requested power and energy is approached by performing an analysis of a large data-set collection [7], [20], obtained from the University of Salerno (UniSa) as part of the activities of the COSMO research project [21]. UniSa parking areas are characterized in terms of conventional vehicles entry time and average parking duration. The first performed analysis is the *incoming vehicles SoC clustering*, used to divide into groups all the EVs arriving at the UniSa Campus from different points of departure and characterized by the same residual SoC. The second one concerns *parking data pattern analysis*, used to identify common behaviors of the incoming vehicles rate in parking areas during the day and in several periods of the year. Monte Carlo based simulations are carried out to correlate real parking duration, charging time and different consumption of each vehicle coming from nearby cities to the UniSa Campus. The used charging profiles are not predetermined and/or

provided by external research organizations, [22], but obtained from real world measurements at UniSa Campus.

### 3.4.1 Data Acquisition: COSMO Research Project

CO.S.MO. (Cooperative Systems for Sustainable Mobility and Energy Efficiency) was a 32-months pilot project co-founded by the European Commission under the Competitiveness & Innovation Program - ICT Policy Support Program [23]. Its scope was to prove the benefits of cooperative mobility services and to quantify their impact on increasing the energy efficiency of transportation infrastructures and vehicles. The project involved the installation of an advanced intelligent transportation system (ITS) related infrastructures and services in three pilot sites: in Göteborg (SE), Vienna (AT), and on the Campus of the University of Salerno (IT).



**Figure 39 - Parking areas in the University of Salerno (Google Maps view).**

Project industrial partners developed and applied to an urban scenario, four applications based on cooperative ITS V2I and vehicle-to-vehicle (V2V) solutions [21]. In particular, among the various equipment, several cameras and antennas systems were installed in the Campus in order to record data related to the occupancy level of parking areas and to allow vehicle to infrastructure (V2I) communication services. The cameras were positioned at the UniSA Campus entrances and exits of each parking areas (outlined in Figure 39). Installed cameras are able to read vehicles plates and thus from date and time it was possible computing the parking time. All data

was stored in a database consisting in more than 200.000 parking events over a one-year period of observation. The collected data are representative of the parking areas used by a significant number of students with their own car.

### 3.4.2 Data Clustering

The UniSA Campus is linked with many cities of Salerno and Avellino provinces. In order to assess the different state of charge (SoC) values in the case of trips made with EVs, several routes are evaluated, considering the origin-destination matrix of students enrolled at the university. The data analysis allows classifying all the different paths to reach UniSA Campus in terms of urban, extra urban and highway routes. The path are converted into electric energy consumption from the batteries of EVs (and, thus, SoC) using as PEV reference vehicle the Nissan Leaf. In detail, Nissan Leaf has a battery storage capacity of 24 kWh, whereas the average consumptions for the different route type are provided from the manufacturer and they are shown in Table 8, [24].

**Table 8 - Nissan Leaf energy consumption (source: Nissan).**

| <i>Route Type</i> | <i>Value<br/>[kWh/km]</i> |
|-------------------|---------------------------|
| Urban             | 0.160                     |
| Extra urban       | 0.126                     |
| Highway           | 0.185                     |
| Mixed             | 0.169                     |



Students PEVs are assumed leaving fully charged from each departure point of the origin-destination matrix, whose values are obtained considering the shortest path, by using Equation 1. All considered paths are divided into clusters, each one with a different residual SoC value at the UniSA arrival.

$$SoC_a = SoC_d - \frac{(c_U \cdot d_U) + (c_E \cdot d_E) + (c_H \cdot d_H)}{C^{Batt}} \quad (1)$$

where  $C^{Batt}$  [kWh] is the EV's battery capacity,  $c_U, c_E, c_H$  [kWh/km] represent the energy consumptions coefficients, and  $d_U, d_E, d_H$  [km]

are the distances covered in the urban, extra urban, and highway route, respectively.

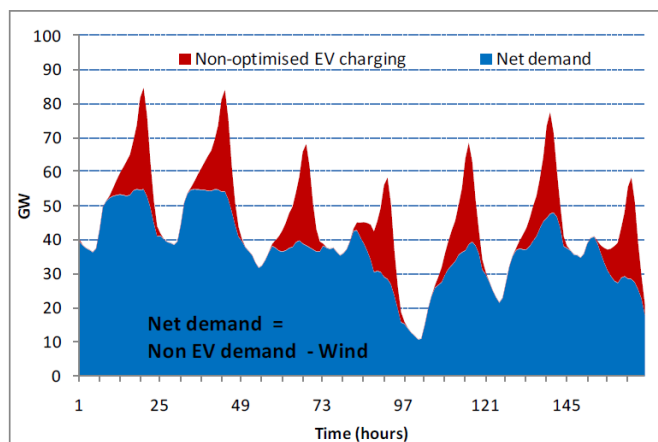
Data related to the parking areas occupancy, collected during the observation period (one year), on a day-by-day base, are analyzed in order to find common features concerning the day of the week, month, and season. Indeed, acquired data show a lower parking areas occupancy level during examination periods, summer vacations, and in the last days of the week. Thus, the variations of the parking areas occupancy are taken into account by splitting the observation period into different patterns. The pattern clustering function is implemented by using k-means algorithm because it ensures a very quickly convergence and it minimizes the total intra-cluster variance among the different patterns. In this way, the hourly rate and the parking time of the incoming vehicles in the parking areas are characterized. COSMO data allows obtaining the average vehicles reaching the Campus every 15 minutes for each day of the week during the year.

### **3.5 EVs Charging Scheduling Algorithm**

Several studies show that effective PEVs charging strategies are able to support a deeper penetration of electric vehicles within distribution networks [9], [25-26]. Thus, the need for optimal scheduling algorithms able to allow PEVs charging while avoiding negative drawbacks on DNs is becoming a relevant issue to face with future power system planning and management actions [12], [27]. Scheduling algorithms, also, aims to optimize PEVs charging cost while introducing charging models based on real-time price information or day-ahead price profiles, in order to consider the relationship between electricity prices and charging load demand, even in the presence of self-production from renewable energy resources, [13], [28-29]. For example, suppose a vehicle is plugged in from 6.00 p.m. until 7.00 a.m., giving an 11-hour window in which the vehicle can charge. If the battery can obtain sufficient charge in one hour, this charge can be scheduled to occur during an ideal hour between 6.00 p.m. and 7.00 a.m., which takes into account the electricity price, electric load, individual vehicle battery SoC and driving schedule. This will reduce consumer cost of charging and help

to balance the electricity supply and the demand (Figure 40). In order for PEV charging to be advantageous for both the PEV owners and the utility, a mechanism is needed that receives information from both the vehicles and the system dispatcher to facilitate vehicle charging. An aggregator manages the communication and electricity distribution between a group of electricity consumers and an electric utility.

### Non-optimized charging



### Smart charging

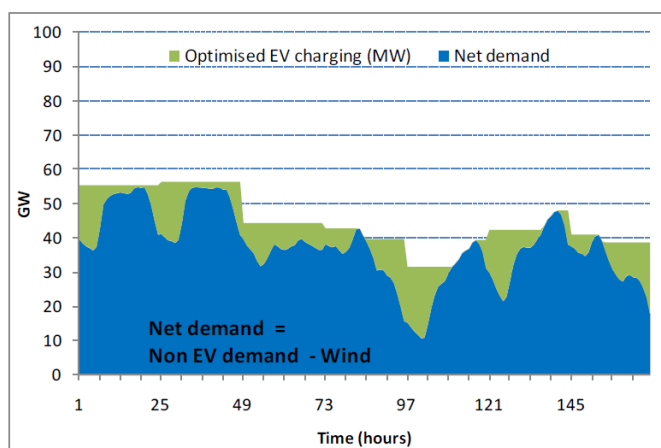


**Figure 40 - Impact of EVs on aggregated demand (source: G. Strbac - Workshop VI: integrating new technologies while maintaining resource adequacy).**

### State of art

Among the scheduling algorithms proposed in the technical literature, it is possible to distinguish two main categories based on centralized or decentralized approaches. Using decentralized algorithms, each local controller is only required to report its PEVs power demand. The supervisor entity, such as an aggregator, broadcasts a few messages from which each local controller computes its PEV charging events, avoiding simultaneous charging of large numbers of PEVs, that could destabilize the grid [30], [31]. Other works deal with distributed algorithms to locally solve the PEV-charging selection problem [32]: the PEVs' charging management strategies determine charging events in response to day-ahead price profiles broadcasted to vehicles by the utilities [28], [33]. On the other hand, the centralized scheduling algorithms provide a higher PEV integration level in the existing grid [34]: in centralized strategies, a single operator controls precisely time duration and rates of vehicles charging actions. Each PEV submits detailed information to a central processing unit, which solves an optimization problem producing the charging schedule for each PEV. These approaches consider various objectives, including power loss and/or load variance minimization, or PEV penetration level maximization [6], [11]. Within the literature, ref. [13] presents a global scheduling optimization problem in which the charging events are optimized to minimize the total PEVs charging cost during the day. Finally, [28] and [29] propose optimized PEV charging strategies in response to time-of-use (ToU) prices in a regulated market.

### **3.5.1 Mathematical Formulation**

Once introduced the main characteristics of the optimized PEVs charging algorithms and the state of the art, Section 3.5 describes the model and the features of the charging station (CS) typologies considered in this analysis. Furthermore, the proposed approach to the PEVs charge scheduling and some details on the real implementation are presented.

### 3.5.1.1 Charging Modes

It is worth to note that the adopted charging mode has a direct effect on the charging time duration. In this analysis, two types of charging modes for the incoming PEVs in the parking areas are considered: *mode 1* (230 V, 3.3 kW) for domestic use charging (AC1) and *mode 2* (230 V, 6.6 kW) for public use charging (AC2), [35]. In any case, the proposed methodology can be applied without any modification even in the case of other types of recharge mode, such as fast-charge and ultra-fast DC charge. For each charging stations  $CS_i$ , with  $i=1, \dots, N_{CS}$  and  $N_{CS}$  number of CS, the  $SoC_i$  variation at time  $dT$  of the battery connected to it is described by using the following model:

$$SoC_i(t + dT) = SoC_i(t) + \frac{V_i \cdot I_i \cdot dT}{3600 \cdot C_i^{Batt}} \quad (2)$$

where  $dT$  is the time step,  $V_i$  and  $I_i$  represent the charging voltage and current respectively at charging station  $CS_i$ , computed according to the battery charging characteristic [29] depicted in Figure 41 and approximated by (3):

$$\begin{cases} I_i = I_i^{cc} \cdot u_i^{SoC} + I_{cc} \cdot \exp\left(-\frac{t}{T_i^{cc}}\right) \cdot (1 - u_i^{SoC}) \\ V_i = V_i^{cv} \left(1 - \exp\left(-\frac{t}{T_i^{cv}}\right)\right) \cdot u_i^{SoC} + V_i^{cv} \cdot (1 - u_i^{SoC}) \end{cases} \quad (3)$$

Here  $I_i^{cc}$  and  $T_i^{cc}$  represent the current and the time constant in the constant current charging mode (*ccm*) of the battery connected to the  $CS_i$ , respectively, whereas  $V_i^{cv}$  and  $T_i^{cv}$  represent voltage and time constant for the constant voltage-charging mode (*cvm*) at the same CS.  $u_i^{SoC}$  is a binary variable to distinguish between the *ccm* and the *cvm*, as described in (4):

$$\begin{cases} u_i^{SoC} = 1 & SoC \in [0, 80]\% \\ u_i^{SoC} = 0 & SoC \in ]80, 100]\% \end{cases} \quad (4)$$

To address the worst case in terms of additional load required at the point of common coupling (PCC), the number of charging stations

available is assumed equal to the capacity of the parking areas considered. In this way, each incoming EV has its own charging station available and the number of maximum charging stations simultaneously active is limited by the maximum power available from the DN. The actual PEV charging time  $t_i^r$  at  $i$ -th CS represents the minimum value between the declared parking time  $T_i^{PARKING}$  and the time  $T_i^{CHARGE}$  requested to fully charge the vehicle connected to  $CS_i$ , computed knowing its  $SoC_i$  and the battery charging characteristics. If  $T_i^{PARKING} < T_i^{CHARGE}$ , then  $t_i^r$  is set to the time to charge the vehicle at a minimum SoC value allowing the EV to come back to its departure site.

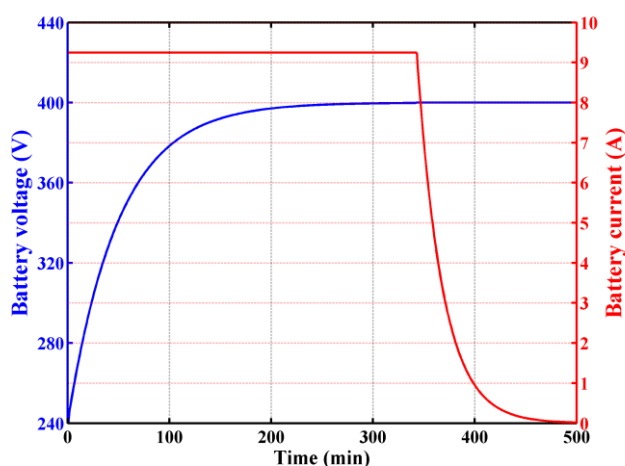


Figure 41 - Approximated battery-charging characteristic.

### 3.5.1.2 Optimized EVs Scheduling Problem

The proposed approach is a scheduling strategy based on a chronological shift of the full charging interval starting time, jointly minimizing the peak demand and the charging cost. The charging action is contained within the estimated PEV parking time according to *FCFS* - *first come first serve* - model. During each scheduling slot  $\Delta t$ , the scheduling procedure checks the parking duration declared by PEV owners and assigns the starting charge time of the vehicle in the next time intervals. The proposed scheduling technique is formulated

in the following as a mixed-integer nonlinear programming (MINLP) problem:

$$\begin{cases} \min J \\ t_i^{START} \in \mathbb{R} \\ J = \sum_{i=1}^{N_{CS}} \int_{t_i^{START}}^{t_i^{START} + T_i^{CHARGE}} M(t - t_i^{START}) \cdot [p_{BASE}(t) + p_i^{CHARGE}(t - t_i^{START})] dt \end{cases} \quad (5)$$

subject to the main constraints (6) and (7):

$$\begin{cases} t_i^{START} \geq N\Delta t \\ t_i^{START} \leq N\Delta t + (T_i^{PARKING} - T_i^{CHARGE}) \\ \int_{t_i^{START}}^{t_i^{START} + T_i^{CHARGE}} p_i^{CHARGE}(t) dt = (1 - SoC_i^{START}) C_i^{Batt} \\ 0 \leq p_i^{CHARGE}(t) \leq P_i^{BATTERY}(SoC_i, t) \end{cases} \quad (6)$$

$$\begin{cases} \sum_{i=1}^{N_{CS}} p_i^{CHARGE}(t) \leq P_{max} - p_{BASE}(t) \\ P_k = \sum_{j=1}^{N_{bus}} |V_k| |V_j| (G_{kj} \cos(\theta_k - \theta_j) - B_{kj} \sin(\theta_k - \theta_j)) \\ Q_k = \sum_{j=1}^{N_{bus}} |V_k| |V_j| (G_{kj} \sin(\theta_k - \theta_j) - B_{kj} \cos(\theta_k - \theta_j)) \end{cases} \quad (7)$$

where  $t_i^{START}$  is the EV charging starting time of the  $i$ -th vehicle connected to the  $CS_i$ ,  $p_{BASE}$  is the base load at time  $dT$ ,  $p_i^{CHARGE}$  is the charging power supplied to the  $i$ -th PEV and  $M$  represents the unit price depending on the hours of the day. In (6),  $N$  is the number of past scheduled slots,  $SoC_i^{START}$  and  $P_i^{BATTERY}$  are the SoC value and the maximum acceptable charging power of the incoming  $i$ -th PEV (3) respectively. Finally, in (7),  $P_{max}$  is the maximum power drawn from the main external DN's PCC, whereas  $P_k$  and  $Q_k$  equations are the power flow constraints, with the classic meaning of the symbols.

### 3.5.2 Solution Algorithm

Distribution network constraints and battery charging characteristic are nonlinear equations. For this reason, a heuristic algorithm based on

genetic algorithm (GA) is proposed to solve the scheduling problem, [36]. GA is an adaptive heuristic search algorithm based on the evolutionary ideas of natural selection and represents very effective techniques to quickly finding a reasonable solution to complex non-linear problems, such as those presented in the section 3.5.1.

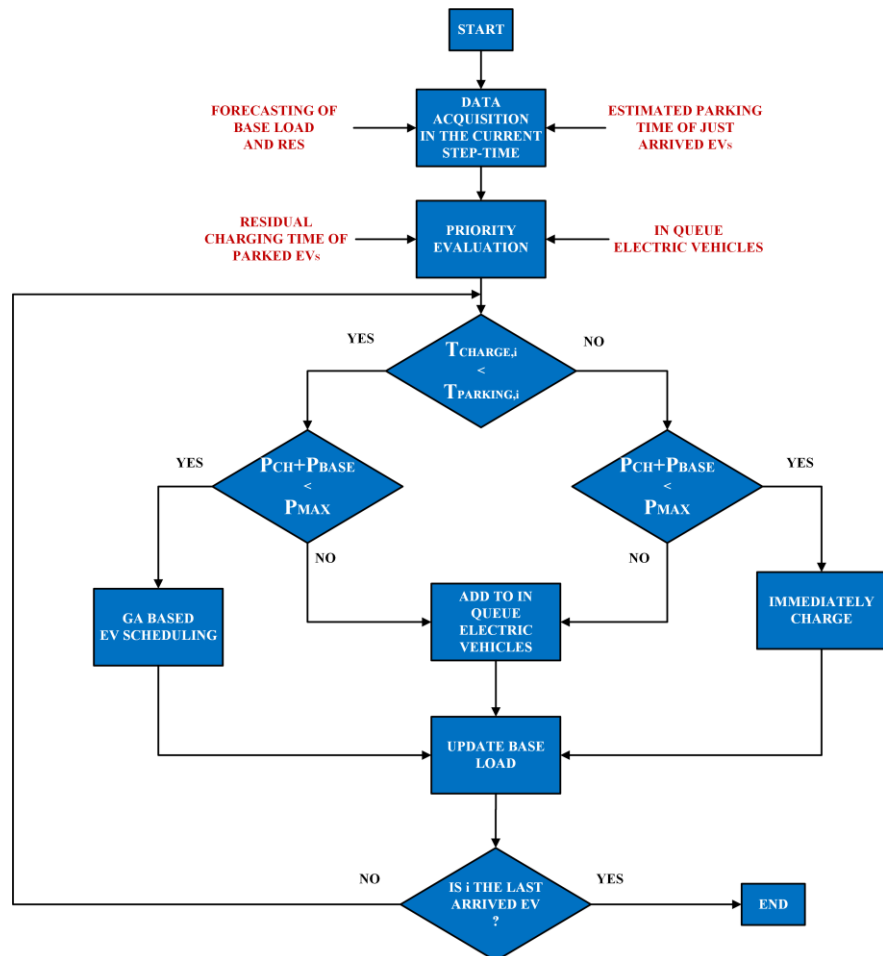


Figure 42 - Scheduling Algorithm Block Diagram.

In a genetic algorithm, a population of candidate solutions (called individuals) to an optimization problem is evolved toward better solutions. Each candidate solution has a set of properties (its chromosomes or genotype) which can be mutated and altered; traditionally, solutions are represented in binary as strings of 0s and

1s, but other encodings are also possible. The evolution usually starts from a population of randomly generated individuals, and is an iterative process, with the population in each iteration called a generation. In each generation, the fitness of every individual in the population is evaluated; the fitness is usually the value of the objective function in the optimization problem being solved. The more fit individuals are stochastically selected from the current population, and each individual's genome is modified (recombined and possibly randomly mutated) to form a new generation. The new generation of candidate solutions is then used in the next iteration of the algorithm. Commonly, the algorithm terminates when either a maximum number of generations has been produced, or a satisfactory fitness level has been reached for the population.

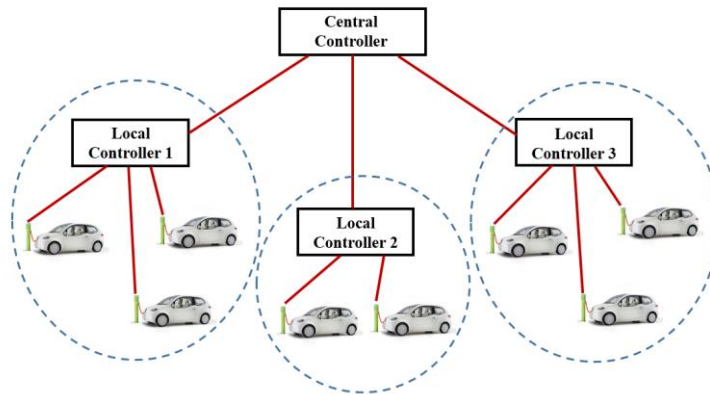
The GA-based scheduler for each incoming PEV computes the time slot sequence available to charge each vehicle. Thus, for each PEV we use a binary chromosome changing its length according to  $T_i^{CHARGE}$  and  $T_i^{PARKING}$ . The chromosome length also affects the simulation speed performance and the reliability of the final solution. Therefore, a limit of 1000 iterations is imposed to the optimization procedure and 20 chromosomes are used to compose the population.

Figure 42 shows the block diagram of the proposed EVs scheduling algorithm. In particular, after receiving the information about the base load and the RES production, the algorithm performs a preliminary analysis on estimated parking time of the just arrived EVs and on the residual charging time of parked EVs, in order to select the vehicles having to wait in queue for the next time slot. For each vehicle arrived in the current time slot, the proposed algorithm performs the scheduling routine. It allows the immediate charge or adds the vehicle to the waiting queue, according to the estimated parking time, the charging time and the maximum power from the drowned main external DN's CCP. Finally, it updates the current value of the base load and the algorithm repeats the cycle for the next EVs arrived in the parking area during the current time slot.

### 3.5.3 Scheduler Architecture and Protocol

In Figure 43 is shown the proposed scheduling scheme: a central controller is assumed receiving the forecasted base load and the

production from renewable sources for the day. Each charging station communicates with local controllers to collect the PEV information. Central controller performs scheduling optimization deciding when to charge each PEV according to provided data. In Table 9, is shown the central and local controller scheduling protocol performed on a daily base.



**Figure 43 - Locally optimal scheduling scheme.**

**Table 9 - Proposed EV scheduling protocol.**

|   |
|---|
| <p><b>Initialize:</b> The central controller forecasts the base load (and eventually the production from renewable energy sources - RES) for the current day.</p>   |
| <p><b>Loop</b> (Each local controller for each time slot):</p> <ol style="list-style-type: none"> <li>1. receive the scheduled charging session for the actual time slot from the central controller;</li> <li>2. acquire new charging request;</li> <li>3. update in charging vehicles status;</li> <li>4. send data to the central controllers.</li> </ol> <p><b>End</b></p>  |
| <p><b>Loop</b> (Central controller for each time slot):</p> <ol style="list-style-type: none"> <li>1. receive the new charging request and the in charging vehicles status for the actual time slot from the central controller;</li> <li>2. run the PEVs scheduling strategy to all the vehicles in the parking area;</li> <li>3. update base load profile adding in charge PEVs and the hourly electricity cost;</li> <li>4. update the forecast of the base load, including the RES</li> <li>5. send data to the local controllers.</li> </ol> <p><b>End</b></p> |
| <p>Evaluation of the PEVs charging service statistics.</p>  |

After receiving the scheduled PEV for the current time, the functionalities of the local controllers in each time slot consist firstly in acquiring the new charging request from the incoming vehicles and then updating the SoC status of the charging PEVs. The central controller receives the new charging request and the PEV status from the local controllers and performs the scheduling optimization updating the base load adding actual charging load for each PEV in the parking lot. At the end of the day, the central controller calculates the data related to the charging service provided to the users in order to evaluate the performance of the scheduling strategy.

## 3.6 Simulation Framework

This Section describes the case study and a representative set of the results obtained from the extensive simulation framework performed. To test the effectiveness of the presented methodology, a Monte Carlo simulation framework is implemented to calculate the PEVs charging power needs starting from an assigned SoC distribution [12]. The adopted method allows evaluating the effects of different charging station typologies on the PEVs power absorption patterns. Starting from the results of the Monte Carlo analysis, the PEVs charging scheduling algorithm is run to evaluate its performance, [35].

### 3.6.1 Case Study

The impact of a deep penetration of PEVs in DNs is investigated by using the model of the University of Salerno (UniSA) microgrid. The UniSA network has several distributed generators (DG) connected to the grid:

- two cogeneration (CHP) units, with a rated power of 580 kW each one;
- eight photovoltaic (PV) power plants for a total PV rated power of 1076 kW installed on the roof of Campus buildings.

CHP units produce both electricity used to supply the loads and thermal energy used to heat water of Campus sport facilities.

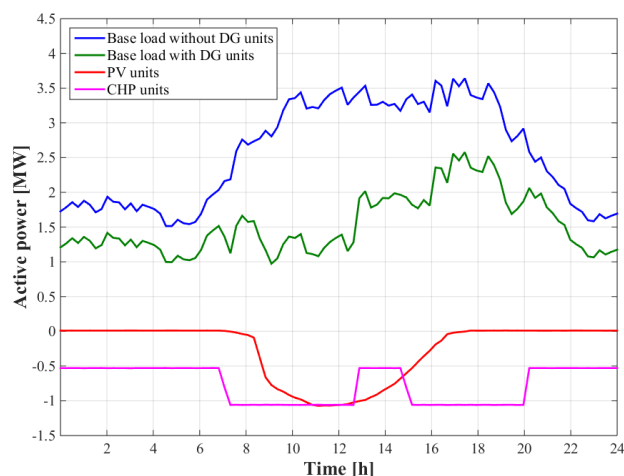


**Figure 44 - Active power drawn from the DN external to the UniSA microgrid.**

Figure 44 shows the typical daily profiles of the net active power drawn from the main external PCC by the UniSA network. Blue and green lines depict the active power absorption with and without internal PVs and CHPs, respectively. Finally, red and pink lines show the average (calculated every 15 minutes) active power generated by the PV and CHP units.

**Table 10 - Daily price categories for the electricity cost.**

| <i>Price Category</i> | <i>Hours</i>  | <i>Days</i>                                    |
|-----------------------|---|--|
| <b>F1 - Peak</b>      | 10:00 - 15:00 /<br>18:00 - 21:00                    | Monday - Friday                                |
| <b>F2 - Mid-level</b> | 07:00 - 10:00 /<br>15:00 - 18:00 /<br>21:00 - 23:00 | Monday - Friday<br>+ Saturday<br>07:00 - 23:00 |
| <b>F3 - Off-peak</b>  | 23:00 - 07:00                                       | All week and<br>holidays                       |

Table 10 shows the three hourly price categories for the electricity cost in the UniSA Campus. Adopting the actual price of electricity in the city, the prices of the peak, mid-level and off-peak load period are 0.187 €/kWh, 0.142 €/kWh and 0.103 €/kWh, respectively [37].

### 3.6.2 Numerical Results

By using the proposed data-pattern method related to the arriving EVs in the parking areas and knowing their SoC distribution, several Monte Carlo simulations are carried out. In this work, 30'000 iterations are imposed by running the proposed algorithm on a workstation with an Intel® Core™ i7 (3.20 GHz, 64 bit) processor, 16 GB of RAM and Matlab™ R2014b. Starting from the results of the Monte Carlo analysis, the EVs charging scheduling algorithm is performed to evaluate its performance.

#### 3.6.2.1 Data Clustering Results

By analyzing parking data of the UniSA Campus and considering the shortest path to reach the Campus, 50 clusters are derived, each one with a different residual SoC value at the UniSA arrival. Assuming the PEVs leaving fully charged from their departure points and taking into account the PEV consumption, Figure 45 shows residual SoC statistical distribution related to the departure sites.

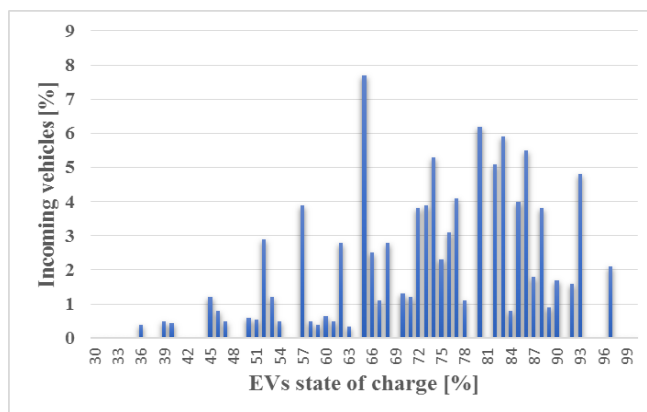


**Figure 45 - Residual SoC distribution of incoming vehicles.**

The average residual SoC value of PEVs arriving at the UniSA is approximately equal to 70%. Figure 46 illustrates the statistical distribution of the EVs average parking time: data analysis shows that the most frequent value of the parking time is between 3 hours and 3.5 hours.

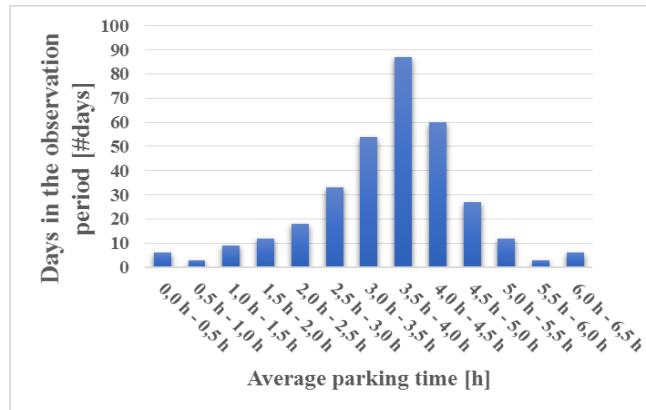


**Figure 46 - Statistical distribution of average parking time.**

In Figure 47, all the observed days are divided into two main clusters: the first one concerning the institutional courses period and the second one related to the examination period. The courses period cluster is characterized by days in which the PEVs' arrival rate is significantly greater than those are in the examination period cluster.

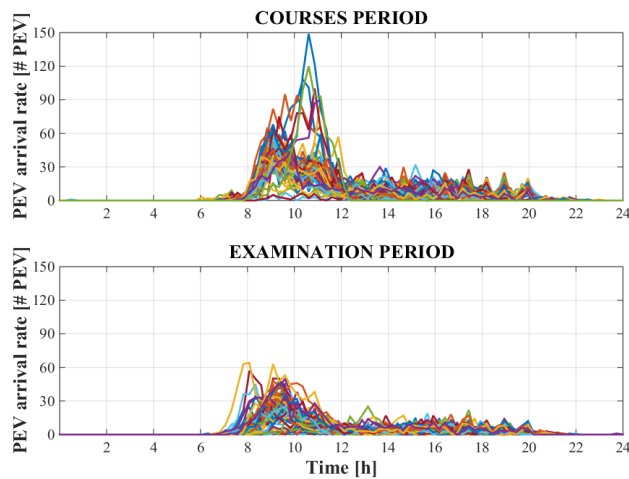


**Figure 47 - Two PEV main arrival rate cluster on all observation days.**

In detail, days in the courses period cluster are characterized by an average PEVs' arrival rate in the hours between 10:00 a.m. and 12:00 p.m. approximately equal to 80 vehicles each 15 minutes. It is possible to subdivide the first main pattern into three other different sub-clusters: from Monday to Wednesday, Thursday and Friday

respectively. In Figure 48 is shown the PEVs’ arrival rate pattern to one parking area for each day of the week, during the institutional courses periods.

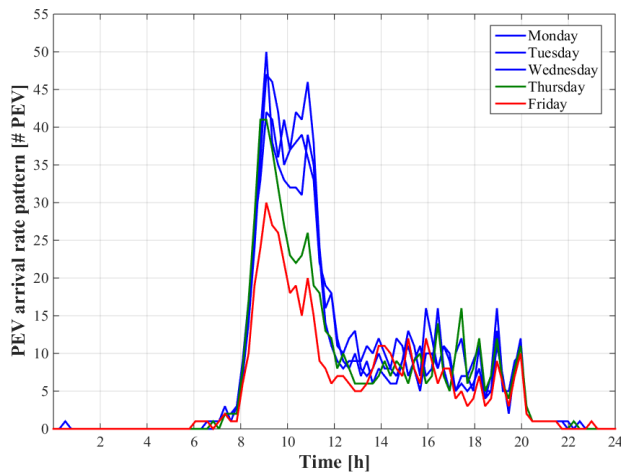


**Figure 48 - Centroids of the PEV arrival rate clusters during courses period.**

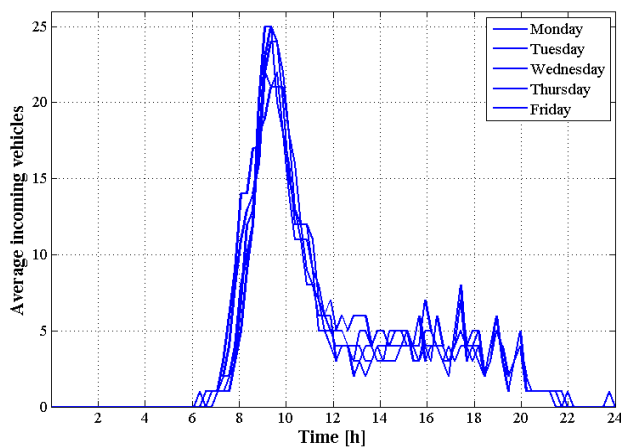


**Figure 49 - Centroid of the PEV arrival rate cluster during examination period.**

The examination period is considered as a single cluster (Figure 49), because of the absence of relevant differences among the weekdays. Thus, four different daily patterns are assumed adequate to describe arrival rate concerning the three parking areas. Since the daily incoming vehicles SoC and arrival order to the parking areas are

not known in advance, but only statistical distributions are available for these data, we implemented a Monte Carlo approach to calculate the EVs charging power for different days related to a given arrival pattern. Thus, the proposed method allowed to evaluate the effect of different charging station technologies on the EVs power absorption patterns.

The following step-by-step procedure of the Monte Carlo based algorithm is implemented for each parking area and for each EVs incoming pattern.

- 1) Generate randomly incoming EVs, such as SoC values by clustering analysis, keeping the same distribution of the student's cities membership.
- 2) Compute EVs charging daily profile according to one incoming vehicles pattern.
- 3) Repeat from Step 1 until reaching the maximum number of iterations in Monte Carlo simulation.
- 4) Compute the average, minimum, and maximum daily charging profile.

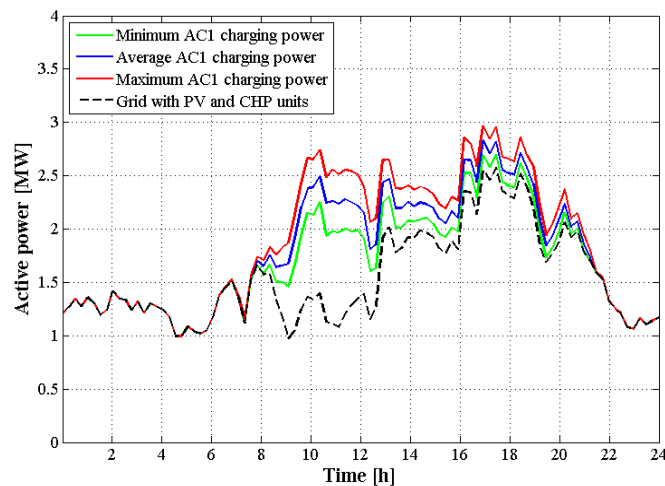


**Figure 50 - Active power absorbed to the delivery node with AC1 charging stations.**

The minimum daily charging profile is obtained by considering the minimum power consumption among all the iterations of the Monte

Carlo simulation every 15 minutes. In a similar way, the average charging profile and the maximum one are computed. Finally, by means of daily-charging profiles for each recognized pattern, the impact on the power grid is assessed in term of absorbed power and energy compared to the normal consumption of the Campus.

Figure 50 and Figure 51 show the grid impact in terms of increased power consumption at the delivery node due to the AC1 and AC2 modes, respectively. The variation of the load profile to the point of common coupling with the external grid (PCC) is more pronounced in the hours between 8:00 a.m. and 12:00 a.m. where the incoming vehicle rate is greater.

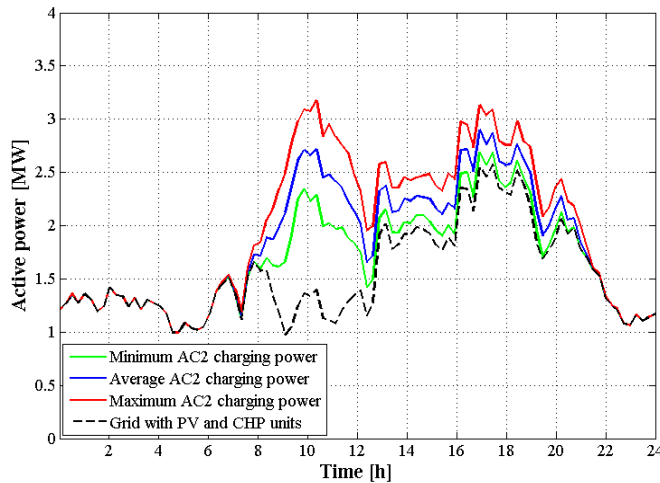
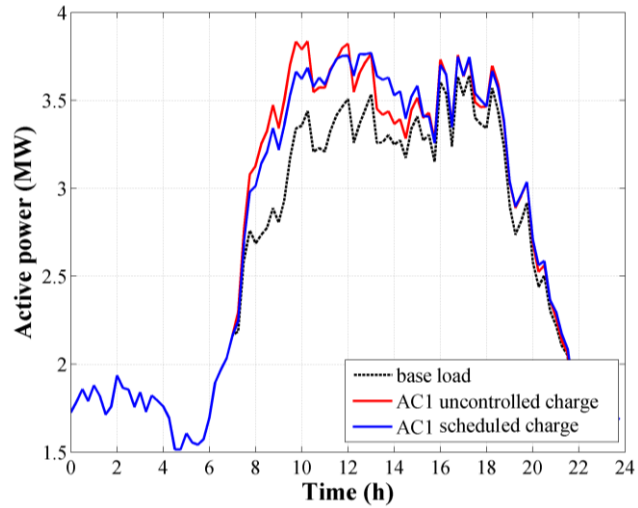


Figure 51 - Active power absorbed to the delivery node with AC2 charging stations.

### 3.6.2.2 Scheduled EV Charging Results

In the following, results obtained from the performed simulation framework are discussed. In particular, it is reported the comparison between the proposed scheduled charging strategy and a conventional charging strategy based on the chronological shift of the full charging interval starting time. The comparison is performed for each one of the considered charging modes (AC1 and AC2).



**Figure 52 - Comparison between uncontrolled and conventional scheduled AC1 charge.**

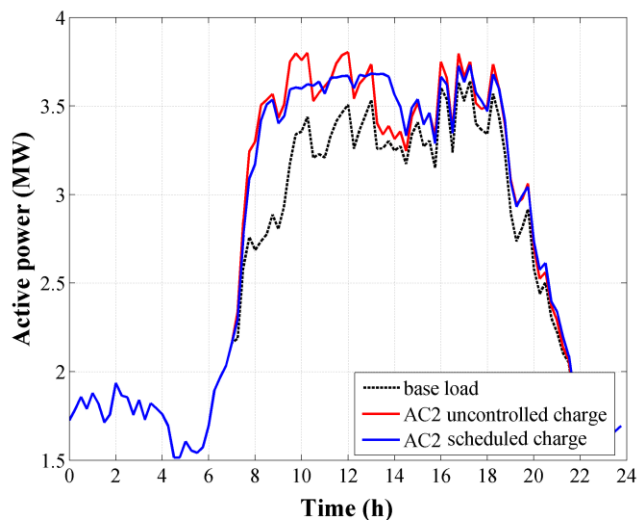


**Figure 53 - Comparison between uncontrolled and conventional scheduled AC2 charge.**

Figure 52 and Figure 53 show the comparison between the uncontrolled charge and the conventional scheduling strategy assuming AC1 and AC2 charging modes, respectively.

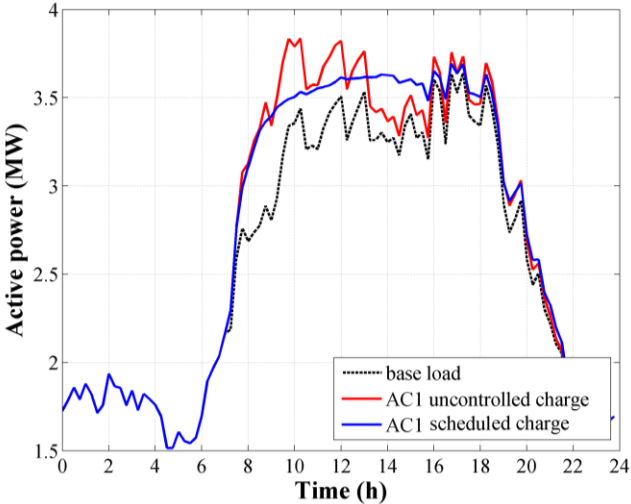


Figure 54 - Comparison between uncontrolled and proposed scheduled AC1 charge.

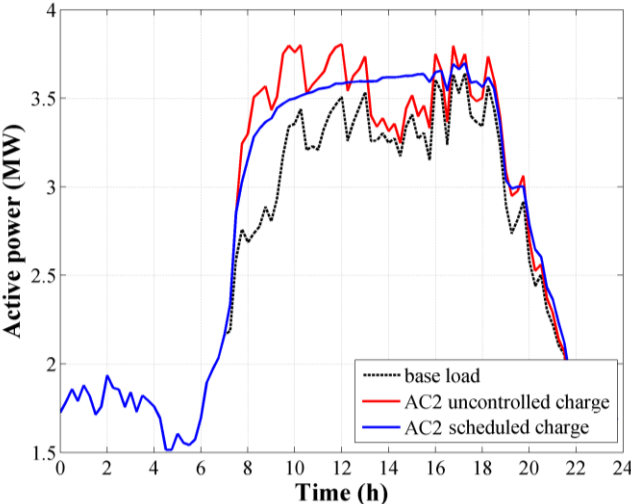
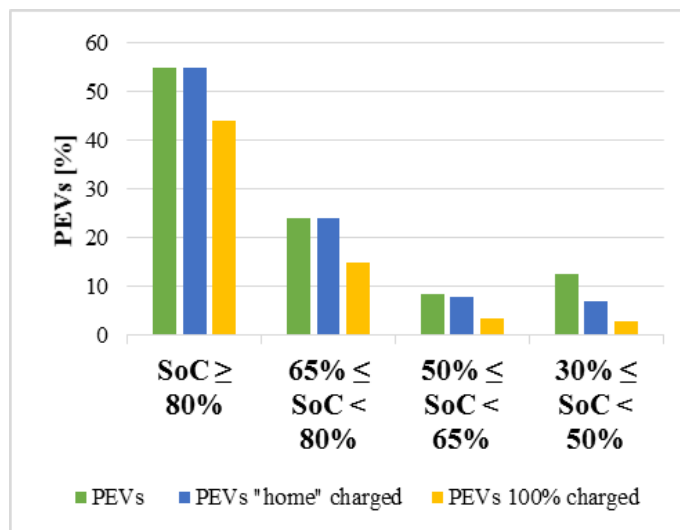


Figure 55 - Comparison between uncontrolled and proposed scheduled AC2 charge.

It is worth to note a flattened load profile and a significant reduction in the active power absorption peak in the hours between 8:00 a.m. and 12:00 p.m. compared to the uncontrolled charging. In particular, we observe a reduction of 184 kW for AC1 charging station and a reduction of 217 kW for AC2 charging station at 9:45 a.m. The

load profile is significantly increased during the hours of low demand, e.g. between 2:00 p.m. and 4:00 p.m. Figure 54 and Figure 55 show the comparison between the proposed scheduling algorithm and the uncontrolled charge for AC1 and AC2 charging modes. The proposed scheduling allows obtaining better performance using the valleys in the demand profile more efficiently. Results show more significant reductions of active power peak absorption than the conventional scheduling strategy. In particular, the proposed algorithm presents, at 9:45, a peak reduction of 392 kW and 383 kW for AC1 and AC2 charging stations, respectively.



**Figure 56 - Average PEVs charged in a day: AC1 scheduling charge.**

Furthermore, Figure 56 and Figure 57 show the comparison on battery SoC level reached by PEVs in a single day between AC1 and AC2 scheduled charge. In particular, PEVs having battery SoC level able to get home the user, and fully charged PEVs are assumed as performance indices. The results show that the scheduling charge using the AC1 mode ensures all users with residual SoC value higher than 50% to come back to their starting point, but not to fully charge their vehicle. For users with residual SoC value less than 50% (about 20% of all PEVs in a single day), the performance indices are higher than 70%. AC2 scheduled charging, however, ensures that all

incoming vehicles in a day are able to come back to their starting point, but only 90% of the PEVs can fully charge their vehicle.

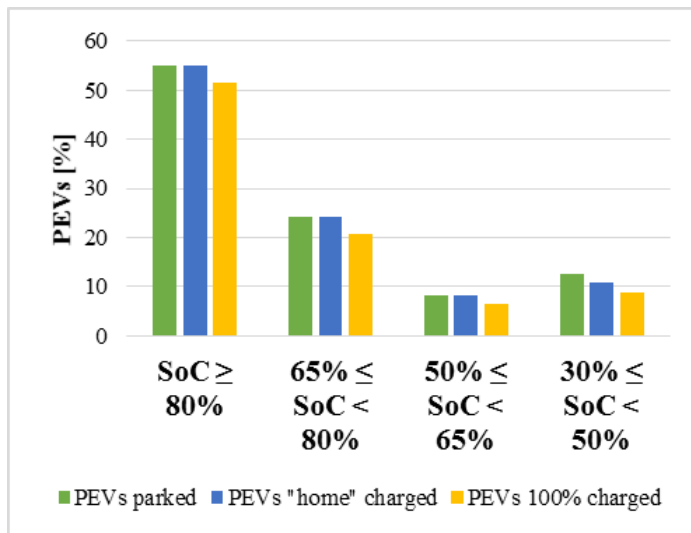


Figure 57 - Average PEVs charged in a day: AC2 scheduling charge.

Table 11 - Charging extra time (AC1 and AC2 mode).

| Residual SoC [%] | Average extra time [min] |          |
|------------------|--------------------------|----------|
|                  | AC1 MODE                 | AC2 mode |
| SoC ≥ 80         | 45                       | 18       |
| 65 ≤ SoC < 80    | 74                       | 30       |
| 50 ≤ SoC < 65    | 99                       | 46       |
| 30 ≤ SoC < 50    | 121                      | 52       |

Table 11, show the comparison concerning the charging extra time by using the proposed scheduling strategy between AC1 and AC2 mode. The average extra time required to complete the PEVs charge, is considered when  $T^{PARKING} < T^{CHARGE}$ . Using AC1 charging mode PEVs with the lowest residual SoC value have to wait for an average extra-time about 2 hours, whereas AC2 charging mode allows obtaining average extra-time less than 1 hour.

Finally, Table 12 show the comparison concerning the average charging cost by using the proposed scheduling strategy. By using the

proposed scheduling strategy, each user has a slight reduction in the average charging cost because the chronological shift of the charge allow obtaining a lower electricity cost. In particular, the user average charging cost is reduced by 16.2% and 18.5% compared to uncontrolled charge and considering AC1 and AC2 mode, respectively.

**Table 12 - Charging cost (AC1 and AC2 mode).**

| <i>PEV charge</i>   | <i>Average charging cost [€]</i> |                 |
|---------------------|----------------------------------|-----------------|
|                     | <i>AC1 MODE</i>                  | <i>AC2 mode</i> |
| <b>Uncontrolled</b> | 1.78                             | 1.62            |
| <b>Scheduled</b>    | 1.49                             | 1.32            |

## References

- [1] J. Larminie, J. Lowry, "Electric Vehicle Technology Explained", *John Wiley & Sons*, 2nd Edition, 2012.
- [2] I. Husain, "Electric and Hybrid Vehicles: Design Fundamentals", *CRC Press*, 2nd Edition, 2010.
- [3] IEC 62196-1 – available on line at URL: <https://webstore.iec.ch/publication/6582>
- [4] <https://www.press.bmwgroup.com/global/pressDetail.html?title=bmw-group-is-pressing-ahead-with-the-development-of-systems-for-inductive-charging-of-electric-and&outputChannelId=6&id=T0186710EN&>
- [5] [https://www.teslamotors.com/en\\_GB/blog/battery-swap-pilot-program?redirect=no](https://www.teslamotors.com/en_GB/blog/battery-swap-pilot-program?redirect=no)
- [6] S. Rezaee, E. Farjah, B. Khorramdel, "Probabilistic analysis of plug-in electric vehicles impact on electrical grid through homes and parking lots", *IEEE Transaction on Sustainable Energy*, vol.4, pp. 1024-1033, Oct. 2013.
- [7] Ashtari, E. Bibeau, S. Shahidinejad, T. Molinski, "PEV charging profile prediction and analysis based on vehicle usage data", *IEEE Transaction on Smart Grid*, vol.3, pp. 341-350, March. 2012.
- [8] Z. Darabi, M. Ferdowsi, "Aggregated impact of plug-in hybrid electric vehicles on electricity demand profile", *IEEE Transactions on Sustainable Energy*, vol.2, no. 4, 2011, pp. 501-508.
- [9] O. Sundstroem, C. Binding, "Flexible charging optimization for electric vehicles considering distribution grid constraints", *IEEE Trans. on Smart Grid*, vol. 3, 2012, pp. 26-37.

- [10] J. Quiros-Tortos, L.F. Ochoa, B. Lees, "A statistical analysis of EV charging behavior in the UK", *Innovative Smart Grid Technologies Latin America (ISGT LATAM), IEEE PES Conference*, 2015, pp. 445-449.
- [11] E. Veldman, R.A. Verzijlbergh, "Distribution Grid Impacts of Smart Electric Vehicle Charging From Different Perspectives", *IEEE Trans. on Smart Grid*, vol. 6, pp. 333-342, Jan. 2015.
- [12] V. Calderaro, V. Galdi, G. Graber, G. Massa, A. Piccolo, "Plug-in EV Charging Impact on Grid Based on Vehicles Usage Data", in *Proc. of Electric Vehicle, IEEE International Conference on 2014*, pp. 1-7.
- [13] He Yifeng, B. Venkatesh, Guan Ling, "Optimal Scheduling for Charging and Discharging of Electric Vehicles", *IEEE Trans. on Smart Grid*, vol. 3, pp. 1095-1105, Sept. 2012.
- [14] Shao Yun Ge, Long Wang, Hong Liu, Liang Feng, "The impact of discharging electric vehicles on the distribution grid", in *Proc. of IEEE Innovative Smart Grid Technologies - Asia (ISGT Asia)*, 2012, pp. 1-4.
- [15] M. Zhang, J. Chen, "The energy management and optimized operation of electric vehicles based on microgrid", *IEEE Transactions on Power Delivery*, vol.29, no. 3, 2014, pp. 1427-1435.
- [16] L. Pieltain Fernández, T.G.S. Román, R.Cossent, C.M. Domingo, P.Frías, "Assessment of the Impact of plug-in electric vehicles on distribution networks", *IEEE Transactions on Power Systems*, vol. 26, no. 1, 2011, pp. 206-213.
- [17] Q. Gong, S. Midlam-Mohler, V. Marano, G. Rizzoni, "PEV charging impact on residential distribution transformer life", in *Proc. of IEEE Energytech*, 2011, pp. 1-6.
- [18] K. Petrou, J. Quiros-Tortos, L.F. Ochoa, "Controlling electric vehicle charging points for congestion management of UK LV networks", in *Proc. of Innovative Smart Grid Technologies (ISGT), IEEE Conference*, 2015, pp.1-6.
- [19] F.H.P. Zamora, H. Kagan, M.A.Pelegrini, L.G. Gardiman, L. Zamboni, M. Gavazzi, M.A.P.Fredes, C.A.M. Gonçalves, J.P. Niggli Silva, "Evaluation of the impact of electric vehicles on distribution systems combining deterministic and probabilistic approaches", in *Proc. of 22nd International Conf. and Exhib. on Electricity Distribution*, 2013, pp. 1-4.
- [20] Gong Qiuming, S. Midlam-Mohler, V. Marano, G. Rizzoni, Y. Guezennec, "Statistical analysis of PHEV fleet data", in *Proc. of Vehicle Power and Propulsion Conference*, 2010, pp. 1-6.
- [21] G. Alcaraz, V. Galdi, A. Trapuzzano, "Cooperative Systems for Energy Efficiency and driver behaviour change: University of Salerno Pilot Site Results", in *Proc. of 9th ITS European Congress*, 4-7 June, 2013.
- [22] V. Calderaro, V. Galdi, G. Graber, G. Graditi, F. Lamberti, "Impact assessment of energy storage and electric vehicles on smart grids", in *Proc. of Electric Power Quality and Supply Reliability (PQ), IEEE International Conference*, 2014, pp. 15-18.
- [23] COSMO (2015), "Co-Operative Systems for Sustainable Mobility and Energy Efficiency." COSMO Website. Accessed October 5, 2015 available on-line at: <<http://www.cosmo-project.eu/>>.

- [24] Nissan, “Nissan Leaf prices and specifications”, available on-line at: <[http://media.nissan.eu/content/dam/pes/GB/leaf/prices\\_and\\_equipment/pdf/New-LEAF-Tech-Spec-and-Pricesv3.pdf](http://media.nissan.eu/content/dam/pes/GB/leaf/prices_and_equipment/pdf/New-LEAF-Tech-Spec-and-Pricesv3.pdf)>, 2013, pp. 1-7.
- [25] P. Rezaei, J. Frolik, P.D.H. Hines, “Packetized Plug-In Electric Vehicle Charge Management”, *IEEE Transaction on Smart Grid*, vol. 5, pp. 642-650, March 2014.
- [26] J. de Hoog,, T. Alpcan, M. Brazil, D.A. Thomas, I. Mareels, “Optimal Charging of Electric Vehicles Taking Distribution Network Constraints Into Account”, *IEEE Transaction on Power Systems*, vol. 30, pp. 365-375, Jan. 2015.
- [27] J. Timpner, L. Wolf, “Design and Evaluation of Charging Station Scheduling Strategies for Electric Vehicles”, *IEEE Transaction on Intelligent Transportation Systems*, vol. 15, pp. 579-588, April 2014.
- [28] P. Balram, T. Le Anh, Guan Ling, “Effects of plug-in electric vehicle charge scheduling on the day-ahead electricity market price”, in *Proc. 2012 IEEE ISGT Europe Int. Conf.*, pp. 1-8.
- [29] Yijia Cao, Shengwei Tang, Canbing Li, Peng Zhang, Yi Tan, Zhikun Zhang, Junxiong Li, “An Optimized EV Charging Model Considering TOU Price and SOC Curve”, *IEEE Trans. on Smart Grid*, vol. 3, pp. 388-393, March 2012.
- [30] Chao-Kai Wen, Jung-Chieh Chen, Jen-Hao Teng, Pangan Ting, “Decentralized Plug-in Electric Vehicle Charging Selection Algorithm in Power Systems”, *IEEE Trans. on Smart Grid*, vol. 3, pp. 1179-1789, Dec. 2012.
- [31] E. Akhavan-Rezai, M.F. Shaaban, E.F.El-Saadany, A. Zidan, “Uncoordinated charging impacts of electric vehicles on electric distribution grids: Normal and fast charging comparison”, in *Proc. of IEEE Power and Energy Society General Meeting*, 2012, pp. 1-7.
- [32] Lingwen Gan, U. Topcu, S.H. Low, “Optimal decentralized protocol for electric vehicle charging”, *IEEE Trans. on Power Systems*, vol. 28, pp. 940-951, May 2013.
- [33] S. Vandael, B. Claessens, D. Ernst, T. Holvoet, G. Deconinck, “Reinforcement Learning of Heuristic EV Fleet Charging in a Day-Ahead Electricity Market”, *IEEE Trans. on Smart Grid*, vol. 6, pp. 1795-1805, Jul. 2015.
- [34] Tang Wanrong, Suzhi Bi, Y.J.A. Zhang, “Online Coordinated Charging Decision Algorithm for Electric Vehicles without Future Information”, *IEEE Trans. on Smart Grid*, vol. 5, pp. 2810-2824, Nov. 2014.
- [35] G. Graber, G. Massa, V. Galdi, V. Calderaro, A. Piccolo, “Performance Comparison between Scheduling Strategies for PEVs Charging in Smart Grids”, in *Proc. of Renewable Energy Research and Applications, IEEE International Conference on*, 2015, pp. 1-6.
- [36] M. Mitchell, “An Introduction to Genetic Algorithms”, *MIT Press*, 1998.
- [37] Enel Distribuzione, “Price categories for the electricity cost”, available on-line at: <<https://www.enelservizioelettrico.it/it-IT/tariffe/altri/bta-6-trioraria>>.



## Chapter 4

# Energy Efficiency in Metro Systems

The expected growth in penetration of electrified mass transportation in urban and suburban areas and significant contribution in terms of energy consumption characterizing the railway and metro services in urban and metropolitan areas is focusing the attention of researcher and technicians mainly to the energy efficiency issue on subways, trams and light rail.

This chapter introduces and discusses some innovative solutions for energy efficiency in urban railway systems, in particular, focusing on energy storage systems and eco-drive train operations in metro networks. In Section 4.1, it is shown the state of the art regarding the design and implementation of energy storage systems (ESSs) and the most widely used techniques to calculate metro vehicle speed profiles minimizing energy consumption. Following, Section 4.2 describes the electrical models describing the railway system. In particular, the train, the contact wire, the electrical substation and the ESSs submodels are analyzed. Sections 4.3 and 4.4 deal with the joint problem of ESSs sizing and positioning along the track and the problem of calculating eco-drive speed profiles for metro vehicle, respectively. The mathematical formulation of these optimization problems and the proposed solution algorithms are illustrated and discussed. Finally, Section 4.5 show simulations results carried out by using a real case study data. The research activities and the obtained results are part of the activities carried out in the research project: “*SFERE - Sistemi Ferroviari: Ecosostenibilità e Risparmio Energetico*”, developed with the financial support of National Operative Program PON R&C.

## 4.1 Innovative Solution for Energy Efficiency

To improve the energy efficiency in electrified transport systems is necessary to know the main components that are responsible for the largest power absorption. The energy consumptions in urban railway system, according to FS (Ferrovie dello Stato Italiane) data, are split in Figure 58, [1].

- Railway traction system
- Infrastructure service utilities (heating, lightning, ...)
- Railway signaling system

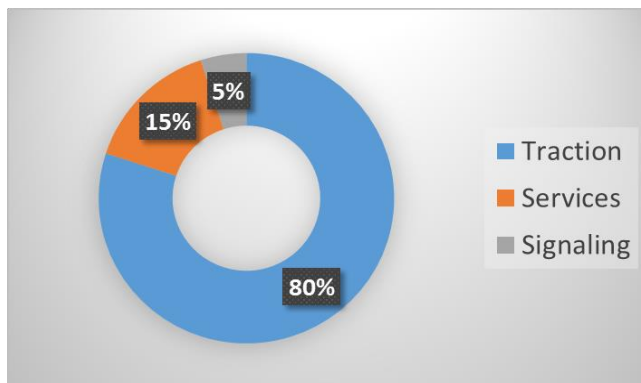


**Figure 58 - Distribution of energy consumption in electrified transport systems (source: RFI Data).**

About 80% of the overall energy supplied to the railway system is used by traction elements, whereas 15% represents the infrastructure service utilities consumption and the railway signaling system requires the remaining 5%. Since the largest contribution to the energy consumption comes from the traction system, therefore we will find the most used solutions to improve the transportation energy efficiency focusing on it. To reduce the energy consumption of railway traction systems, research mainly focuses on development of more efficient technologies and designs.

In the field of *component-based lightweight design*, the use of new materials or innovative traction components offer substantial potential

for mass reduction [2]. As in past years, the aluminum car-bodies have replaced the steel constructions, in the future the developments in car-body construction point in the direction of an increasing use of carbon fiber materials. For the mass reduction of bogies, which account for over one third of the train weight, several innovative and conventional concepts exist. However, they usually entail changes in the whole system design of the train and have to be considered as *system-based lightweight design*. One of the promising option is to replace conventional 2-axle bogies with single axle bogies. For suburban and regional vehicles, modern curve-steered single-axle running gear exists and is successfully in use. In recent years, mechatronic revolutionized suspension technologies for railways based on sensors, controllers and actuators and it considerably reduced train weight. Developments in this field range from electronically controlled single-axle running gear to wheel-sets with two.

Mechanical friction comprises all the dissipative effects of wheel-rail interaction, mainly linear friction caused by dissipation in the wheel-rail interface and curve resistance is the additional resistance in curves due to increased frictional forces in curves [3]. The sum of the two effects usually accounts for less than 10% of a train's energy consumption. Rail lubrication aims at reducing lateral friction between rail and wheel. This is especially effective in curves but can also be applied on tangent tracks. Since linear friction is proportional to train mass, reduced friction is an automatic side effect of light weight efforts. Aerodynamic aspects are also of great interest for railway operation, not only for energy considerations, but also for noise reduction and passenger comfort [3]. Two features mainly determine the air drag experienced by a travelling train: its external geometry and its surface roughness. Since a major part of the air resistance is due to transitions between laminar and turbulent flows, the aerodynamics of sides and roofs can be effectively improved by avoiding sharp changes in the vehicle's surface geometry. Measures include covering the underfloor equipment, optimizing windows, doors and the transition between coaches as well as coating the train surface with an aerodynamically smooth materials.

Regarding the drive train components, Figure 59 shows the power losses distribution in the metro vehicle propulsion system: the power transformer represents the largest source of energy waste, then the

electric motor and at least the power converter represents a small part of losses [1].

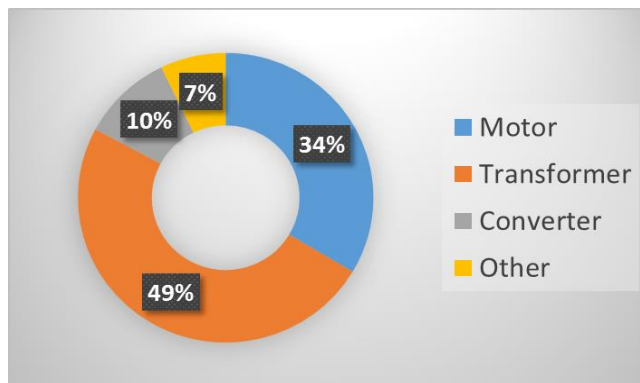


**Figure 59 - Distribution of the power losses in railway vehicle (source: FS Data).**

Transformers are usually the more efficient the heavier they are. Thus, dimensioning this component always involves a compromise between efficiency and mass. As an alternative to conventional transformers, two innovative concepts are discussed: the high-temperature superconductors (HTSC) transformer, which dramatically increases efficiency by using superconducting material, and the medium-frequency transformer, which saves mass and losses by exploiting the fact that induction increases with frequency. Asynchronous traction motors have become the standard solution in electric railway technology, [3]. In long-term perspective, permanent magnet motors may prove an interesting alternative to asynchronous motors in some areas. Permanent magnet motors and transversal flux motors are potential candidates for such a wheel-mounted construction, such as in tram, trolley-bus and electric bus. In the field of power converters, the main efficiency advances lie in power electronics technology. With IGBTs replacing GTOs, efficiency of these components in new stock has generally improved. Finally, the gears play a minor role in traction losses, but there is R&D going on to develop a direct traction motor without gears, [4].

On the other hand, one of the most effective methods to reduce the energy consumption in metro networks is to recover the electrical regenerative braking, [5]. In a conventional metro feeding network, braking energy is only usable if other vehicles are simultaneously

demanding energy. Obviously, these conditions are not always provided and the recovered energy that can be fed back to other vehicles depends on the traffic density. However, if another train does not absorb the energy, the catenary voltage rises and it is necessary to activate the braking resistors. One possible approach consists in improving the substations technology, converting them into reversible substations able to inject into the upstream AC network from the DC feeding line whenever there is energy from braking trains. Currently, the cost of reversible (or regenerative) substations is still quite high, considering also that replacing or to upgrading to a large number of substations in service on existing metro lines may not be economically viable. Energy storage systems represent a very interesting option, which allows for a much wider energy utilization scenario, [6]. ESSs can store the metro vehicles braking energy, making it available for the next traction operation with lower use of energy from the feeding network and resulting in an improvement in the energy efficiency.

Finally, another way, immediately applicable, to increase energy saving in railway systems is to use optimization procedures for energy-efficient speed profile definition during train operations; this mode is often referred in literature as *eco-driving*, [7]. Relationship between energy consumption and operational times in railways has been widely studied in the last years and, briefly, reduction of the first can take place with an extra availability of the latter. Reserve times are part of the scheduled timetable and can be classified in time for recovering train small delays (running time reserve, dwell time reserve) and time for avoiding delay propagation between different trains. In the literature, reserve times are usually considered as the extra time available for implementing energy efficiency strategies.

### 4.1.1 Energy Storage Systems

Most of rectifiers in the conventional metro network are unidirectional, thus regenerative braking energy is only usable if other vehicles are simultaneously demanding energy, otherwise, it is wasted as heat on the vehicles braking resistors. Energy storage systems represent a very interesting option to store the vehicles braking energy making it available for the next traction operation with consequent lower use of energy from the DC feeding network. An efficient energy

storage system not only reduces the energy consumption but also it stabilizes the line voltage and reduces the peak input power, resulting in lower losses in the electric lines [8].

Two main ESS configurations can be implemented for urban railway systems: mobile ESSs, installed on-board vehicle, and stationary ones, installed at the substation level or along the track. On-board ESSs can provide a few hundred meters of autonomy to the vehicle in case it is needed, they can store the whole vehicle braking energy if properly sized, and they can shave the power peaks requested to the network. They also reduce the line losses and allow, eventually, a higher traffic density with an increase of the simultaneous departure of trains without increasing the substations power. In contrast, they have the disadvantage of the weight and space they require on the vehicles, [9].

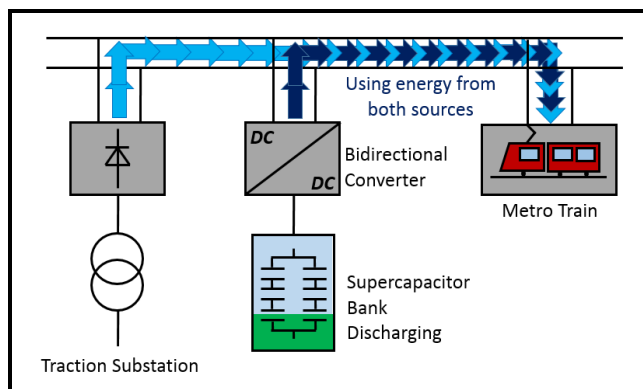


**Figure 60 - Stationary ESS during train traction phase.**

Stationary ESSs have the advantage to not be subject to weight and size constraints imposed by vehicle and to be able to balance the voltage at weak points of the network. They, also, can recover energy from several braking vehicles simultaneously. The drawback is that owing to voltage boundaries on the line, sometimes, it is not possible for a distant vehicle to send all the energy to the stationary ESS because of the voltage drop on the line. Besides, the current circulating on the network will not be reduced, and therefore, line losses will remain similar.

The metro trains generate high instantaneous currents when they brake. The braking time is around 10-15 s, therefore the ESS power is

very high and it is hard to find a convenient ESS that can store these high currents in such a few periods.

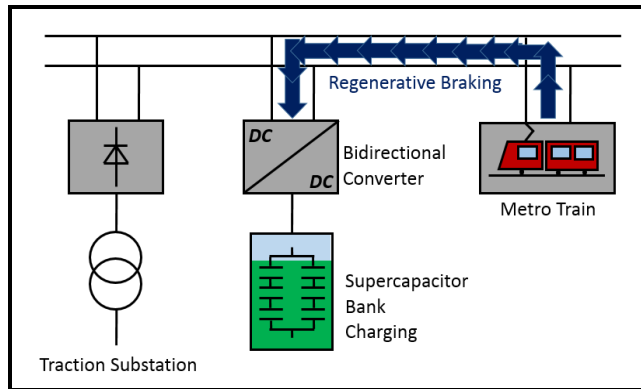


**Figure 61 - Stationary ESS during train braking phase**

Several solutions are proposed in literature: new battery technologies, supercapacitors (SCs), and flywheels, [10], [11]. Among them, SCs based ones seems to be the most attractive due to the long life cycle, rapid charging, low internal resistance, high power density, and the expected development of this technology. In particular, Figure 60 and Figure 61 show the stationary ESS supporting the main substation during the train traction phase, and recovering energy during the train-braking phase, respectively.

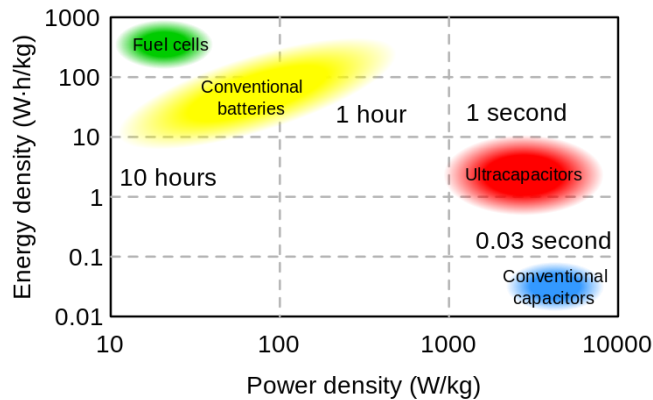


**Figure 62 - Ragone chart - energy density depends on power density (source: www.maxwell.com).**

The SC is a double layer capacitor: two electrodes, a separator and an electrolyte constitute it. Charge transfer at the boundary between electrode and electrolyte allows to store the electrical energy. The amount of stored energy is a function of electrodes surface area, the size of the ions, and the level of the electrolyte decomposition voltage. Due to their technology, these devices exhibit energy densities (about 10 Wh/kg) lower than those of batteries and flywheels, as shown in Figure 62, but higher power densities (about 10 kW/kg), with discharge times ranging from ten of seconds to minutes, [12].

#### State of art

Several papers are written on stationary ESSs implementation in metro systems, [13-15]. Several different ESSs technologies are proposed for energy saving in railway systems and several analyses are performed in terms of cost, efficiency, electrical capacity, discharge behavior, lifetime, maturity and applications for each ESS technology, [9], [10]. Up to now, the classic problems of sizing and siting are mainly analyzed in the literature in a separated way: the only SCs sizing is usually designed equating the maximum kinetic energy of the metro vehicles with the energy that can be stored by SCs [16], or using an optimization approach without considering the related SCs siting [17]. In [18], *Clemente et al.* address the SCs sizing problem using a stochastic approach by calculating the probability density function of the interest variables. On the other hand, the only SCs siting problem, is usually solved placing the SCs in arbitrary position along the track or using heuristic method to find the best position [19]. Only a few papers consider jointly siting and sizing design issues, for instance, formulating and solving the optimization problem by using the Lagrange multiplier [20].

### **4.1.2 Eco Drive Speed Profiles**

Given a train with assigned physical characteristics (mass, aerodynamic profile, traction equipment, etc.) and a trip from point A to B, energy consumption is far from being established, [21]. Since the number of stops and subsequent accelerations as well as the average speed have significant influence on the train's energy demand, thus it is important to look at the driving pattern, i.e. the speed over time

diagram. From a theoretical point of view, the energetically most efficient trip would be one at low speed and with no intermediate stops, [2]. For obvious reasons this is not an option for railway operators: customer orientation and cost efficiency drive timetable planning rather than energy efficiency. Nevertheless, there is not always a conflict between an energy efficient and a customer-oriented timetable.

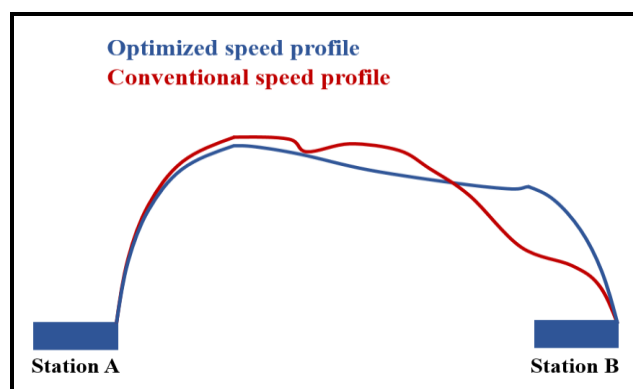


**Figure 63 - Optimized vs. conventional speed profile.**

There is a variety of energy efficient driving strategies making use of time buffers (Figure 63). The most important ones are reported in the following.

- *Coasting*: the driver shuts off the traction motors as early as possible in order to reach the station on time. This avoids braking and leaves deceleration to air resistance and friction, [21], [22].
- *Continuous speed optimisation*: a more sophisticated approach consists in a continuously optimization of the trip speed pattern and speed recommendations are calculated in real-time for the driver (i.e. train speed reduction before entering a steep downhill grade in which the train will accelerate due to gravity), [23].

An eco-drive cycle consists in selecting a speed profile for a given drive train configuration, among all the possible, which ensures the same trip distance, equivalent stops, and the same final time, but with lower energy consumption. The resulting optimal driving style contains an effective combination of four basic control regimes:

acceleration, cruising at constant speed, coasting (zero traction force), and deceleration, as shown in Figure 64.

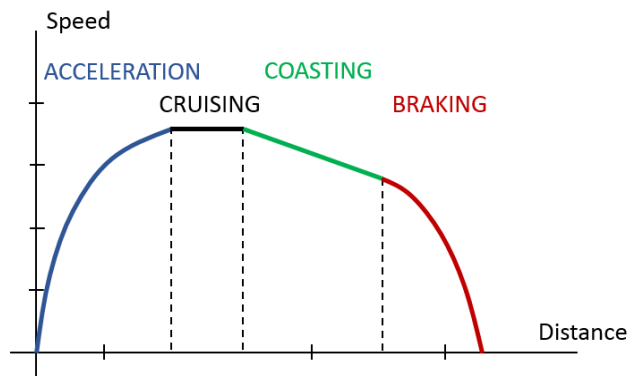


**Figure 64 - Metro vehicle optimized speed profile.**

Energy efficient driving cycles require no unexpected stops and delays occurring on the way. These conditions become more and more difficult to realize in today's railways since existing infrastructure has reached its capacity limits in many countries. Traffic fluidity is a major issue for energy efficiency since any additional stop (and subsequent acceleration) along the way requires additional traction energy. Such train conflicts are especially relevant in bottlenecks of the infrastructure, such as the junctions and the part of lines with high traffic density.

#### State of art

Optimization of speed profiles is a well-known problem in literature [24]-[26]. As stated in [27], reference trajectory planning for trains, i.e. the optimal selection of the four control regimes, can be formulated as an optimal constrained control problem. The heavy nonlinearity of both motion equations and problem, linear and nonlinear constraints make the optimization problem difficult to solve numerically as well as analytically. There were many studies on optimal speed profile, which assumed use of mechanical brake [28], [29] however, regenerative braking completely changed conditions of optimal speed profiles. Several approaches can be found where researchers optimize the energy utilization of metro vehicles for a given trip. Pontryagin's Maximum Principle [27] and the Dynamic Programming Optimization (DPO) method [22], [30] are commonly

used optimization methods to solve the energy utilization problem for metro vehicles. In [31] the optimal speed profile for energy saving problem is formulated as a Mixed Integer Linear Programming (MILP) problem, solved efficiently by using of existing commercial software tools. In [32], *Kang et al.* present an optimal algorithm for a train speed profile using Genetic Algorithm (GA) by controlling the coasting point. Finally, in [33], an algorithm of energy minimization using Particle Swarm Optimization (PSO) is introduced for a catenary-free mass transit system.

## 4.2 Models of the Metro Systems

In the next Sections, in order to compute the energy supplied by the main substation and to estimate the power flows along the feeding line, a steady state analysis is proposed. Thus, the simplified models of the metro railway system, suitable for the purpose, are presented in this Section. The metro system electric model is obtained by the integration of three different sub-models: one related to the metro vehicle and its kinematics, the second one related to the stationary ESSs, and the last one related to the supply system.

### 4.2.1 Metro Vehicle

Usually, in the literature the metro vehicle kinematic is modelled by using the mass-point model of metro train [22], [30], [31]. The longitudinal dynamic of trains evolves according to the force balance equation expressed by

$$\begin{cases} m\rho \frac{dv}{dt} = u(t) - R_{BASE}(v) - R_{LINE}(x) \\ x = x_0 + v_0 t + \frac{1}{2} \frac{dv}{dt} t^2 \\ v = \frac{dx}{dt} \end{cases} \quad (1)$$

where  $m$  is the mass of the vehicle,  $\rho$  is a factor that takes into account the rotating mass,  $v$  and  $x$  are the metro train speed and position

respectively (in particular,  $v_0$  and  $x_0$  are the  $t=0$  values),  $u(t)$  is the traction or braking force, which is lower and upper bounded, [26].  $R_{BASE}(v)$  is the basic resistance, including roll resistance and aerodynamic drag, and  $R_{LINE}(x)$  is the line resistance due to the track slopes and curves, expressed by:

$$\begin{aligned}
 R_{BASE} &= m(\alpha_1 + \alpha_2 v^2) \\
 R_{LINE} &= mg \sin(\gamma(x)) + mg \frac{a}{r(x)-b}
 \end{aligned}
 \tag{2}$$

In (2)  $\alpha_1$  and  $\alpha_2$  depend on the train mechanical characteristics and the train speed, and can be calculated by the train data or obtained by literature. Second term of  $R_{LINE}$  is the curve resistance given by empirical formulas, as the Von Röckl's formula, where  $r(x)$  is curvature radius, and  $a, b$  are coefficients which depend on the track gauge, tabled as in [3]. Finally,  $g$  is the gravitational acceleration and  $\gamma(x)$  is the slope grade.

The power at the wheels is calculated starting from a given speed cycle (Figure 65). This power is required to overcome the vehicle inertia, slopes and curves, aerodynamic drag, and rolling friction. Going upstream the vehicle components and their related efficiencies, the power requested from the electric grid is determined by the following equation:

$$\begin{aligned}
 P_{VEHICLE} &= \frac{\left( m \frac{dv}{dt} + F_r \right) v}{\eta_g \eta_m \eta_i} + P_{ACCESSORIES} \\
 I_{VEHICLE} &= \frac{P_{VEHICLE}}{V_{LINE}}
 \end{aligned}
 \tag{3}$$

In (3),  $P_{ACCESSORIES}$  is the necessary power for lighting and cooling (or heating) services,  $m$  is the total mass of the metro train - including the passengers -,  $v$  is the vehicle speed,  $\eta_g, \eta_m,$  and  $\eta_i$  represent the gear box efficiency, the motor efficiency, and the inverter efficiency, respectively.  $F_r$  is total resistive forces, computed as sum of two terms: the basic resistance  $R_{BASE}$ , and the line resistance  $R_{LINE}$ , defined in (2). In order to bring into account that the voltage along the track is not constant, metro trains are modelled as current sources absorbing power at the accelerating time or generating power at the regenerative

breaking time. The ideal current generator value,  $I_{VEHICLE}$ , is calculated as the ratio between vehicle power and line voltage  $V_{LINE}$ , (3).

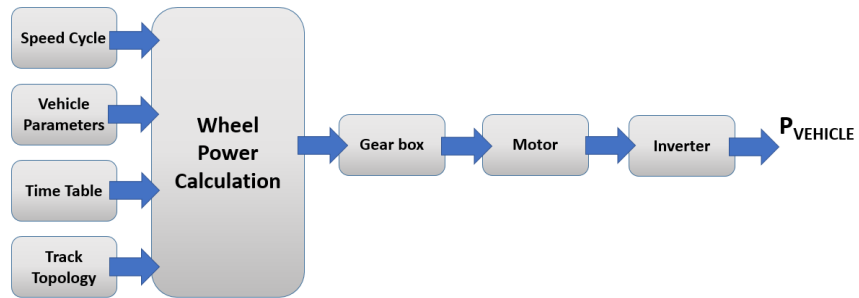


Figure 65 - Metro vehicle electric power computation.

## 4.2.2 Energy Storage System

The stationary ESS electrical model includes the SC modules, the DC/DC converter and the power flow controller (Figure 66). During the charging period, SCs receive the regenerative power from the vehicles and during the discharging period they deliver power to the metro trains: therefore, the ESSs are modelled as ideal current sources, whereas the ideal buck and boost converter equations model the bidirectional power converter. In Table 13  $V_o$ ,  $I_o$  ( $V_i$ ,  $I_i$ ) are the output (input) voltage and current, respectively;  $D$  is the duty cycle value and  $\eta$  is the bidirectional converter efficiency taking into account power losses.

Table 13 - Bidirectional power converter equation.

| <i>BUCK Converter</i>      | <i>BOOST Converter</i>    |
|----------------------------|---------------------------|
| $V_o = DV_i$               | $V_o = \frac{1}{1-D} V_i$ |
| $I_o = \frac{\eta}{D} I_i$ | $I_o = \eta(1-D) I_i$     |

A power flow controller commands the DC/DC converter to charge or discharge the SCs, using an energy management strategy, according to the line voltage and the SCs State of Charge (SoC). The second-order equivalent circuit of SC consists of four elements, as depicted in Figure 66, [13].

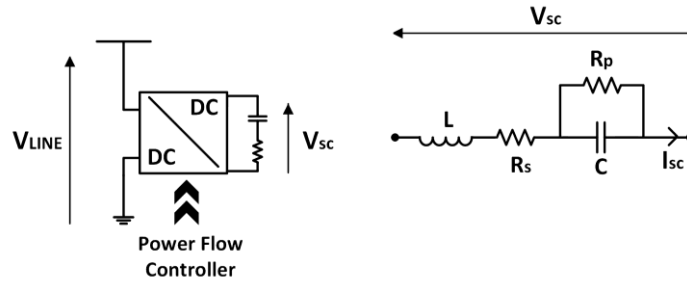


Figure 66 - ESS and SC module electric model.

The equivalent series resistance  $R_s$  represents the power loss during the charging and discharging operations; the self-charge resistance  $R_p$  models the losses due to the leakage current; the inductance  $L$  results primarily from the SC physical construction and its value is usually very small. Finally, the capacitor  $C$ , that models SC's capacity, changes linearly with the SC electrodes voltage  $V_{sc}$  according to the following:

$$V_{sc}(t) = V_{sc}(0) + \frac{1}{C} \int_{\Delta t} I_{sc}(\tau) d\tau + R_s I_{sc}(t) \quad (4)$$

$$C = C_0(1 + \lambda V_{sc})$$

where  $I_{sc}(t)$  is the SC current,  $C_0$  is the SC's capacity constant value and  $\lambda [V^{-1}]$  represents the SC's capacity voltage coefficient.

#### 4.2.2.1 Power Converter Control Algorithm

The ESS controller ensures the storage system supplying or recovering energy keeping the line voltage within an interval defined by a lower and upper threshold value that are lower enough than protections line [8]. The block diagram of the proposed ESS control algorithm is shown in Figure 67, where it is possible to note an external control action on the maximum current supplied from the ESS and an inner control action for the line voltage regulation. In particular, if the line voltage exceeds the upper threshold value,  $V_{max}$ , (usually if one or more vehicles are in braking phase), according to the battery modules SoC, the ESS stores the regenerative braking energy, reducing the line voltage. Instead, if the line voltage is below the lower threshold value,  $V_{min}$ , (as when a train accelerates or starts), the

ESS supports the railway system by using the previously stored energy to the feeding the contact line.

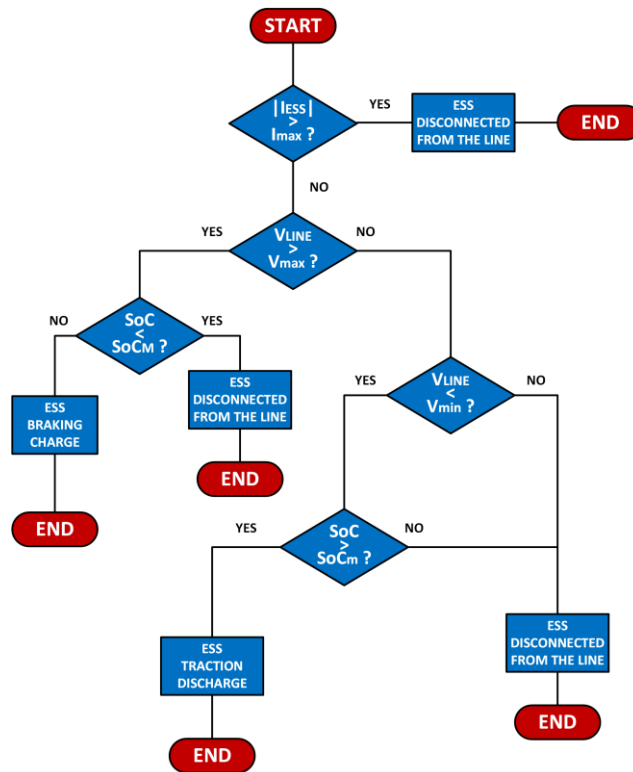


Figure 67 - ESS control algorithm flow-chart.

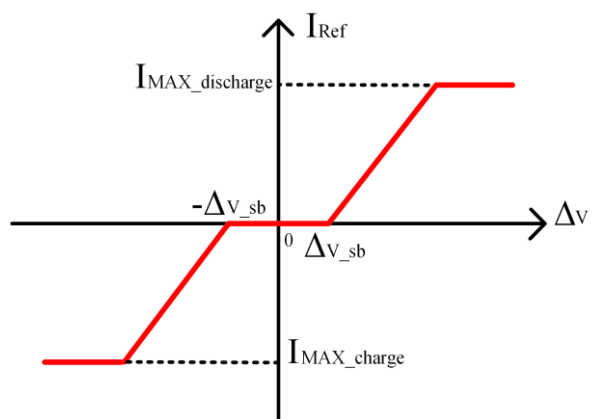


Figure 68 - ESS current control function.

Figure 68 illustrates the operational characteristic of the ESS control function (CF) linking the ESS reference current  $I_{Ref}$  and the line voltage variation related to its nominal value  $\Delta V$ . If the line voltage is increased by regenerative braking, the battery is charged ( $I_{Ref} > 0$ ), and it is discharged ( $I_{Ref} < 0$ ) when the line voltage is decreased by powering trains [8]. The maximum charging current  $I_{MAX\_charge}$  is set to the battery maximum current and it depends on the battery technology and characteristics, for absorbing the regenerative energy as large as possible. The maximum discharge current  $I_{MAX\_discharge}$  is chosen in a similar way. If the voltage values at connection point ( $V_{CP}$ ) of the ESS is within the  $V_{rated} \pm \Delta V_{sb}$  interval, we are in the standby region and no actions are required. When the variation  $|\Delta V|$  of the voltage at connection point  $V_{CP}$  is greater than  $|\Delta V_{sb}|$ , the ESS is ready to supply/recover energy; it is more or less responsive according to the slope of the CF and the  $I_{MAX\_charge}$  and  $I_{MAX\_discharge}$  values.

### 4.2.3 Feeding Network

The electrical substation (Figure 69), converting the AC voltage into DC voltage, can be very simply described through a DC voltage generator with a downstream diode rectifier. The choice of the suitable model depends on the analysis to be performed.

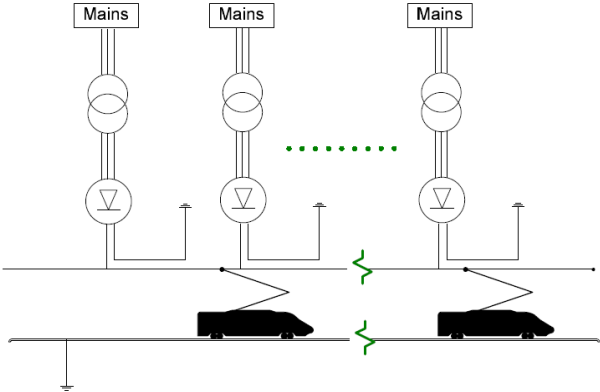


Figure 69 - Conventional metro line.

In this analysis, focusing primarily on power flows affecting the metro vehicle and the DC feeding line, it is sufficient to consider the

main substation represented by an ideal DC voltage generator with internal resistive losses, whose voltage value is equal to the DC voltage of the downstream diode bridge. Thus, conventional substations are modelled by ideal DC voltage sources with series resistance and series diode, in the case of not reversible substations, [15].

Usually, the line impedance is described by the series of a resistance and of an inductance, able to model the first order transients too. Obviously, since we are interested in a steady state analysis, it is possible referring to the model, which takes into account only a variable line resistance. Thus, the contact wire is modelled as a set of electric resistances varying with the vehicle position [13], [15]. If  $x(k\Delta t)$  is the metro train position at the time  $k\Delta t$ , the value of the resistance upstream  $R_a$  and downstream  $R_b$  to the metro vehicle towards a generic node of the railway electric power feeding system (electric substation, ESS or another train) are calculated by:

$$\begin{cases} R_a = r x(k\Delta t) \\ R_b = r [d - x(k\Delta t)] \end{cases} \quad (5)$$

where,  $R_a$  and  $R_b$  are expressed in  $[\Omega]$ ,  $r$   $[\Omega/\text{km}]$  represents resistive coefficient,  $d$   $[\text{km}]$  is the distance between the two nodes, upstream and downstream the metro train, and  $x(k\Delta t)$   $[\text{km}]$  is the distance between the train and the upstream node at each time step  $k\Delta t$ .

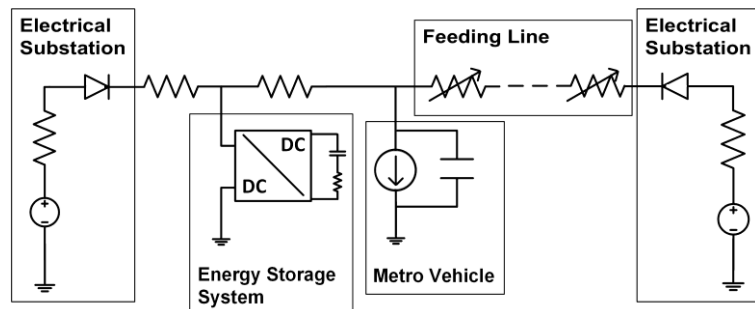


**Figure 70 - Metro network overall electric model.**

The electric model of the overall network with the substations, the SC storage units, and the metro vehicle is shown in Figure 70. Furthermore, it is necessary to improve the model with some small capacitances in parallel to the vehicles in order to describe the

receptivity of the network under regenerative braking conditions [15]. Indeed, if the capacitance was not present, it would not be possible to simulate the energy fed back to the line because all the paths for the current flow would be closed when there are no receptors (i.e. vehicles consuming energy) and substations are blocked. Its effect is a voltage rise when trying to feed back to the line an amount of power higher than the power being consumed by other vehicles at that instant. The ESS controller manages the power flow handling this variable.

### **4.3 ESSs Sizing and Positioning Problem**

Amongst various advantages of stationary ESSs, there is the easily feasible integration into the existing infrastructure, independently by the train design, as well as the flexibility in size, weight, number and position. From the economical point of view, the possibility of individual sizing for each track carries particular importance. Each track between two stations of the metro network varies in distance, as well as maximum speed and acceleration. Therefore, the resulting kinetic energy of the trains differs from track to track (and from train to train, obviously). This directly affects the amount of recoverable energy and demands individual sizing of the supercapacitors depending on their location along the line in order to enable full capacity utilization. To avoid energy transport losses, it is advisable to install the supercapacitors close to where the trains usually stop and restarts: at the passenger stations. Furthermore, the voltage level on the overhead line becomes more unstable the larger the distance to the next traction power substation. Due to this fact, the weakest point could be located between two traction power substations and therefore would be the ideal position to install the supercapacitors in order to stabilize the voltage along the track.

#### **4.3.1 Mathematical Formulation**

The problem to solve consists in finding the optimal number, positioning and sizing of ESSs on the track, taking into account its topology, the electric characteristics of the feeding line, the vehicle

mechanical features, and its timetable. The positioning of the ESSs and their related capacity are the input variables of the optimisation problem, [9], [13]. The objective function is the sum of energy supplied by the substation during the trip and the energy stored by all the ESSs, thus the minimization problem can be written as

$$\begin{cases} \min_{\substack{\vec{P} \in \mathbb{R}^N \\ \vec{C} \in \mathbb{R}^N}} (J) \\ J = [\alpha \cdot E_{SS}(\vec{P}, \vec{C}) + \beta \cdot E_{SC}(\vec{C})] \end{cases} \quad (6)$$

where  $\alpha$  and  $\beta$  are the fitting weight coefficients,  $\vec{P}$  is the SCs position vector,  $\vec{C}$  is SCs capacity vector and  $N$  is the number of ESSs on the track.  $E_{SS}$  is the energy supplied by the main substation and  $E_{SC}$  is the total energy that can be stored by all the ESSs on the track. In particular,

$$\vec{P} = [p_1, p_2, \dots, p_n, \dots, p_N]$$

$$\vec{C} = [c_1, c_2, \dots, c_n, \dots, c_N]$$

$$E_{SC}(\vec{C}) = \sum_{n=1}^N \frac{1}{2} c_n V_{SCmax}^2 = \frac{1}{2} V_{SCmax}^2 \sum_{n=1}^N c_n \quad (7)$$

In (7)  $c_n$  is the SC capacity of the  $n$ -th ESS, and  $V_{SCmax}$  is the maximum allowable voltage at the SC terminals. Furthermore, the following constraints are considered:

$$\begin{cases} V_{LINE\_min} \leq V_{LINE} \leq V_{LINE\_max} & \forall t \leq T \\ 0 \leq I_{SSE} \leq \frac{P_{SSE\_max}}{V_{LINE\_min}} & \forall t \leq T \\ P_{BRAKE\_max} \leq P_{Train} \leq P_{TRACTION\_max} & \forall t \leq T \\ V_{SC\_min} \leq V_{SCn} \leq V_{SC\_max} & \forall t \leq T, \quad \forall n = 1, \dots, N \\ SoC_{min} \leq SoC_n \leq SoC_{max} & \forall t \leq T, \quad \forall n = 1, \dots, N \\ SoC_n(t=T) \geq SoC_n(t=0) & \forall t \leq T, \quad \forall n = 1, \dots, N \end{cases} \quad (8)$$

where  $T$  is the total simulation time,  $V_{SCn}$  is the maximum allowable voltage at the  $n$ -SC terminals,  $I_{SSE}$  and  $P_{SSE}$  are the substation current and power, respectively;  $P_{Train}$  is the vehicle absorbed (or generated) power,  $P_{BRAKE}$  is the maximum vehicle generated power during the

braking phase,  $P_{TRACTION}$  is the maximum vehicle absorbed power during the traction phase. Finally,  $SoC_n(t)$  represents the value of the  $n$ -SC state of charge defined in (9).

$$SoC_n(t) = \frac{V_{SCn}^2(t)}{V_{SCmax}^2} \quad (9)$$

The isoperimetric constraint of SoC - the last in (8) - used in the optimisation problem guarantees that the energy stored by SC is the same at the beginning and at the end of the trip cycle.

### 4.3.2 Solution Algorithm

The optimization of the SC joint positioning and sizing can be formulated as a Mixed-Integer Non-Linear Problem (MINLP). The great difficulty and the too computationally demand in solving these problems, has suggested to find heuristic algorithms to explore more quickly the solution space. So the optimisation problem is addressed using a PSO based algorithm as solving method.

PSO is a quite recent heuristic method inspired by the choreography of a bird flock [34]. In the real number space, each individual possible solution is modelled as a particle that moves through the problem hyperspace. At each iteration, the velocities of the individual particles are stochastically adjusted according to the historical best position for the particle itself and the neighbourhood best position. Both the particle best and the neighbourhood best are derived according to a user defined fitness function. The position of each particle is determined by the  $x_i \in R^n$  vector and its movement by the velocity of the particle  $v_i, \in R^n$  as shown in (10).

$$\begin{aligned} \bar{x}_i(t) &= \bar{x}_i(t-1) + \bar{v}_i(t) \\ \bar{v}_i(t) &= \bar{v}_i(t-1) + \phi_1 \cdot rand_1(\bar{p}_i - \bar{x}_i(t-1)) + \dots \\ &\quad \dots \phi_2 \cdot rand_2(\bar{p}_g - \bar{x}_i(t-1)) \end{aligned} \quad (10)$$

The coefficients  $\phi_1, \phi_2$  are two positive numbers and  $rand_1, rand_2$  are two random numbers with uniform distribution in the range of [0.0, 1.0];  $\bar{p}_i$  is the best position ever found by the  $i$ -th particle, whereas  $\bar{p}_g$  is the best position ever found by all particle. The block

diagram of the proposed PSO siting and sizing algorithm is shown in Figure 71.

The objective function is evaluated using a railway simulation tool implementing the models described in Section 4.2 and able to calculate the energy supplied by the substations for a particular siting and sizing configuration. The metro network model is implemented in a simulation routine based on the 'quasi static' backwards looking method, due to its short simulation times for estimating energy consumption of vehicles following an imposed speed cycle [6], [15]. The speed cycle is divided in time steps during which all the variables are supposed to be in the steady state. The power needed to satisfy the speed cycle is determined at the wheel level. Then, the power provided by the feeding line is estimated calculating the consumption of the upstream vehicle components. The calculation direction is the opposite of the real power flow direction.

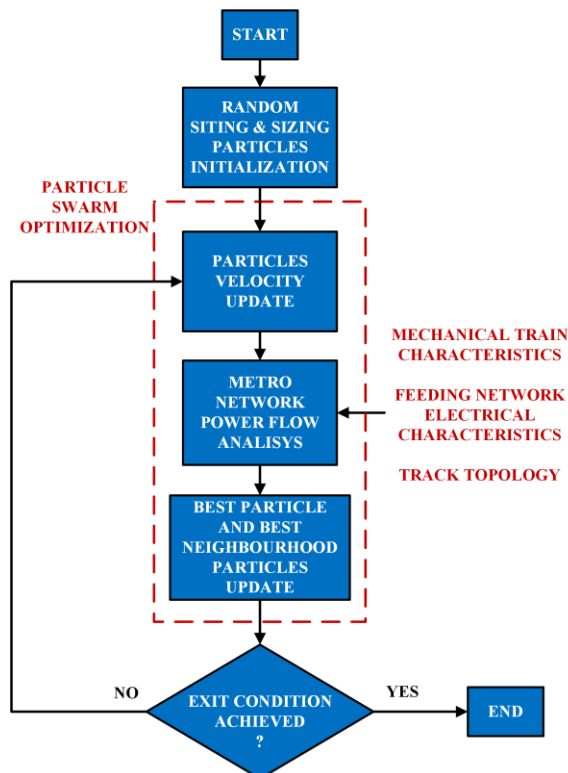


Figure 71 - PSO based algorithm flow-chart.

## 4.4 Eco-Drive Speed Profiles Problem

The calculation of optimal driving strategies for metro trains is a challenging task. Reference trajectory planning for metro vehicles, i.e. the optimal selection of the four control regimes (acceleration, cruising at constant speed, coasting), can be formulated as an optimal constrained control problem. The heavy nonlinearity of both motion equations and problem linear and nonlinear constraints makes the optimization problem difficult to solve numerically as well as analytically.

All solved problems, however, propose the analysis of single aspects, introducing simplifications in electric models, often without considering energy recovery by regenerative braking, or modelling of the train kinematics. The optimization problem solved in this work consists in finding the sequence of basic control regimes able to minimize the energy consumed for a given path. In particular, the problem formulation takes into account: i) the track topology - slopes and curves -, ii) the mechanical characteristics of the vehicle and the electrical ones of the feeding line, iii) the effect of regenerative braking, assuming also stationary ESSs on the track, [21], [24].

### 4.4.1 Mathematical Formulation

The problem to solve consists in finding the optimal speed profile obtained as sequence of basic control regimes that leads to the minimization of energy consumed for a given trip. Moreover, in the pointed out model are taken into account the track topology, the electric characteristics of the feeding line, the vehicle mechanical features and its timetable. The traction or braking force  $u$  is the control variable, and the state variables are the train position  $x$  and its speed  $v$ . Thus, the optimization problem can be written as:

$$\begin{cases} \min_{u(t)} (J) \\ J = \int_0^T P_{SS}(u(t)) + \beta \left| \frac{du(t)}{dt} \right| dt \end{cases} \quad (11)$$

subject to the train dynamics equations (1), coded by means of the following constraints:

$$\begin{aligned}
 u_{\min} &\leq u(t) \leq u_{\max} \\
 0 &\leq v(t) \leq V_{\max}(x) \\
 \left(\frac{dv}{dt}\right)_{\min} &\leq \frac{dv}{dt} \leq \left(\frac{dv}{dt}\right)_{\max}
 \end{aligned} \tag{12}$$

and the boundary conditions:

$$\begin{aligned}
 s(0) &= 0, & s(T) &= L \\
 v(0) &= 0, & v(T) &= 0
 \end{aligned} \tag{13}$$

The proposed optimization problem is also subjected to the following electrical constraints imposed by the proper operation of the DC feeding line:

$$\begin{cases}
 V_{LINE\_min} \leq V_{LINE} \leq V_{LINE\_max} & \forall t \leq T \\
 0 \leq I_{SS} \leq \frac{P_{SS\_max}}{V_{LINE\_min}} & \forall t \leq T \\
 P_{BRAKE\_max} \leq P_{Train} \leq P_{TRACTION\_max} & \forall t \leq T
 \end{cases} \tag{14}$$

In (11)...(14),  $J$  is the weighted sum of the energy supplied by the electrical substation  $P_{SS}$  during the trip, whereas the passenger riding comfort is taken into account reducing the number of transitions and the rate of change of the control variable  $u$ , [30]. The control variable  $u$  is also constrained by the maximum braking force  $u_{min}$  and the maximum traction force  $u_{max}$ ;  $V_{max}(x)$  is the maximum allowable speed, that depends on the train characteristics and the line conditions, and it is usually a piecewise constant function of the coordinate  $s(t)$  [31]. The derivative of the train speed  $dv/dt$  is also constrained by the maximum deceleration value  $(dv/dt)_{min}$  and the maximum acceleration value  $(dv/dt)_{max}$ . In (13),  $s(0)$ ,  $s(T)$ ,  $v(0)$  and  $v(T)$  are position and speed at the beginning and the end of the trip respectively, with  $L$  and  $T$  the trip distance and the trip duration usually, imposed by the timetable. Finally,  $V_{LINE}$  is the line voltage, which is lower  $V_{LINE\_min}$  and upper  $V_{LINE\_max}$  bounded,  $I_{SS}$  and  $P_{SS}$  are the substation current and power, respectively;  $P_{Train}$  is the metro vehicle power,  $P_{BRAKE}$  is the maximum vehicle generated power during the braking phase, and

$P_{TRACTION}$  is the maximum vehicle absorbed power during the traction phase.

### 4.4.2 Solution Algorithms

The eco-drive speed profiles computing can be formulated as a Mixed-Integer Nonlinear Programming problem (MINLP). The high computational demand of deterministic algorithms in solving these problems, has suggested to find heuristic algorithms to explore more quickly the solution space, even finding a suboptimal solution. In order to compare the performances of deterministic and heuristic algorithm, the optimization problem is addressed using both, a DPO and PSO based solution methods.

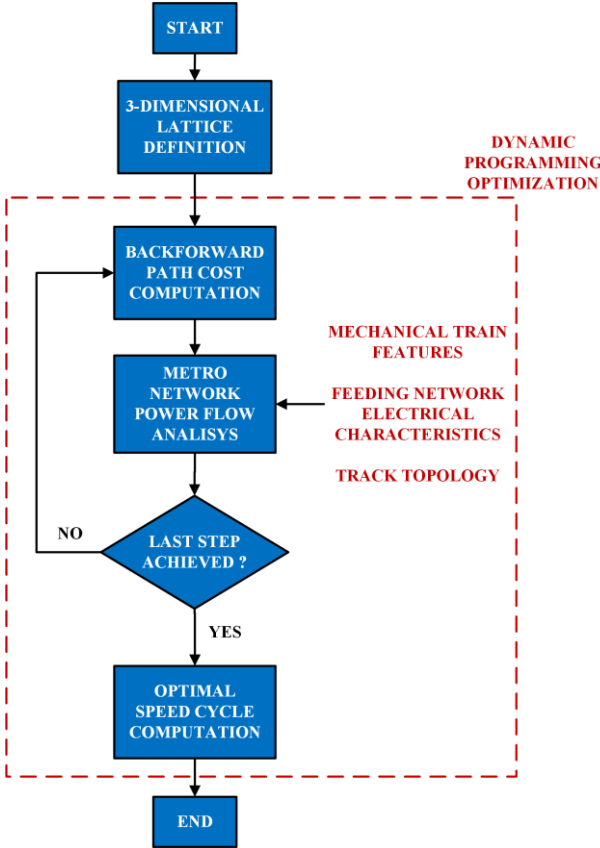


Figure 72 - DPO based algorithm flow-chart.

Widely used in the literature to solve the problem of energy minimization for the railway vehicles (11)...(14), DPO, firstly, performs the calculation of the cost of each single decision, working backwards from the final state to the initial one; secondly, since is known the cost of each possible decision, DPO calculate the optimal policy minimizing the objective function, [35]. In the present case, the optimal policy, that the DPO allows to build, is the metro vehicle speed profile that minimizes the energy consumption.

In the following, DPO in the three dimensional approach will be used, [22]. In each state, three variables describing the vehicle kinematics are defined: time ( $t$ ), distance ( $x$ ) and speed ( $v$ ). We have built a three dimensional lattice in which they are imposed temporal resolution  $\Delta t$  and distance resolution  $\Delta x$ ; furthermore, it is used an interpolation procedure to fix the resulting distance  $x(k+1)$  and speed  $v(k+1)$  for a given time  $k\Delta t$ , traction effort  $u(k)$  and speed  $v(k)$  to the defined lattice. Problem (11) in discrete form is expressed by:

$$\begin{cases} v(k+1) = v(k) + \frac{\Delta t}{m\rho} [u(k) - (R_{BASE}(v(k)) + R_{LINE}(x(k)))] \\ x(k+1) = x(k) + \frac{1}{2}v(k+1)\Delta t + \frac{1}{2}v(k)\Delta t \end{cases} \quad (15)$$

The block diagram of the proposed DPO siting and sizing algorithm is shown in Figure 72. The objective function is evaluated using a railway simulation tool implementing the models presented in Section 4.2 and based on the 'quasi static' backwards looking method, as stated in Section 4.3.2 [13]. The DPO based algorithm fully explores the solution space by finding the optimal solution but showing against a computational cost very high. Hence, the computation time of a dynamic programming optimization grows exponentially with the dimension size, [22]. For example, given a problem with two dimensions and  $K$  possible values, at each dimension the method searches, at each of the  $K$  possible time steps, the  $K$  possible state values.

The computational cost becomes  $K*KC = K^2C$ , where  $C$  is the cost to calculate one edge. However, when the problem consists of three dimensions (as here), and again  $K$  possible values are given for each dimension, the method has to search each of the  $K$  time steps at all possible combinations ( $K^2$ ) of the other two variables. The resulting computational cost becomes  $K*K^2C=K^3C$ .

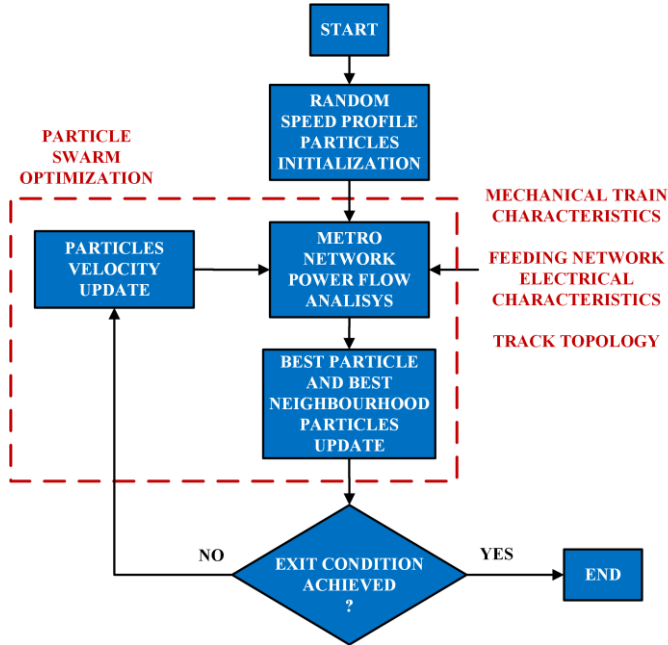


Figure 73 - PSO based algorithm flow-chart.

More often, the optimal solution search is not a feasible approach due to the high computing time. For different applications from planning where computing time is not a binding constraint, another possible approach consists in using heuristic algorithms. In problem solving, the heuristic approach employs a practical method not guaranteed to be optimal or perfect, but sufficient for the immediate goals. Where finding an optimal solution is an impractical approach, heuristic methods can be used to speed up the process of finding a satisfactory solution.

For these reasons, it was implemented a heuristic based algorithm to solve the problem of searching the speed profiles minimizing energy consumption. In particular, the PSO based algorithm is able to find a sub-optimal solution very close to the optimal solution by using a calculation time significantly lower. The block diagram of the proposed PSO eco-drive algorithm is shown in Figure 73. The metro kinematics in discrete form is expressed as in DPO by equation (15) and the objective function is evaluated by using the metro network model implemented in a simulation routine.

## 4.5 Simulation Framework

In order to establish the performances of the proposed solution methods for the joint ESSs siting and sizing and eco-drive cycles computing problems, respectively, a real case study is presented, [9], [13]. The ESSs design solution is implemented by using commercially available SC modules and the substations energy saving with and without stationary SCs on the track are evaluated. The eco-drive problem instead is solved by using two different algorithms and a comparison between the computing time and the goodness of the obtained solution is performed, [21], [24]. The railways infrastructure simulation tool and the solution algorithms are coded in Matlab™.

### 4.5.1 Case Study

The tests are performed on the track EUROPA–MOMPIANO–CASAZZA, a portion of the Italian line PREALPINO–S.EUFEMIA of the Brescia metro network. The metro DC line is fed by two electric substations and consists in two subway line sections and three stations, one intermediate and two located at the beginning and the end of the line, in correspondence of the substations.

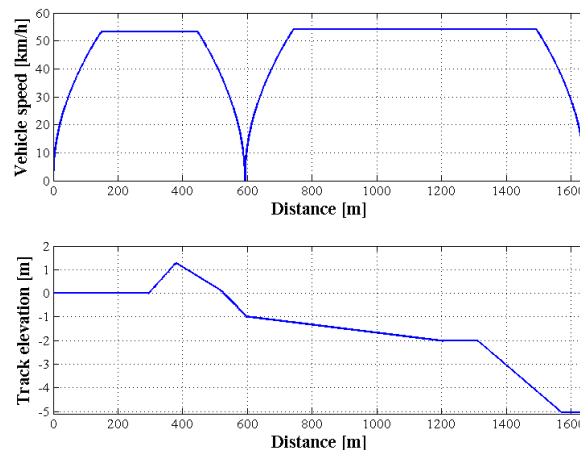


Figure 74 - Vehicle drive cycle and track elevation EUROPA-CASAZZA.

Driving cycle and track elevation are shown in Figure 74: reference speed cycles consist in repeating two times a first phase of acceleration, followed by a stretch of line path at a constant speed and finally ending with the braking phase. We considered only one metro vehicle moving along the track and its maximum speed over the entire trip is 60 km/h. Metro vehicle and feeding network are characterized by the parameters listed in Table 14 and Table 15, respectively.

**Table 14 - Metro vehicle parameters.**

| <i>Parameter</i>                                    | <i>Value</i> | <i>Unit</i> |
|---|--------------|-------------|
| Net weight  | 59357        | kg          |
| Loaded weight<br>(6 passengers per m <sup>2</sup> ) | 88170        | kg          |
| Rotating mass                                       | 10.46        | %           |
| Max. traction power                                 | 630          | kW          |
| Accessories power                                   | 90           | kW          |
| Coefficient of auxiliary use                        | 0.75         | -           |
| Gear box efficiency                                 | 0.98         | -           |
| Motor efficiency                                    | 0.85         | -           |
| Inverter efficiency                                 | 0.90         | -           |

**Table 15 - Metro network parameters.**

| <i>Parameter</i>               | <i>Value</i> | <i>Unit</i> |
|--------------------------------|--------------|-------------|
| Track's length                 | 800          | m           |
| Rail electric resistance       | 0.0133       | Ω/km        |
| Substation DC voltage          | 750          | V           |
| Substation internal resistance | 0.0125       | Ω           |
| Maximum line voltage           | 900          | V           |
| Minimum line voltage           | 500          | V           |

### 4.5.2 Numerical Results

Several simulations are carried out for the described case study in the previous subsection, in which one metro train moves in the two opposite directions implementing the same driving cycle. The optimization algorithms are characterized by 10 time-steps in the

3-dimensional DPO and 50'000 iterations by using 25 particles in the PSO. The proposed algorithms are run on a workstation with an Intel® Core™ i7 (3.20 GHz, 64 bit) processor, 16 GB of RAM and Matlab™ R2014b.

#### 4.5.2.1 SCs Positioning and Sizing Results

The comparison between the case study assuming only one ESS, designed by using the proposed method, and without ESSs, is summarized in Table 16.

**Table 16 - 1-ESS Siting and Sizing.**

| <i>Line</i>    | <i>Siting [m]</i> | <i>Sizing [F]</i> | <i>Substation supplied energy [kWh]</i> |
|----------------|-------------------|-------------------|---|
| EUROPA-CASAZZA | 100               | 140               | 6.491                                   |
|                | -                 | -                 | 7.636                                   |
| CASAZZA-EUROPA | 200               | 0                 | 9.239                                   |
|                | -                 | 169               | 10.197                                  |

Figure 75 shows the energy supplied by the electrical substations when there is only one ESS on the track. To minimize the substations delivered energy in both directions is necessary to have the ESS near the point where the vehicle should perform an uphill acceleration.

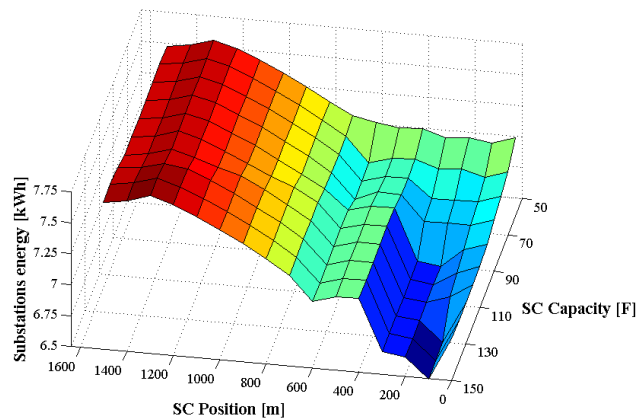


**Figure 75 - Siting and sizing of one ESS on the line EUROPA-CASAZZA.**

Even though, the installed ESS capacity is equal, the reduction of the supplied energy is different according to the track direction. In particular, the ESSs should be positioned at a distance of 100 m from

the first substation and 1440 m from the second, respectively. On the line EUROPA-CASAZZA, there is a reduction of the absorbed energy by 15.1%, while in the opposite direction there is a smaller reduction equal to 9.4%.

**Table 17 - 5-ESSs Siting and Sizing.**

| <i>Line</i>             | <i>Siting [m]</i> | <i>Sizing [F]</i> | <i>Substation supplied Energy [kWh]</i> |
|-------------------------|-------------------|-------------------|---|
| <b>EUROPA – CASAZZA</b> | 150               | 20                | 6.505                                   |
|                         | 300               | 130               |   |
|                         | 1000              | 60                |   |
|                         | 1150              | 10                |   |
|                         | 1500              | 10                |   |
| <b>CASAZZA – EUROPA</b> | 200               | 170               | 8.901                                   |
|                         | 600               | 20                |   |
|                         | 800               | 10                |   |
|                         | 1000              | 70                |   |
|                         | 1500              | 10                |   |

The results of the PSO siting and sizing procedure assuming the number  $N$  of ESSs on the track  $N = 5$  are in Table 17. The coefficients  $\alpha$  and  $\beta$  in the objective function are chosen both equal to 1. The position and the capacity of the ESSs are discretised. In particular, the ESSs siting varies by 100 metres steps along the track and the SC capacity size varies by steps of 10 F, starting from zero up to 300 F. The ESSs on the line EUROPA-CASAZZA, lead to a reduction of the absorbed energy by 19%, while in the opposite direction there is a smaller reduction equal to 12.7%.

**Table 18 -Theoretical and Real ESSs Sizing.**

| <i>Siting [m]</i> | <i>Theoretical sizing [F]</i> | <i>Substation supplied energy [kWh]</i> | <i>Real sizing [F]</i> | <i>Substation supplied energy [kWh]</i> |
|-------------------|-------------------------------|---|------------------------|---|
| 200               | 10                            |   | 0                      |   |
| 300               | 150                           |   | 154.5                  |   |
| 800               | 20                            | 6.392                                   | 0                      | 6.505                                   |
| 1200              | 160                           |   | 169                    |   |
| 1500              | 20                            |   | 0                      |   |

Table 18 reports the comparison, in the same siting conditions, between the theoretical ESSs sizing and a real design solution obtained using commercially available SCs modules. The theoretical sizing is implemented by using the proposed PSO algorithm, considering both the track directions, and testing the results in terms of energy supplied by the substation on the line EUROPA-CASAZZA.

The real sizing, instead, is obtained by implementing the theoretical sizing with commercial SCs module. Each ESS module consists in the series of four SC units to obtain SC modules with rating voltage 500 V and nominal capacity 15.75 F: each SC unit has as rating voltage 125 V, a nominal capacity of 63 F, as well as the commercially available [12]. The real sizing allows to obtain a slightly higher (1.7%) value of energy delivered by the substations compared to those obtained with the theoretical sizing because the real sizing presents, in the same siting condition, a lower overall ESSs capacity.

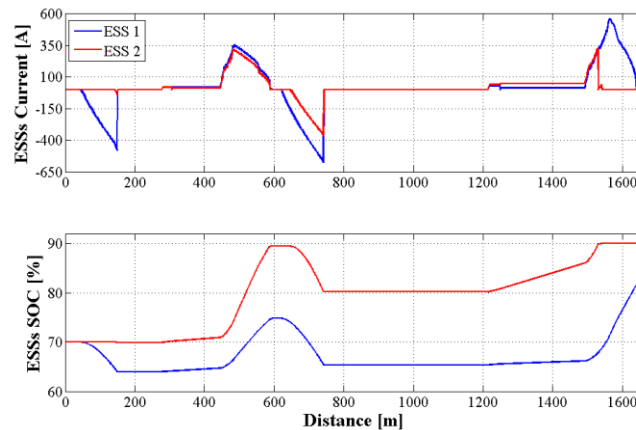


**Figure 76 - ESSs current and SoC trends on the line EUROPA-CASAZZA.**

Figure 76 shows the ESSs current trends related to their SoC trends on the line EUROPA-CASAZZA. The current recovered/supplied by the ESSs on the DC line reaching a peak value equal to 600 A. The SC modules held their SoCs value within the minimum and maximum value equal to 40% and 90%, respectively. The line voltage trend without ESSs on the track and with ESSs sized and positioned using the proposed method, is proposed in Figure 77. Although the line voltage has voltage drop well below the lower limit, the voltage drop

obtained with ESSs on the track is slightly lower than the previous one. The ESSs held also the line voltage value much lower than the maximum limit such as it makes unnecessary to switching on the braking chopper and waste energy.

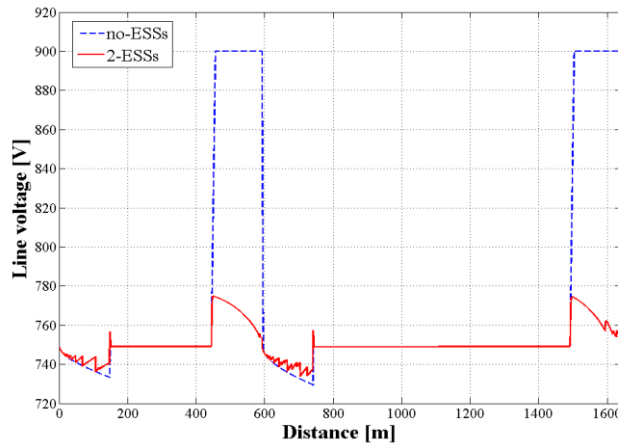


Figure 77 - Comparison on line voltage: no ESSs and real ESSs sizing case (line EUROPA-CASAZZA).

Finally, the comparison between the current trends supplied from the substation without ESSs on the track and with ESSs, on the line EUROPA-CASAZZA, respectively, is proposed in Figure 78.

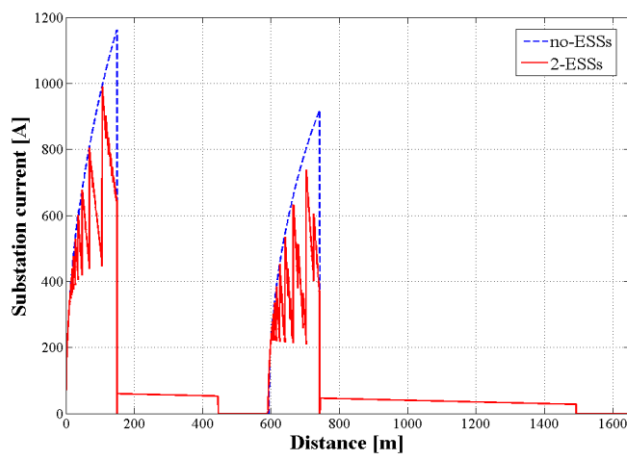
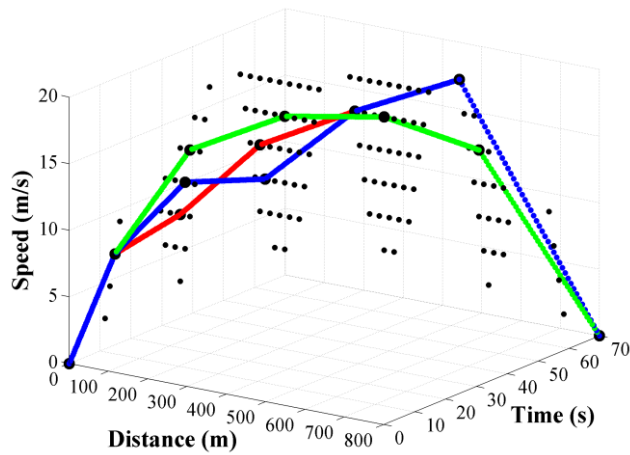


Figure 78 - Comparison on substation current: no ESSs and real ESSs sizing case (line EUROPA-CASAZZA).

Obtained results, show a significant reduction (15%) in the supplied peak current, with consequent savings in delivered energy, and, in addition, on the sizing of the power components and the substations converters too.

#### 4.5.2.2 Eco-Drive Speed Profiles Results

In Figure 79 is shown the comparison between the reference speed cycle and the minimum energy consumption speed profile computed using DPO and PSO based algorithms.



**Figure 79 - Comparison between DPO and PSO based eco-drive speed cycle (7-time step).**

The speed trajectories are plotted on a three-dimensional lattice in which there are all and only the possible *time-space-speed* states and in which all the speed profiles satisfying the imposed constraints must lie. Green line represents the reference speed cycle whereas red line and blue line represent the DPO and PSO eco-drive algorithms, respectively.

**Table 19 - DPO vs PSO based algorithm comparison (10-time step).**

|            | <i>Computing time [s]</i> | <i>Substation supplied energy [kWh]</i> |
|------------|---------------------------|---|
| <b>DPO</b> | 64853                     | 6.491                                   |
| <b>PSO</b> | 25362                     | 6.880                                   |

The comparison between the DPO and PSO eco-drive algorithms, in terms of computing time and goodness of solution, is summarized in Table 19. Although the eco-drive heuristic algorithm allows to obtain a sub-optimal solution, it shows energy saving performance slightly lower ( $< 6\%$ ) but a computing time considerably lower than the DPO algorithm. The effect of the control variable on the speed profiles and thus, on the energy saved is shown in Figure 80 and in Table 20. The speed profile generated with 9 different values of the control variable  $u$  allows to obtain the great energy saving value because it has more freedom degrees than the generated speed cycle by using are 7 and 5 values of  $u$ , respectively.

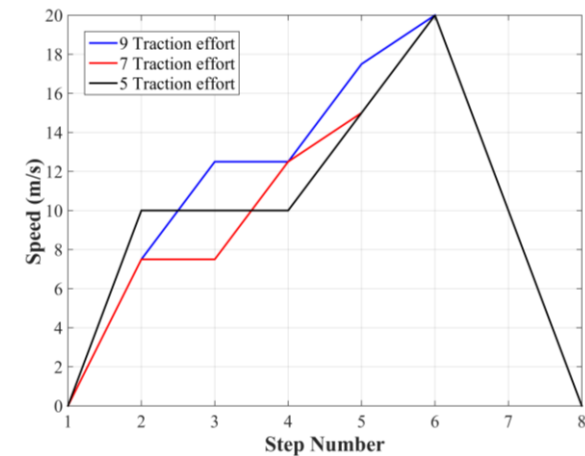


**Figure 80 - Control variable effect on drive cycle (7-time step).**

A greater number of  $u$  freedom degrees, i.e. the traction/braking effort, allows to better control the vehicle dynamics and therefore to obtain speed profiles with higher performance in terms of energy consumption.

**Table 20 - Control variable effect on energy saving (7-time step).**

| <i>Control variable values</i><br>[% $u_{max}$ ]      | <i>Substation supplied energy</i> [kWh] | <i>Comparative evaluation</i> [%] |
|---|---|-----------------------------------|
| 0, $\pm 50\%$ , $\pm 100\%$                           | 7.567                                   | +17                               |
| 0, $\pm 50\%$ , $\pm 75\%$ , $\pm 100\%$              | 6.832                                   | +5                                |
| 0, $\pm 25\%$ , $\pm 50\%$ , $\pm 75\%$ , $\pm 100\%$ | 6.491                                   | ref. value                        |

In Figure 81 are plotted the eco-drive speed profiles found by using the PSO based algorithm and by increasing the iterations maximum number. The optimal eco-drive speed profile computed by DPO based algorithm is represented in black dotted line, and it is compared to those obtained by the PSO based algorithm using different iterations number. The results show that the performance of the PSO based algorithm can already match the DPO algorithm by using 50'000 iterations and thus, a further increase in the iterations value is not required as it only increases the computing time.

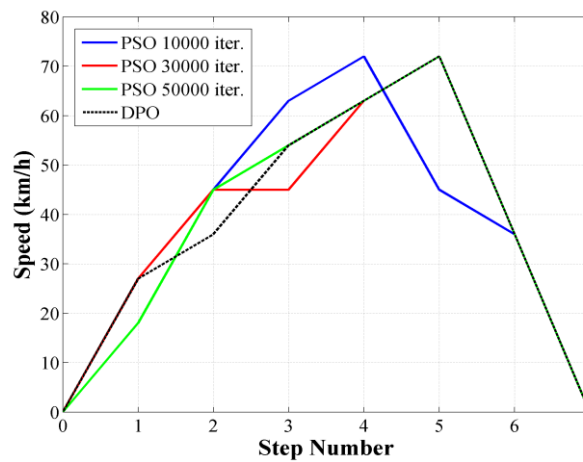


Figure 81 - Iterations effect on PSO eco-drive algorithm (7-time step).

Table 21 presents the performance of the PSO algorithm changing the maximum number of iterations. The results show an improved performance of the heuristic algorithm in terms of goodness of solution, increasing the maximum number of iterations.

Table 21 - PSO algorithm iterations vs performance (10-time step).

| <i>Iterations</i> | <i>Computing time [s]</i> | <i>Substation supplied energy [kWh]</i> | <i>Comparative Evaluation [%]</i> |
|-------------------|---------------------------|---|-----------------------------------|
| 10'000            | 5073                      | 8.256                                   | ref. value                        |
| 20'000            | 10'145                    | 7.912                                   | - 4.16                            |
| 30'000            | 15'217                    | 7.568                                   | - 8.33                            |
| 40'000            | 20'289                    | 7.224                                   | - 12.5                            |
| 50'000            | 25'362                    | 6.880                                   | - 16.6                            |

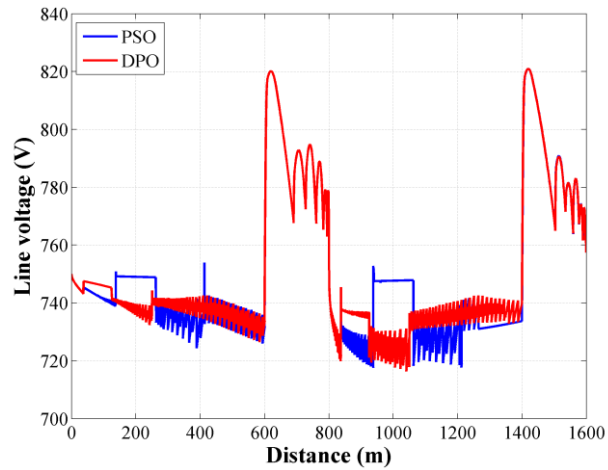
In particular, increasing from 10'000 to 50'000 the maximum number of iterations of the PSO based algorithm, it is possible to obtain a decrease of the energy supplied by the substations equal to 22%. This benefit is paid by an almost linear increase in computing time, which remains still lower than DPO algorithm one by using 50'000 iteration. The comparison between the DPO and PSO eco-drive algorithms, in terms of reserve time effect on the goodness of solution, is summarized in Table 22. The results show worst performance of the PSO algorithm increasing the reserve time and, at the same time, keeping the time step and the number of iterations at a constant value, because the solution space is expanded. It is necessary to increase the number of iterations (i.e. computing time) to achieve the same performance of the DPO based algorithm, otherwise the results of the two eco-drive algorithms have a mean deviation of 9.6%.

**Table 22 - Reserve time effect on energy saved (7-time step).**

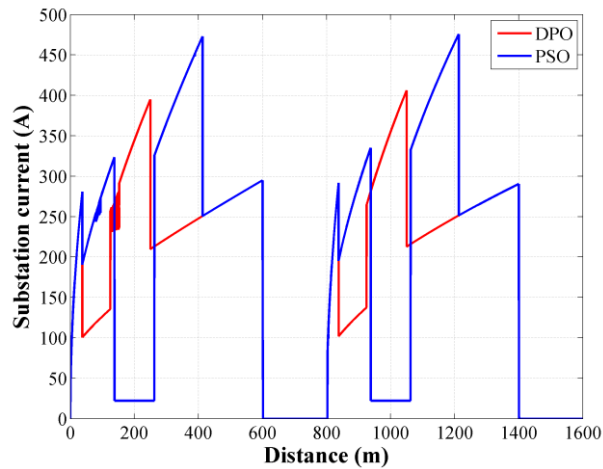
| <i>Reserve time [s]</i> | <i>DPO substation supplied energy [kWh]</i> | <i>PSO substation supplied energy [kWh]</i> | <i>DPO vs PSO Comparative Evaluation [%]</i> |
|-------------------------|---|---|--|
| 5                       | 6.572                                       | 6.937                                       | + 5.25                                       |
| 10                      | 6.491                                       | 6.880                                       | + 5.62                                       |
| 15                      | 6.101                                       | 6.467                                       | + 5.69                                       |
| 20                      | 5.712                                       | 6.054                                       | +5.75  |

Figure 82 shows the line voltage trend related to the reference and the eco-drive speed profiles, repeated twice. The first one leads to a greater drop (15%) in the line voltage because it has a steeper acceleration phase. During the braking phase, optimized speed profiles present a higher overshoot in the line voltage (12.6%) because the deceleration is greater and, therefore, it is possible recovers more braking energy.

Figure 83 highlights the comparison between the substation current trends related to the reference and the eco-drive speed profiles, repeated twice (A⇒B trip – 0⇒800 m - is equal to B⇒C – 800 m⇒1600 m - one). Compared to the reference speed profile, DPO and PSO speed cycles show a significant reduction (17%) in the supplied peak current, with consequent savings in energy delivered.



**Figure 82 - Comparison on line voltage: DPO and PSO based algorithms (7-time step).**



**Figure 83 - Comparison on substation current: DPO and PSO based algorithms (7-time step).**

Eco-drive speed cycles differ slightly each other in terms of substation peak current: DPO algorithm show a peak current value equal to 398 A, whereas the value of the PSO based algorithm is 482 A.

## References

- [1] Ferrovie dello Stato Italiane, “Rapporto di sostenibilità 2014”, available on line at URL: <http://www.fsitaliane.it/cms-file/allegati/fsitaliane/Impegno/Rapporto diSostenibilit%C3%A02014.pdf>
- [2] X. Yang, X. Li, B. Ning, T. Tang, “A Survey on Energy-Efficient Train Operation for Urban Rail Transit”, *Intelligent Transportation Systems*, IEEE Transactions on, 2016, Vol. 17, pp. 2-13.
- [3] F. Perticaroli, “Sistemi elettrici per i trasporti”, 2<sup>nd</sup> Edition, 2001, CEA.
- [4] M.C Falvo, R. Lamedica, R. Bartoni, G. Maranzano, “Energy saving in metro-transit systems: Impact of braking energy management”, in *Proc of Power Electronics Electrical Drives Automation and Motion (SPEEDAM), International Symposium on*, 2010, pp. 1374-1380.
- [5] P. Radcliffe, J.S. Wallace, L.H. Shu, “Stationary applications of energy storage technologies for transit systems”, in *Proc. of Electric Power and Energy (EPEC), IEEE Conference*, 2010 , pp. 1-7.
- [6] R. Barrero, X. Tackoen, J. van Mierlo, “Stationary or onboard energy storage systems for energy consumption reduction in a metro network”, *Journal of Rail and Rapid Transit*, 2010, Vol. 224, pp. 207-225.
- [7] M. Domínguez, A. Fernández-Cardador, A.P. Cucala, R.R. Pecharromàn, “Energy Savings in Metropolitan Railway Substations through Regenerative Energy Recovery and Optimal Design of ATO Speed Profiles”, *Automation Science and Engineering, IEEE Transactions on*, 2012, Vol. 9, pp.496-504.
- [8] A. Rufer, D. Hotellier, P. Barrade, “A supercapacitor-based energy storage substation for voltage compensation in weak transportation networks”, *Power Delivery, IEEE Transactions on*, 2004, Vol. 19, pp. 629-636.
- [9] V. Calderaro, V. Galdi, G. Graber, A. Piccolo, “Siting and Sizing of Stationary Supercapacitors in a Metro Network”, in *Proc. of AEIT Annual Conference, 2013*, pp.1-5.
- [10] M. Ceraolo, R. Giglioli, G. Lutzemberger, M. Conte, M. Pasquali, “Use of electrochemical storage in substations to enhance energy and cost efficiency of tramways”, in *Proc. of AEIT Annual Conference, 2013*, pp. 1-6.
- [11] ZongYu Gao, JianJun Fang, YiNong Zhang, Lan Jiang, Di Sun, Wenrong Guo, “Control of urban rail transit equipped with ground-based supercapacitor for energy saving and reduction of power peak demand”, *Electrical Power and Energy Systems, Elsevier*, 2015, Vol. 67, pp. 439-447.
- [12] Maxwell, “Ultracapacitors module 125 V datasheet”, available on line at: [http://www.maxwell.com/images/documents/125vmodule\\_ds\\_1014696-7.pdf](http://www.maxwell.com/images/documents/125vmodule_ds_1014696-7.pdf)
- [13] V. Calderaro, V. Galdi, G. Graber, A. Piccolo, “Optimal Siting and Sizing of Stationary Supercapacitors in a Metro Network using PSO”, in *Proc. of*

- Industrial Technologies, IEEE International Conference on*, 2015, pp. 2680-2685.
- [14] T. Ratniyomchai, S. Hillmansen, P. Tricoli, “Energy loss minimisation by optimal design of stationary supercapacitors for light railways”, in *Proc. of Clean Electrical Power (ICCEP), IEEE International Conference on*, 2015, pp. 511-517.
- [15] R. Barrero, X. Tackoen, and J. Van Mierlo, “Quasi static simulation method for evaluation of energy consumption in hybrid light rail vehicles”, in *Proc. of Vehicle Power and Propulsion (VPPC), IEEE International Conference*, 2008, pp. 1-7.
- [16] R. Teymourfar, B. Asaei, H. Iman-Eini, R. Nejati Fard, “Stationary supercapacitor energy storage system to save regenerative braking energy in a metro line”, *Energy Conversion and Management, Elsevier*, 2012, Vol. 56 pp. 206-214.
- [17] U. Sirmelis, J. Zakis, L. Grigans, “Optimal supercapacitor energy storage system sizing for traction substations”, in *Proc. of Power Engineering, Energy and Electrical Drives (POWERENG), IEEE International Conference on*, 2015, pp. 592-595.
- [18] G. Clemente, M. Fantauzzi, D. Lauria, “Energy savings in urban mass transit systems: A probabilistic approach for sizing electric energy storage devices”, in *Proc. of Clean Electrical Power (ICCEP), IEEE International Conference on*, 2013, pp. 610-613.
- [19] S.J. Kashani, E. Farjah, “Applying Neural Network and Genetic Algorithm for Optimal Placement of Ultra-Capacitors in Metro Systems”, in *Proc. of Electrical Power and Energy (EPEC), IEEE International Conference on*, 2011, pp. 35- 40.
- [20] T. Ratniyomchai, S. Hillmansen, P. Tricoli, “Optimal Capacity and Positioning of Stationary Supercapacitors for Light Rail Vehicle systems”, in *Proc. of Power Electronics Electrical Drives Automation and Motion (SPEEDAM), International Symposium on*, 2014, pp. 807-812.
- [21] V. Calderaro, D. Coglianò, V. Galdi, G. Graber, A. Piccolo, “An Algorithm to Optimize Speed Profiles of the Metro Vehicles for Minimizing Energy Consumption”, in *Proc. of Power Electronics, Electrical Drives, Automation and Motion, IEEE International Symposium on*, 2014, pp. 813-819.
- [22] F. Mensing, R. Trigui, E. Bideaux, “Vehicle trajectory optimization for application in ECO-driving”, in *Proc. of Vehicle Power and Propulsion (VPPC), IEEE International Conference*, 2011, pp. 1-6.
- [23] A. Albrecht, P. Howlett, P. Pudney, Xuan Vu, “Optimal train control: Analysis of a new local optimization principle”, in *Proc. of American Control Conference (ACC)*, 2011, pp. 1928-1933.
- [24] V. Calderaro, V. Galdi, G. Graber, A. Piccolo, “Deterministic vs Heuristic Algorithms for Eco-Driving Application in Metro Network”, in *Proc. of*

- Electrical Systems for Aircraft, Railway, Ship Propulsion and Road Vehicles (ESARS)*, *IEEE International Conference on*, 2015, pp. 1-6.
- [25] Shuai Su; Xiang Li; Tao Tang; Ziyu Gao, “A Subway Train Timetable Optimization Approach Based on Energy-Efficient Operation Strategy”, *Intelligent Transportation Systems, IEEE Transactions on*, 2013, Vol. 14, pp. 883-893.
- [26] Jiateng Yin; Dewang Chen; Lingxi Li, “Intelligent Train Operation Algorithms for Subway by Expert System and Reinforcement Learning”, *Intelligent Transportation Systems, IEEE Transactions on*, 2014, Vol. 15, pp. 2561-2571.
- [27] E. Khmelnitsky, “On an optimal control problem of train operation”, *Automatic Control, IEEE Transactions on*, 2000, Vol.45, pp. 1257-1266.
- [28] B. Németh, P. Gàspàr, “Optimised speed profile design of a vehicle platoon considering road inclinations”, *Intelligent Transport Systems, IET*, 2014, Vol. 8, pp. 200-208.
- [29] Jungme Park, Y.L Murphey, R. McGee, J.Q. Kristinsson, M.L. Kuang, A.M. Phillips, “Intelligent Trip Modelling for the Prediction of an Origin–Destination Traveling Speed Profile”, *Intelligent Transportation Systems, IEEE Transactions on*, 2014, Vol. 15, pp. 1039-1053.
- [30] J. Wollaeger, S.A. Kumar, S. Onori, D. Filev, U. Ozguner, G. Rizzoni, S. Di Cairano, “Cloud-computing based velocity profile generation for minimum fuel consumption: A dynamic programming based solution”, in *Proc. of American Control Conference (ACC)*, 2012, pp. 2108-2113.
- [31] Yihui Wang, B. De Schutter, Bin Ning, N. Groot, T.J.J. van den Boom, “Optimal trajectory planning for trains using mixed integer linear programming”, in *Proc. of Intelligent Transportation Systems (ITSC), IEEE International Conference on*, 2011, pp. 1598-1604.
- [32] Moon-Ho Kang, “A GA-based Algorithm for Creating an Energy-Optimum Train Speed Trajectory”, *Journal of International Council on Electrical Engineering*, 2011, Vol. 1, No. 2, pp. 123-128.
- [33] K. Colak, D. Czarkowski, F. de Leon, “Energy minimization for catenary-free mass transit systems using Particle Swarm Optimization”, in *Proc. of Electrical Systems for Aircraft, Railway, Ship Propulsion and Road Vehicles (ESARS), IEEE International Conference on*, 2012, pp. 1-5.
- [34] Y. del Valle, G.K. Venayagamoorthy, S. Mohagheghi, J.-C. Hernandez, R.G. Harley, “Particle Swarm Optimization: Basic Concepts, Variants and Applications in Power Systems”, *Evolutionary Computation, IEEE Transactions on*, 2008, Vol. 12, pp. 171-195.
- [35] D. E. Kirk, “Optimal Control Theory: An Introduction”, 2004, Dover Publications on Electrical Engineering.

## Chapter 5

### Conclusions

This dissertation set out to investigate the challenge of urban mobility in the smart cities of the future. In particular, the impact on the smart grid of the urban electrified transport systems and the transition of road transport towards electric propulsion is analyzed and discussed. This final chapter will review the research contributions of this dissertation, as well as discuss directions for future research.

#### 5.1 Summary of Dissertation

The growing phenomenon of *Smart Cities* has led city managers to look beyond traditional city planning and to find ways of giving people a place to live that is environmentally, economically and socially sustainable. In this scenario, mobility policies are the key of effectiveness of all the choices. In fact, *transportation* is the backbone of the existing economy and society; it enables trade, which is essential for social growth and economic development in the urban area. However, transport produces several negative impacts and problems for the quality of life in cities. *Sustainable Mobility* is one of the most promising topics in smart city, as it could produce high benefits for almost all the city stakeholders. The boldest and imminent challenge awaiting sustainable mobility in smart cities is the introduction of the electricity as energy vector instead of fossil fuels, concerning both the collective and the private transports.

On the other hand, the electric mobility highlights new problems both in terms of energy efficiency in public transport systems and in

terms of expected impact on distribution networks due to the EVs charging. In fact, Electric transport modes, such as electric light rail, tramway, electric buses and EV fleets, are power demanding adding significant pressure on the power system, including the local power utilities. *Smart Grid* technologies offer a potential solution to these problems, and, in so doing, contribute to the establishment of a power system that is more energy efficient, secure and sustainable from a growing base of renewable resources.

The main research contributions of this dissertation, in the reference context described above, are:

- **GRLS problem under uncertainty conditions.** The three following points lay the foundations for Chapter 2 and represent its main contributions: 1) the possibility to apply GRLS management strategies in microgrids that could improve the reliability level of the distribution systems in the presence of DERs. 2) the necessity to formulate GRLS problem in microgrids considering the uncertainty due to not-programmable DERs and no well-known load demand profiles; 3) to develop a complete strategy to support the continuity of service in case of faults by completing the only rescheduling scheme already proposed. In Chapter 2, a GRLS problem for microgrids is formulated and solved in order to determine a stable equilibrium state following outage for increasing continuity of service. The solution takes into account the uncertainty due to the fact that: i) lower and upper limits of some of the dominant constraints are not sharp but rather soft, ii) the load profiles in MV distribution system are not deterministic, iii) a part of distributed renewable generation and EVs charging load introduces uncertainty in power production and demand, respectively.
- **EVs charging profile prediction and scheduling.** The contributions are mainly described in the Chapter 3 and they consist of three parts, which can be summarized as follows: 1) it shows a simple and effective methodology to analyze measured data and to identify typical load pattern for the PEVs charging. We use an approach based on the analysis of a large data-set collection characterizing parking areas in terms of conventional vehicles entry time and average parking duration.

- 2) It proposes a novel scheduling problem formulation flattening the demand load profile and minimizing the PEVs charging costs, according to the electricity prices during the day. The charging action is evaluated according to the battery charging characteristic and it is contained within the estimated PEV parking time assuming domestic and public charging modes for the incoming PEVs in the parking areas. 3) It evaluates the impact of PEVs demand on a real micro grid and the benefits introduced by the proposed charging scheduling algorithm. Obtained results confirm the effectiveness of the proposed scheduling algorithm, ensuring the satisfaction of PEVs charging needs while flattening the demand profile at the same time.
- **Energy efficiency in urban railway systems.** Chapter 4 introduces and discusses two particular solutions for energy efficiency in urban railway systems: energy storage systems and eco-drive train operations. The main contributions consist of two parts: 1) it propose a heuristic method for the joint siting and sizing design of stationary SCs in metro network, taking into account: i) the track topology - slopes and curves - ii) the electrical features of the feeding line, iii) the mechanical characteristics of the vehicle and its time-table. The proposed design solution allows to maximize energy efficiency, to minimize the number of installation sites and the total size of SCs reducing, consequently, the costs. 2) It formulates and solves the eco-drive problem for metro vehicles. In particular, the problem formulation takes into account: i) the timetable, ii) the characteristics of the metro system, iii) the effect of regenerative braking, assuming stationary energy storage systems on the track. Deterministic and heuristic solution algorithms, based on DPO and PSO method, are presented and compared in terms of the time spent to search a feasible solution and the goodness of the obtained solution.

In the following, they are listed the works published by the author in proceedings of international conferences or in journals during the PhD program and supporting this dissertation.

- [1] V. Calderaro, V. Galdi, G. Graber, A. Piccolo, "Optimal Generation Rescheduling in Microgrids under Uncertainty", in *International Review of Electrical Engineering* - Num. 5 (October 2013), vol. 8.
- [2] V. Calderaro, V. Galdi, G. Graber, G. Graditi, F. Lamberti, "Impact Assessment of Energy Storage and Electric Vehicles on Smart Grids", in *Proc. of Electric Power Quality and Supply Reliability (PQ)*, *IEEE International Conference*, 2014, pp. 15-18.
- [3] V. Calderaro, V. Galdi, G. Graber, A. Piccolo, "Generation Rescheduling and Load Shedding in Distribution Systems under Imprecise Information", in *IEEE Systems Journal*, vol. PP, no. 99, pp.1-9, Feb. 2016.
- [4] V. Calderaro, V. Galdi, G. Graber, G. Massa, A. Piccolo, "Plug-in EV Charging Impact on Grid Based on Vehicles Usage Data", in *Proc. of Electric Vehicle, IEEE International Conference on* 2014, pp. 1-7.
- [5] G. Graber, G. Massa, V. Galdi, V. Calderaro, A. Piccolo, "Performance Comparison between Scheduling Strategies for PEVs Charging in Smart Grids", in *Proc. of Renewable Energy Research and Applications, IEEE International Conference on*, 2015, pp. 1-6.
- [6] V. Calderaro, V. Galdi, G. Graber, A. Piccolo, "Siting and Sizing of Stationary Supercapacitors in a Metro Network", in *Proc. of AEIT Annual Conference, 2013*, pp.1-5.
- [7] V. Calderaro, V. Galdi, G. Graber, A. Piccolo, "Optimal Siting and Sizing of Stationary Supercapacitors in a Metro Network using PSO", in *Proc. of Industrial Technologies, IEEE International Conference on*, 2015, pp. 2680-2685.
- [8] V. Calderaro, D. Cogliano, V. Galdi, G. Graber, A. Piccolo, "An Algorithm to Optimize Speed Profiles of the Metro Vehicles for Minimizing Energy Consumption", in *Proc. of Power Electronics, Electrical Drives, Automation and Motion, IEEE International Symposium on*, 2014, pp. 813-819.
- [9] V. Calderaro, V. Galdi, G. Graber, A. Piccolo, "Deterministic vs Heuristic Algorithms for Eco-Driving Application in Metro Network", in *Proc. of Electrical Systems for Aircraft, Railway, Ship Propulsion and Road Vehicles (ESARS), IEEE International Conference on*, 2015, pp. 1-6.

## 5.2 Future Research Direction

The research that was undertaken for this dissertation is just a step of a complex and long path: several areas where information is lacking were highlighted in the literature review and whilst some of these were addressed by the research in this dissertation, others remain.

In particular, Chapter 2 showed how the integration of fuzzy possibility theory and Monte Carlo simulations allow obtaining a large interval of solutions corresponding to power system scenarios with high or low possibility. Furthermore, the interpretation of the solutions is easy because the uncertainty characterizing both load and power generation is modeled on human's intuition. The main benefits of the proposed approach are due to the fact having real rescheduling and load shedding solutions with different degree of possibility, so that technicians and operators can accept the proposed solutions with an aware risk level.

Borders of this approach are due to the real rescheduling optimization and fuzzy check procedure: in some cases, it is not possible to find a  $\alpha = 0$  rescheduling solutions, but only one that has a possibility  $\alpha > 0$ . Furthermore, the optimization procedure is based on a classical solution method that uses as input data the central values of fuzzy numbers. An approach based on a solution method that manipulates fuzzy numbers could be more accurate and with higher performance results. In the future works, research activities should be focused on the development of a fuzzy method to solve optimization power system problems.

In Chapter 3, the impact of EVs demand on DNs in terms of requested power an energy is approached by performing an analysis of a large data-set collection, obtained from the University of Salerno as part of the activities of the COSMO research project. Several Monte Carlo simulations are carried out to assess the benefits introduced by the proposed scheduling algorithm on a real case study, in terms of reduction in the cost of user's charge, satisfaction of PEVs charging needs, and flattening of the demand load profile.

A wider set of data referred to the behaviour of different kind of nodes (like shopping centres, interchanges such as railway stations, ports and airports bus terminal, public offices, factories, etc.) must be collected and handled.

In this work, it is assumed a centralized scheduling architecture requiring a central node able to receive all the vehicle information from each EVs charging station and perform the scheduling algorithm for all vehicles in the parking areas. Future developments include the extension of the proposed algorithm for decentralized or hierarchical architectures, much more realistic in larger smart grid. In addition, the

proposed algorithm can be further enhanced by adding priority mechanisms, charging reservation or personalized services, etc. Finally, it is interesting to evaluate the performance of a greedy algorithm, having a lower computing time, compared to those of the optimization problem solution algorithm.

Chapter 4 deals with the joint problem of stationary ESSs sizing and positioning along the track and the eco-drive speed profiles computation problem for metro vehicle. In particular, the optimized design solution maximizes the covered braking energy and to minimize the number and capacity of ESSs along the track. The eco-drive problem consists in finding the optimal speed profile obtained as sequence of basic control regimes that leads to the minimization of energy supplied by the electrical substation for a given trip, take into account line power losses.

Directions for future research activities include the performance comparison between different ESSs technologies and the introduction into the optimization procedure of a cost function that takes into account the energy price and the costs related to the installation and maintenance of the ESSs. On the other hand, development of control techniques and stored energy management strategies, in order to improve the performance of the ESS in terms of energy efficiency could be very interesting.

Regarding the possibility of research on algorithms for computing eco-drive profiles, the proposed work lays the foundation for planning the timetable in driverless metro systems, but it does not address the issues related to the real-time updating of the speed profiles according to human driver guide styles. Finally, eco-drive algorithms are very interesting even in the automotive field, where the problems are exacerbated because private cars run on non-dedicated lanes.